Analysis of Radiation Embrittlement Reference Toughness Curves

NP-1661
Research Project 886-1

Final Report, January 1981

Prepared by

FRACTURE CONTROL CORPORATION
340 South Kellogg Avenue, Suite G
Goleta, California 93017

Principal Investigators
W. L. Server, Editor
R. A. Wullaert
G. R. Odette*
W. Oldfield**

*University of California
Department of Chemical and Nuclear Engineering
Santa Barbara, California 93106

**Materials Research and Computer Simulation
340 South Kellogg Avenue, Suite K
Goleta, California 93017

Prepared for

Electric Power Research Institute
3412 Hillview Avenue
Palo Alto, California 94304

EPRI Project Manager
T. U. Marston

Water Reactor System Technology Program
Nuclear Power Division

ORDERING INFORMATION

Requests for copies of this report should be directed to Research Reports Center (RRC), Box 50490, Palo Alto, CA 94303, (415) 965-4081. There is no charge for reports requested by EPRI member utilities and affiliates, contributing nonmembers, U.S. utility associations, U.S. government agencies (federal, state, and local), media, and foreign organizations with which EPRI has an information exchange agreement. On request, RRC will send a catalog of EPRI reports.

NOTICE

Prepared by
Fracture Control Corporation
Goleta, California

EPRI PERSPECTIVE

PROJECT DESCRIPTION

The embrittlement of ferritic pressure vessel materials resulting from exposure to fast neutrons is a key element in the assessment of reactor vessel structural integrity. RP886-1, Evaluation and Prediction of Neutron Embrittlement of Reactor Pressure Vessel Materials, evaluates and develops techniques for the measurement and prediction of radiation damage. This project is part of the characterization of the Materials Phase of the Pressure Boundary Technology Program within the Nuclear Tower Division, as described in EPRI Special Report NP-1540-SR, Pressure Boundary Technology Program: Progress in 1979.

PROJECT OBJECTIVES

The appropriateness of the existing methods for predicting radiation-induced embrittlement contained in the codes, standards, and regulations has been under question by the technical community. This project addressed the development of statistical, reference fracture toughness curves; the generation and evaluation of fracture toughness data from modified surveillance (Charpy impact) specimens; and the development of a radiation-damage model incorporating thermal aging and in-situ annealing. Verification tests were conducted wherever possible.

PROJECT RESULTS

The research results indicated that a Charpy-based, statistically developed, reference fracture toughness approach was a better predictor of fracture toughness than the existing RT_{NDT} approach contained in the ASME Code. An additional project, RP1021-4, was initiated to complete the development, and a PVRC/MPC task group was established to assess the approach for possible codification. Certain Charpy specimen modifications were developed and confirmed to facilitate fracture toughness measurement from surveillance specimens. A simple and inexpensive technique for reconstituting surveillance specimens for additional testing was developed and verified on both irradiated and unirradiated specimens. Finally, the radiation-damage model research clearly identified the importance of the time-at-exposure temperature on radiation embrittlement. Overall, the project identified several areas of improvement in radiation-damage predictions.

The information contained in this report should be of interest to those involved with licensing questions concerning radiation damage and reactor vessel integrity and those generally interested in service-induced changes in material properties.

Theodore U. Marston, Project Manager
Nuclear Power Division

ABSTRACT

The objective of this program was to establish statistical and experimental insight into the development of a methodology for producing radiation embrittlement reference toughness curves. To meet this objective, three major tasks were performed: (1) statistical analysis and development of reference fracture toughness curves, (2) evaluation of fracture toughness data from surveillance (small) specimens, and (3) radiation damage analysis and modeling. The results from the first task provided techniques for statistical experimental design of radiation embrittlement programs and proper collection and qualification of experimental mechanical property data. The main accomplishment was the development of global tolerance and confidence bounds from precracked Charpy and Charpy V-notch normalization using a reference fracture toughness curve approach. The second task provided a single-specimen procedure for measuring ductile initiation toughness with side-grooved precracked Charpy specimens; additionally, excellent predictions of fracture toughness by critical stress and critical strain fracture models were made. Instrumented Charpy-type data were also maximized using various approaches. A surrogate material was developed to simulate radiation-induced damage by shock hardening. Perhaps of greatest interest was the utilization of reconstituted surveillance specimens produced from previously broken Charpy specimens. The radiation damage task produced information necessary to treat radiation embrittlement and dosimetry analysis in an improved manner. A physically-based damage correlation model and a microstructural defect development model provided additional insight into radiation damage observations.

CONTENTS

ILLUSTRATIONS

TABLES

SUMMARY

This final report covers the work performed by Fracture Control Corporation during a three-and-one-half year program with the Electric Power Research Institute under Contract RP886-1. The principal investigators for this program were Dr. R.A. Wullaert and W.L. Server from Fracture Control Corporation and consultants, Dr. W. Oldfield and Dr. G.R. Odette, from Materials Research and Computer Simulation and University of California, Santa Barbara, respectively. A large number of other individuals made significant contributions to the material presented here; these individuals are identified within the report with respect to their work.

The research program consisted of three major tasks, each of which will be summarized in the following discussion.

STATISTICAL ANALYSIS AND DEVELOPMENT OF REFERENCE FRACTURE TOUGHNESS CURVES

The uncertainty in the degree of conservatism in the Nuclear Regulatory Commission (NRC) radiation embrittlement trend curves (Regulatory Guide 1.99) indicates the deficiencies in the existing radiation embrittlement data base. Any new experimental test program should be designed in a statistical manner to reap the maximum benefit that can be obtained from an expensive radiation embrittlement study. The requirements and options available in developing an efficient experimental design were reviewed. This review included a quantitative definition of program objectives and relating these quantities to the anticipated variance in the measurements to be made. Specific probability diagrams were developed for the detection of temperature shifts in Charpy V-notch curves. The importance of not confounding the quantities being measured with extraneous variables was stressed. Two sources of bias which can be confounded with main effects in irradiation experiments are "between capsule" and "between positions in the capsule" variations. Suggestions for a balanced, but flexible, experimental design were made.

Additionally, a round robin test program was performed to determine the test variability associated with the instrumented precracked Charpy test. This test

can be used as an indexing parameter (for example, in the new statistically-based reference fracture toughness curve procedure). Thus uncertainties in the indexing parameter are reflected in a reference curve. A homogeneous, relatively strain rate insensitive material (6061-T651 aluminum) was used in an effort to separate material variability from test variability. The round robin data were generated using a comparative experimental design and analyzed using the analysis of variance procedure. The results indicated that instrumented impact testing was not yet properly controlled and that there was a clear need for improvement in the test procedures.

A critical aspect of developing a statistically-based reference curve is the existence of a pedigreed data base. The existing EPRI procedures for testing and data analysis were simplified and revised to include current state-of-the-art techniques, particularly for elastic-plastic fracture toughness testing. New data report forms were developed to assure that all pertinent data are recorded with all terms and symbols defined and sample calculations provided. The development of a radiation embrittlement data base also requires the characterization of the radiation environment through proper irradiation analysis. A detailed review of the magnitude and sources of dosimetry uncertainties associated with past radiation embrittlement studies was made.

Fracture toughness data from various EPRI programs were qualified (pedigreed), statistically analyzed, and consolidated in a new computer data base which was published as a topical report; this expanded data base includes chemical analysis, processing history, curve-fit parameters, statistics, and tables and graphs of all mechanical properties data. The revised data base, which also included valid J integral initiation (R-curve), upper shelf data, was used to develop new procedures for referencing fracture toughness in lieu of the current RT_{NDT} indexing parameter. Coefficients from tanh curve fits to instrumented pre-cracked Charpy data (PCVN method) were used to reference fracture toughness data and develop prediction limits. This method was improved by developing a weighted non-linear regression scheme and developing global tolerance bounds. The net result was a simplified, statistically-based technique by which any suitable test could be properly referenced to fracture toughness to give a reference curve. The referencing technique was therefore extended to the use of Charpy V-notch data (CVN method). Both the PCVN and CVN methods were used to predict fracture toughness mean, confidence, and global tolerance bounds for a specific heat of material, test type and stress intensity rate. These predictions were compared to actual fracture toughness data for the same heat and test

conditions. The CVN referencing method has excellent potential since it relates directly to the current surveillance test specimen.

Unirradiated and irradiated V-notch and precracked Charpy data from an associated EPRI program (RP886-2) were entered into a computer data bank, curve-fitted with tanh functions, and prepared for use in generating a statistically-based lower bound reference curve for the limited irradiated data available.

FRACTURE TOUGHNESS DATA FROM SURVEILLANCE SPECIMENS

A variety of experimental and analytical techniques were examined for estimating the fracture toughness of nuclear pressure vessel steels from small surveillance-type specimens. Static and dynamic fracture toughness data were generated using an older generation steel (SA302B surveillance correlation heat), a currently used steel (SA533B-1, HSST Plate 02) and a submerged arc weld metal. The multi-specimen R-curve method was used to obtain ductile initiation J-integral data for a "valid" data base (including static and dynamic data) to compare with the small specimen results. Different methods of measuring crack length influenced the R-curve slope but not the value of J_{Ic}.

To study a single specimen J_{Ic} technique, the J-integral value at maximum load (J_{max}) was measured as a function of side groove depth in precracked Charpy-type specimens under both slow bend and impact loading. J_{max} approached J_{Ic} for a total side-groove depth of about 30% of the specimen thickness. The effect of side-grooving (in producing $J_{max} = J_{Ic}$) was found to be a function of the fracture toughness level and the remaining ligament length (b), but the technique provides excellent potential for assessing the loss in upper shelf fracture toughness due to irradiation exposure. Another technique for obtaining J_{Ic} from J_{max} values was also investigated and involved measuring J_{max} as a function of specimen width while holding all other specimen dimensions constant. This approach is not, however, a single specimen approach.

A predictive scheme to develop fracture toughness information from Charpy and tensile-type data was developed using critical stress and strain models for fracture initiation. The application of these models involved determination of critical stress and strain values, knowledge of precise analyses for the elastic-plastic stress and strain distributions ahead of sharp cracks, and an evaluation of microstructural size parameters which control the fracture event. Critical fracture stress (σ_f^*) values were determined from notched bend bars and

used in a critical stress model to accurately predict low temperature, slip-initiated cleavage fracture toughness up to the Nil Ductility Transition Temperature (both unirradiated and irradiated). Notched tensile specimens were used to obtain upper shelf critical strain values (ε_f) as a function of stress state; these values were used in a critical strain model to predict unirradiated upper shelf fracture toughness where fracture involves a fully ductile rupture (microvoid coalescence) mechanism. Predictions of toughness on the upper shelf for irradiated materials were not possible at this time due too the absence of irradiated ductility-stress state data and the sparce upper shelf toughness results for comparison with the model.

Several investigations were performed in order to maximize Charpy-size specimen data. The effect of notch root radius (ρ) on cleavage and fibrous-initiated fracture toughness was measured to determine if an effective root radius (ρ_0) exists for which the fracture toughness is the same as for a sharp fatigue flaw. Values of ρ_0 were obtained for cleavage-initiated fracture, but there were no such values for fibrous-initiated fracture. Charpy V-notch and precracked Charpy tests under both impact and slow bend loading were analyzed in terms of load-temperature diagrams and energy partitioning. These analyses allow further insight into the different material response between the SA302B and SA533B-1 steels and the differences due to specimen orientation within the plate. A fractograph study was also conducted in which the two steels were characterized with respect to the stretch zone existing at the end of the fatigue precrack of previously tested precracked Charpy specimens. The stretch zone height was carefully measured and related to the crack tip opening displacement, another measure of fracture toughness.

It was also undertaken to develop a surrogate material to simulate radiation embrittlement by explosively shock-hardening an SA533B-1 steel plate. The plate material was then machined into Charpy V-notch specimens, and the subsequent testing produced results consistent with that observed for neutron irradiation damage, i.e., there was a shift in properties to higher temperatures and marked decrease in the Charpy upper shelf energy level.

A final investigation was conducted to develop reconstituted surveillance specimens with final emphasis on stud welding end tabs on broken Charpy V-notch specimens. The study welding procedure was maximized for pressure vessel steels, and specimens were prepared from both unirradiated and irradiated broken Charpy halves. The results of testing the reconstituted specimens were very

encouraging and agreed well with the original test results. Both Charpy V-notch and precracked Charpy testing were performed.

RADIATION DAMAGE ANALYSIS AND MODELING

The assessment of the historical accuracy of the dosimetry component of embrittlement analysis has revealed the most significant source of uncertainty is the flux-fluence measurements based on combinations of reactor physics calculations and nuclear reaction rate measurements for both test and surveillance irradiations. An overall scatter in the fluence parameter in the current embrittlement data base can be as high as a factor of 4. The status of light water reactor damage analysis programs was also reviewed and recommendations were made concerning future experiments and coordination of the overall programs. Interaction was made with a Nuclear Regulatory Commission program on dosimetry improvement; contributions in terms of experimental design, material procurement, and specimen machining were made to augment two experimental aspects of this program [the Oak Ridge Reactor Pool-Side Facility (PSF) space compatible test program and the void box experiment]. It is the type of data which will be generated from this NRC program (plus additional mechanistic results) which will provide the basis for an improved embrittlement data base. Therefore, it is important that the dosimetry data generated in EPRI programs be compatible and of the same quality. To help achieve this goal in conjunction with the Naval Research Laboratory (NRL) program RP886-2, a dosimetry mapping study was conducted to provide neutron spectral information for the NRL-EPRI irradiation experiments.

An overview of the critical processes involved in irradiation embrittlement was developed with emphasis on primary defect production, development of damage microstructure, and the relationship between microstructure and mechanical properties (i.e., embrittlement). These processes were incorporated into a physically based, semi-empirical correlation model for predicting embrittlement. The model was calibrated using irradiated data from the SA302B surveillance correlation heat, with supplemental post-irradiation annealing data used to check the self-annealing part of the model. A key aspect of the model was the determination of the influence of thermal aging, flux, fluence and irradiation temperature on embrittlement (shift in the Nil Ductility Transition Temperature, NDTT). The model was able to predict quantitatively, and with reasonable accuracy, the results of recent observations of a damage rate effect in low lead-factor surveillance experiments. Another computer model called SODAK was developed to track the development of defect microstructures during irradiation, post-irradiation annealing and reirradiation. The model explicitly considered the effect

of both irradiation induced defects and impurity or alloying elements such as copper. The results from SODAK supported the phenomenological modeling approach previously developed. It was shown that the various models, even with their limitations, were useful in providing a systematic identification of future experimental efforts. It was concluded that significant progress in current modeling and data correlation efforts cannot be made until additional microstructural and kinetics data are obtained, and the irradiation environment is more precisely defined. Some of this needed information will be obtained through the PSF space compatible program and the void box experiment.

Section 1

INTRODUCTION

BACKGROUND

Pressure-temperature limitations for heatup and cooldown of the reactor coolant system during operation and test conditions are provided in the Technical Specifications for each plant. These pressure-temperature limits are imposed on the reactor coolant pressure boundary to provide adequate safety margins against nonductile or rapidly propagating failure of the ferritic pressure vessel materials. Appendices G and H of 10 CFR 50 specify the requirements for the reactor vessel pressure-temperature limits. These limits are based on the ASME Code, Section III, Appendix G, which provides a fracture mechanics basis for determining allowable limits. The Electric Power Research Institute (EPRI) has recently completed a large research program (RP232-1, -2, -3) which established a data base for verifying the reference toughness curve (K_{IR}) in Appendix G of the ASME Code. Another EPRI funded program (RP696-1) has developed procedures for defining a statistically-based K_{IR} curve. As a result of these EPRI sponsored programs, the initial limitations for reactor heatup and cooldown related to fracture toughness considerations can be developed with a specified degree of confidence.

Once the reactor is placed in service, the neutron environment alters the mechanical properties of the reactor vessel in the beltline region. The reactor operating curves must therefore be adjusted to account for the anticipated embrittlement. Trend curves of change in fracture toughness versus fluence are used to predict the embrittlement for a specific type of steel, residual element content, and operating temperature of the reactor. These trend curves are used by reactor vendors and operators to predict the operating pressure-temperature limitations of their reactors until actual embrittlement data are obtained from surveillance programs. Recently, the Nuclear Regulatory Commission has issued Regulatory Guide 1.99 which specifies radiation embrittlement trend curves.

There are several problems inherent in the current approach to establishing radiation embrittlement trend curves:

- The variability of test data is not properly treated. If the K_{IR} curve represents a lower bound referenced by RT_{NDT} (which is commonly based upon a Charpy V-notch test) it already incorporates the variability inherent in the unirradiated Charpy V-notch test. Consequently, the additional use of an upper bound on the shift of irradiated Charpy data may represent a double inclusion of data variance. A unified treatment of variance for unirradiated and irradiated data leading to a properly developed lower bound on properties is needed. Since the variability in unirradiated Charpy data can lead to a measured shift of about 40°F (22°C) (approaching the currently defined radation induced shift of 50°F [28°C] for defining beltline materials), a proper treatment of embrittlement data variability is essential.

- The data base available for establishing trend curves is inadequate. Recent attempts to analyze and curve fit existing test data revealed that the data base as presently assembled is seriously deficient, and it cannot be used in an efficient manner to provide guidance. Consequently, regulatory guides based upon it may be highly conservative. Any new experimental irradiation embrittlement programs should be statistically designed to maximize the data obtained and to respond to the deficient areas in the existing data base. To provide adequate statistical information, a large number of expensive tests are generally required; methods for possibly reusing already broken irradiated specimens would greatly enhance any attempt to add to the current data base.

- Test data generated by capsule irradiations must be extrapolated to predict the behavior of irradiated pressure vessels (which might have a substantially different neutron environment). Such extrapolation has been subject to large errors because of inadequate fluence measurements. Recent developments in irradiation analysis make it possible to control the errors of such extrapolation, provided that the capsules are properly monitored with dosimeters. Past irradiation experiments were not always properly monitored.

- The trend curves are based on the change in fracture toughness as measured by the Charpy V-notch test. The desired fracture toughness embrittlement information which is consistent with the initial design of the pressure vessel is fracture mechanics data. Additionally, the current commercial surveillance specimen is the Charpy V-notch bar; thus, a more thorough understanding of the Charpy V-notch test (and/or other small specimen tests) and the relationship to fracture mechanics parameters is needed. Since current irradiation trend curves are not derived from experimentally based reference toughness (K_{IR}) curves, the completion of RP232-1, -2, -3, and RP696-1 provide a basis for developing a unified treatment of fracture toughness which was not previously available.

PROGRAM DESCRIPTION

The primary objective of this research program was to establish statistical and experimental insight into the development of a methodology for producing radiation embrittlement reference toughness curves. To achieve this primary objective, the following items had to be addressed:

- Develop test, data analysis, and statistical evaluation procedures to assure that a pedigreed radiation embrittlement data base can be obtained.
- Develop a statistical approach for predicting the lower bound fracture toughness of irradiated reactor pressure vessel materials.
- Establish the relationship between radiation embrittlement measured by the small specimen, Charpy V-notch test and fracture mechanics tests.
- Establish the magnitudes of uncertainties in establishing neutron exposures and provide a strategy for producing self-consistent data of high relative precision.

The research activities of the current program were divided into three tasks for reporting purposes:

Task I--Statistical Analysis and Development of Reference Fracture Toughness Curves

Task II--Fracture Toughness Data From Surveillance Specimens

Task III--Radiation Damage Analysis and Modeling

The research activities in Task I are concerned with the acquisition, qualification, and ultimate application of radiation embrittlement data, whereas the work in Task II is concerned with developing new techniques for obtaining these data from existing surveillance specimens. Task III is concerned with the qualification, improvement, and ultimate application of radiation exposure parameters and the modeling of radiation damage.

A methodology for defining a statistically based lower bound reference fracture toughness curve has evolved from the RP232-1 and RP696-1 programs (1-4). This methodology was extended and improved to handle the additional variables associated with radiation embrittlement. One of the important aspects of the program was the development of the philosophy underlying reference toughness curves. For example, these curves could be based on Charpy V-notch or fracture toughness data; they could be lower bound or mean curves; and they could be based on a single type of test or a combination of test types. The statistical analysis used to generate reference curves is dependent on the reference curve approach selected, and the type of reference curve approach selected dictates the type of new data required and thus future experimental designs.

Another important aspect of the program concerned the quality (pedigree) of the data from which the radiation embrittlement reference curves are generated. The

quality of the data must be verified with respect to equipment calibration, test and data analysis procedures, acceptance criteria, and neutron environment.

Also of practical importance was the maximization of data obtained from surveillance programs. The use of local and global fracture criteria relative to small specimen testing was examined and predictions were made based upon simple models. Unique approaches for obtaining fracture toughness results from small specimens were also investigated. Additionally, physically-based correlation modeling of radiation embrittlement provided qualitative predictions of observed trends in existing data.

A more detailed description of each task, along with the pertinent results, will be reported separately in the next three sections of this report.

PRIOR PROGRESS REPORTS

This final report covers the total scope of work performed by Fracture Control Corporation and its consultants during a three-and-one-half year program with the Electric Power Research Institute under Contract RP886-1. Work performed during the first three years was reported in semi-annual reports (5-8) and a special topical report (9).

RELATED EPRI PROGRAMS

Two other EPRI programs have evolved from this initial program, RP1021-4 and RP1240-1. The first program is currently under contract to Materials Research and Computer Simulation, and a complete discussion of the program is available in the first annual report (10); briefly, this program was designed to consolidate the new reference curve developments and facilitate their incorporation into revised codes for pressure vessel design and operation. The latter program, RP1240-1, was performed by Fracture Control Corporation and the results will soon be available (11); emphasis was placed on obtaining and qualifying the existing mechanical property and irradiation history data for irradiated pressure vessel steels and developing a weighting procedure whereby the "quality" of the data is systematically assessed and used in comparisons between experimental data.

Section 2

TASK I

STATISTICAL ANALYSIS AND DEVELOPMENT OF REFERENCE FRACTURE TOUGHNESS CURVES*

INTRODUCTION

The scope of this task has evolved with changes in emphasis throughout the research program. There have been considerable achievements in four technical areas: (1) development of statistically-designed irradiation studies, (2) collection, format, and qualification procedures for data, (3) reference fracture toughness curve development, and (4) preliminary analysis of Naval Research Laboratory (NRL) irradiated data obtained under EPRI Research Program RP886-2. The following discussion describes each of these areas of accomplishment.

STATISTICAL EXPERIMENTAL DESIGN

Initial emphasis in Task I was to develop a statistical experimental design to maximize the data obtained in future radiation embrittlement test programs. The requirements and options available in developing an efficient experimental design were reviewed (5). Briefly, the benefits of using an experimental design through which the efficiency of experimentation is maximized and the odds of success or failure are weighed before the experiment is performed, are manifold. Most obvious is the idea that replication of tests reduces the random variation of the mean result. Consequently, the number of replicates required (n) is an important variable. To ascertain the value of n needed to achieve desired results, the experimental program must define three quantities:

1. The size of the effect sought (δ) in comparison to the anticipated variance of the measurements (σ). The ratio of σ/δ is a measure of the sensitivity of the experiment.

2. The required confidence in the result. This confidence is determined in terms of the probability (α) that an effect δ will be asserted to exist when in fact it arose from chance fluctuations in the data.

*Contributions by W. Oldfield (Materials Research and Computer Simulation) and W.L. Server, R.A. Wullaert, and J.W. Sheckherd (Fracture Control Corporation).

3. The acceptable level of risk that no effect will be found to be significant when in fact a real effect does actually exist. This probability of risk is designated β.

These ideas can most simply be illustrated in a "single-sided" situation where a change can only be in one direction.* In Figure 2-1(a), the interpretation of the probability α is shown. Even though there is no real difference between two measurements, the results of repeated comparisons will be distributed about some mean with perhaps a Gaussian shape. There is a size of difference, Δ, which can be exceeded with a probability α even though no real difference exists. Figure 2.1(b) contrasts the hypothetical situation when there is no difference (curve on the left) and when a difference δ exists (curve on the right). The area β is the probability that a real difference, δ, will lie in the range Δ such that no difference will be asserted.

Probability Diagrams

To make the experimental design process more relevant, an experimental design program related to the temperature shift at the Charpy V-notch energy 30 and 50 ft-lbf (41 and 66 J) levels (Cv_{30} and Cv_{50}) caused by irradiation was studied for plate and weld material. Charpy V-notch energy curves were assumed to have been constructed from data which included eight data points on the property transition portion of the curve. On the basis of variance estimates obtained from the existing unirradiated data base (9) the relationship between the size of effect (shift in the Charpy curve), experiment size (n ≡ number of repeated curves), and α and β were computed. The results were formalized in terms of probability diagrams, such as shown in Figure 2-2 for manual metal arc weld metal tests. The computations assumed a 95% confidence level (α = 5%) and curves for β ranging from 0.1% to 10% were determined. Consider an experimental design which compares single Charpy V-notch energy curves to show the effect of material composition (copper content for example) on the properties of manual arc welds. Referring to Figure 2-2, if the variance observed in unirradiated welds still applies, a shift of the Charpy V-notch curves of about 41°F (23°C) can be detected from a single curve (n = 1) with α = 5% and β = 10%. However, if the variance is inflated by irradiation, as it may likely be, a much broader band will apply.

This work showed that in the main experiment, with $\alpha = \beta = 0.05$, comparisons of single Charpy impact test curves of irradiated SA533B-1 base material could

*For a "double-sided" test, the probabilities of α and β are double.

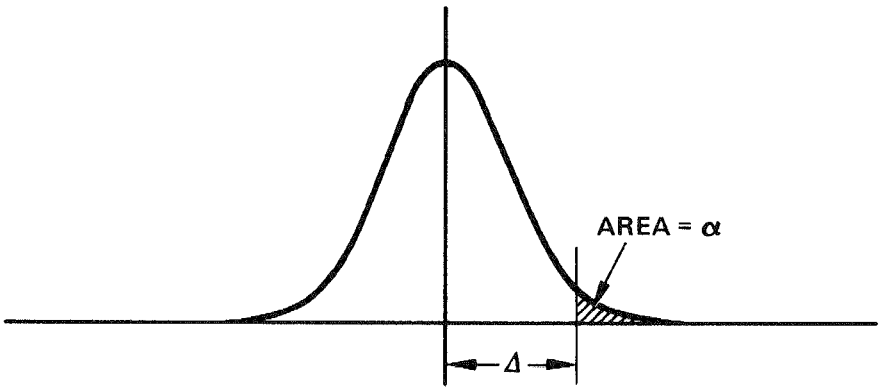

(a)

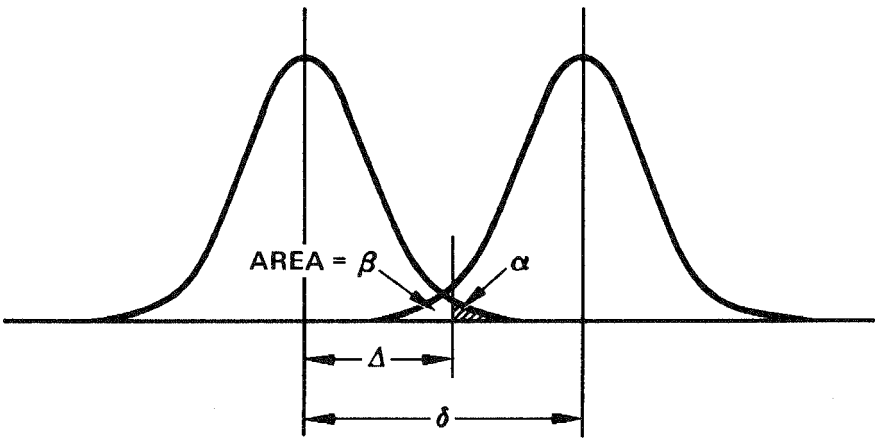

(b)

Figure 2-1. Single-sided situation illustrating the probabilities of α and β.

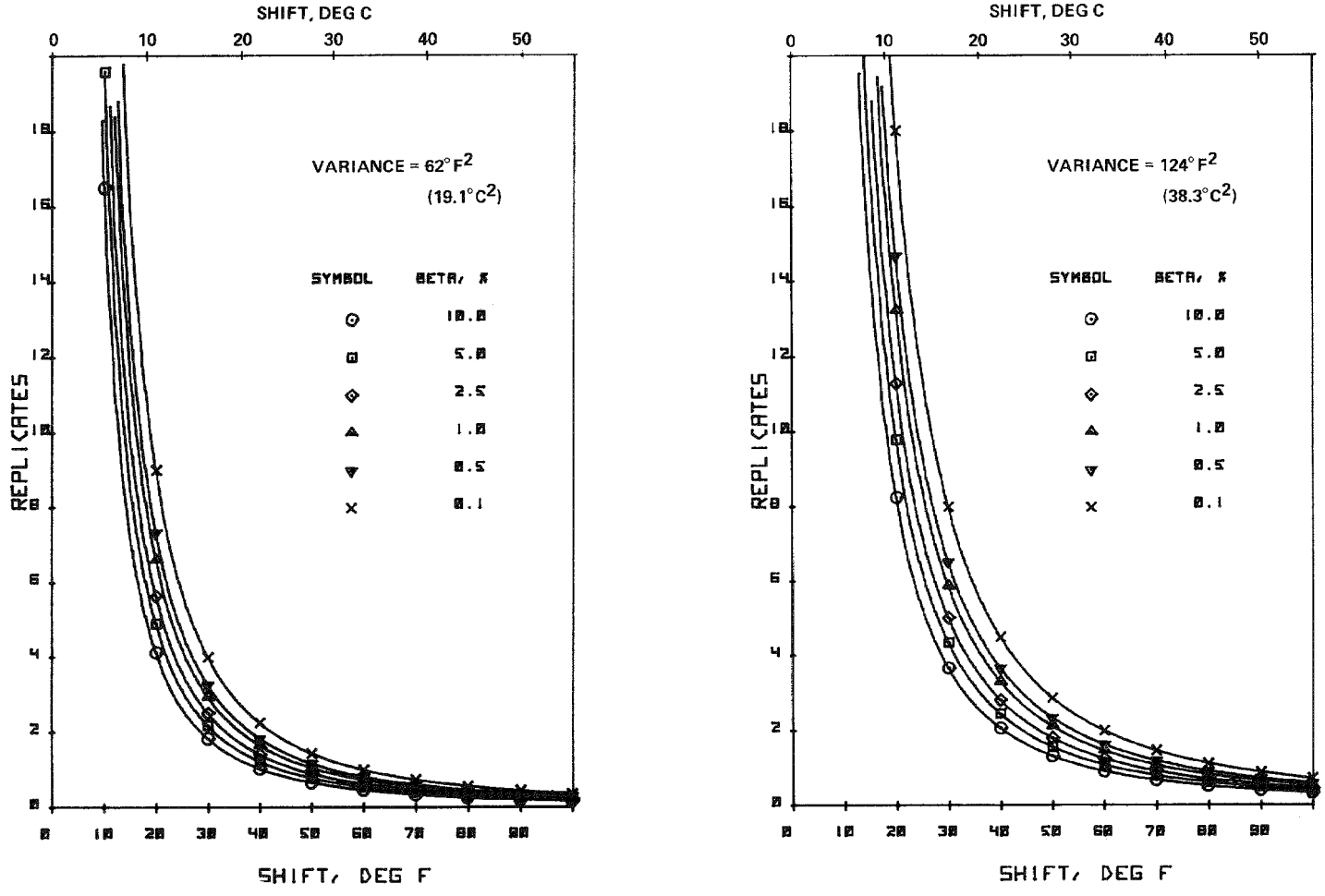

Figure 2-2. Size of the Charpy shift for unirradiated manual metal arc weld metal using (a) the real variance and (b) a two-fold increase in variance.

detect a shift of about 30°F (17°C). Similar tests using manual arc weld metal might detect shifts of about 62°F (34°C). Of course, the precision of the experimentation is increased if more curves are used in the comparisons.

Confounding and Balance

It is good experimental practice to measure important quantities without introducing bias through extraneous variables. When two quantities are irretrievably mixed in this way, they are said to be confounded. It is important not to confound the quantities being measured with extraneous variables. In irradiation experiments, two important sources of bias which might be confounded with the main effects are "between capsule" differences and "between positions in the capsule" variation. Techniques can be used to avoid these problems using reference standards and randomization procedures.

Confounding can also be used in a constructive fashion in statistical experimental design. Take as a starting point a factorial experiment in which every variable is studied at each level for each variable. The size of the experiment may be prohibitively large, and it will measure a number of effects (mainly interactions between the experimental variables) which might be relatively unimportant. By confounding, mixing unimportant comparisons together, the experiment size can be considerably reduced. In fact, the size is cut in half with each quantity confounded.

Properly designed experiments are characterized by their efficiency (as well as their freedom from bias). Two features contribute to this efficiency. First is the use of a balanced design, so that all measurements have more or less equal accuracy. It can easily be shown that a balanced design provides the greatest precision for a given number of tests. The second is the use of appropriate analytical techniques, such as analysis of variance procedures (13), to analyze the data.

If the objectives of an irradiation program are specified along with defined restrictions (α,β,δ), there is a matrix design which can provide optimum performance. By employing confounding techniques and fractional factorial designs, considerable gains in efficiency can be obtained. Comparisons made between properly designed irradiation experiments and conventional matrices reveal up to a four-fold increase in sensitivity.

As an example of a proper statistically-designed test matrix, a traditionally-designed irradiation test matrix was studied; this original matrix employed twelve capsules, eight materials, and two fluence levels. Instead of using the eight materials in an unbalanced, inefficient statistical array, a completely balanced study of six materials at two fluence levels utilizing the twelve available capsules is possible. This approach would provide compact, precracked Charpy, and Charpy V-notch data at both high and low fluences, providing a verification of the NRC Regulatory Guide 1.99 concept without being tied to the shortcoming imposed on the regulatory authorities by the paucity of experimental data. The matrix suggested is based upon a Latin Square and is shown in Table 2-1; this matrix allows complete capsule-to-capsule effects to be determined as well as material-to-material effects. Another alternative is also possible if four critical materials were studied instead of three fluence levels. An intermediate fluence level could prove valuable since the high and low fluence levels would generally be at the extremes of the needed information. Other options in design are also possible including confounding of the between-capsule variance and the between-heats variance by placing specimens from a single heat of each material in each capsule.

To further illustrate experimental statistical design, an experiment was designed for calibration of the equipment used in small specimen instrumented impact testing. A comparative experimental design was developed using a fully characterized and homogeneous 6061-T651 aluminum plate in which the operating procedure and instrumentation from different laboratories were evaluated (5,8). This aluminum round robin should reveal baseline information regarding experimental variability which can impose difficulties on eventual lower bound reference fracture envelopes. Details of this experiment are presented in Appendix A. It is clear from the analysis of the round robin data that there is an incentive to improve the calibration of the instrumented Charpy test.

COLLECTION AND QUALIFICATION OF DATA

An important aspect of any data base is that the data must be pedigreed. Since many of the test methods in use do not have ASTM Standards to follow, certain guidelines must be established for both collecting and analyzing data. The original RP232-1 test procedures (14) provided an initial attempt at establishing a tentative procedure for dynamic fracture toughness testing and elastic-plastic analysis.

Table 2-1

STATISTICAL EXPERIMENTAL DESIGN FOR TEST IRRADIATIONS

Capsule	Material	Fluence
1	A and B	Low
2	B and C	
⋮	⋮	
6	F and A	
7	A and B	High
8	B and C	
⋮	⋮	
12	F and A	

Considering capsules 1 and 2 as an experimental unit plus a capsule lay-out of about 6 compact (CS) and 14 Charpy-size spaces allows both Charpy (CV) and precracked Charpy (PC) curves to be developed.

	Capsule 1	Capsule 2
Material A	3 CS	3 CS
	14 CV	14 PC
Material B	3 CS	3 CS
	14 PC	14 CV

The existing EPRI procedures were simplified and revised to include current state-of-the-art techniques, particularly for elastic-plastic toughness testing (2,5,12). New data report forms were developed to assure that all pertinent data are recorded. Figure 2-3 shows a data record for a static compact fracture specimen test. A summary of the calculations and raw data required along with a list of definition of terms and symbols was included with each different data sheet (5); Appendix B of this report lists this information for the static compact test record shown in Figure 2-3.* Forms were developed (5) for the tensile test, Nil Ductility Transition Temperature (NDTT) test, instrumented Charpy V-Notch test, instrumented precracked bend test (both static and dynamic), and

*Note that SI units are used in the forms.

Compact Specimen Test Data Report

Identification

Laboratory FCC Test Date 9/13/76
Operator(s) [illegible] Specimen Code BBB-T22
Material A508-2 STEEL

Test Parameters

Electronic Response Time (T_R) = 3C μs Test Temperature (T) = 177 °C
Free Running Speed = 5.037 mm/s

Test Data

A. Post Fracture Specimen Photograph Attached
B. Graphs of Load-Time and Load-Displacement Records Attached
C. All Scales Identified on Test Records

Specimen Dimensions

Thickness (B) = 25.46 mm Crack Length (a) = 26.08 mm
Width (W) = 50.80 mm Ligament Area (A) = 629.9 mm²
Ligament Depth (b) = 24.72 mm

Test Results

Loads:
5% Secant (P_Q) = 42,700 N
Maximum (P_M) = 64,050 N
Yield Stress at ~ i (σ_Y) = 443 MPa
Flow Stress at ~ i (σ_{fl}) = 517 MPa
Strength Ratio (R_σ) = —

Times:
t_Q = 71 x 10³ ms
t_M = 178 x 10³ ms
P_M/P_Q = 1.50
Conditional Toughness (K_Q) = — MN-m$^{-3/2}$
J-Integral Value (J_M) = 420.4 kJ/m²

Stress Intensity Factor (K_{IC} or K_Q) = 288 MN-m$^{-3/2}$
Stress Intensification Rate (K̇) = 1.6 MN-m$^{-3/2}$/s
$2.5(K_Q/\sigma_Y)^2$ = — mm $50(J_M/\sigma_{fl})$ = 40.1 mm
t_Q/T_R = 2.4 x 10⁹ $0.5\delta(J_M/\sigma_{fl})$ = 0.45 mm
Acceptable Test? YES Fracture Initiation Mode FIBROUS
Remarks INTERRUPTED TEST & HEAT-TINTED (R-CURVE)
Δā FROM THREE-POINT AVERAGE = 1.26 mm

FCC.CS Jun 77

Fatigue Precracking

Conditions:
Relative Humidity = 51 %
Temperature = 24 °C
Stress Intensity Factor (K_f)
Maximum = 24.1 MN-m$^{-3/2}$
Last 2.5% of δ = 14.8 MN-m$^{-3/2}$

Number of Cycles = [illegible]
Notch: Depth (a_n) = 21.41 mm
Radius (ρ) = 0.13 mm
Other —
Fatigue Crack Extension ($\bar{a}a_0$) = 4.67 mm

Crack Length:
a(¼B) = 25.91 mm
a(½B) = 26.14 mm
a(¾B) = 26.09 mm
Average (ā) = 26.08 mm

a(Surface 1) = 24.46 mm
a(Surface 2) = 24.69 mm

Acceptable Precrack? YES
Remarks —

Fibrous Crack Extension

S1 = 0.18 mm
1/8 B = 0.31 mm
1/4 B = 0.47 mm
3/8 B = 1.85 mm
1/2 B = 2.64 mm
5/8 B = 1.65 mm
3/4 B = 0.86 mm
7/8 B = 0.32 mm
S2 = 0.10 mm
Average (Δā) = 0.91 mm

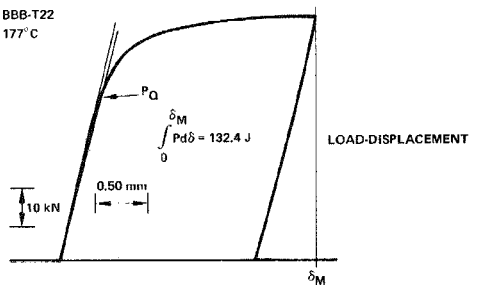

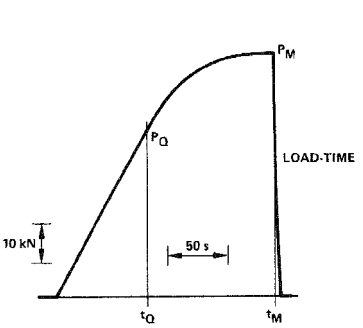

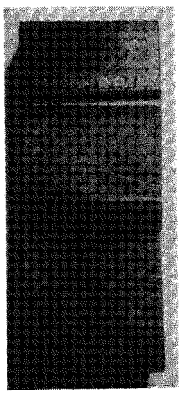

Figure 2-3. Elastic-plastic interrupted static compact test record.

compact specimen test (both static and dynamic). These data forms are available from EPRI as masters.

The development of a radiation embrittlement data base also requires the characterization of the radiation environment through a proper irradiation analysis. A detailed review of the magnitude and sources of dosimetry uncertainties associated with past radiation embrittlement studies was presented in Reference (5), and specific recommendations were made to significantly reduce these uncertainties in future programs. Conclusions from this study are presented later in Section 3. Data forms for extracting the necessary radiation environment data from past programs were developed in another program, RP1240-1 (11).

One of the less obvious but important features of our work has been related to the unirradiated EPRI data base. Considerable effort was expended into the consolidation and clarification of the data base to form the basis for a future irradiated data base. The original EPRI data base was finalized at the end of 1975, and the results were printed in a two volume (three part) report (1). A second data base also existed for the control material round robin program (on HSST Plate 02) performed at the beginning of the RP232 program (15). An adjunct program on high temperature gas-cooled reactor (HTGR) steels was also conducted and a third separate data base established (16). At the time the data were generated (1974-75), techniques for elastic-plastic fracture mechanics were unsettled, and maximum load was used as a fracture initiation point (even though it was recognized that maximum load was a non-conservative estimate of initiation). Also, procedures for dynamic servo-hydraulic machine testing and instrumented impact testing were developed (14) and tested (17,18) without having established ASTM guidelines.

Since the time of the data generation effort by the three laboratories involved (Combustion Engineering, Babcock and Wilcox, and Effects Technology) (19-21), additional research, with respect to dynamic experimental procedures has produced revised criteria for acceptable testing and analysis (5,12). Also, additional research with respect to fibrous crack growth (2,22,23) has produced upper shelf initiation data for selected steels from the original RP232 programs. Furthermore, the understanding of the relationship between specimen size and the validity of the test results has improved (24).

The above comments make it clear that there was a need to update the original EPRI data base report (1). A comprehensive loose-leaf (revisable) topical

report was therefore written (9).* As part of this topical report, the entire data base of fracture toughness data (including over 1,100 precracked Charpy results) was reanalyzed with respect to the following changes:

- Initiation or maximum load (equivalent energy) toughness values were separated.
- An elastic-plastic size criterion was applied to the appropriate data; third order polynomial regressions to the tensile data were performed to evaluate this criterion.
- Revised acceptance criteria with respect to specimen precrack length and dynamic loading were applied.
- All precracked Charpy curves were refit using the latest non-linear regression scheme and the complete statistics related to the curve fits were stored in the data base.
- The proper calculation for the J-integral were performed for the compact specimens (which includes the tensile-axial components as well as the bending component).
- Upper shelf, multi-specimen, initiation data were reanalyzed using a linear regression to the J-crack extension results.

In addition to expanding and updating the data base, a great deal of software had to be developed to serve the new data base. Since all the entries (records) in the base are unambiguously identified by a set of up to eight numbers termed keywords, the software deals with many tasks and is able to enter all groups of data within the base and select from it predetermined sets of data on the basis of the keywords. One task is obviously that of simply extracting, printing, and perhaps plotting specified groups of data. Another task is curve fitting or regression analysis; a major effort has related to fitting sigmoidal (tanh function) curves to impact and fracture toughness data. Much of the software relates to statistical analysis. This software package is written mainly in FORTRAN (some minor programs are in BASIC) and is portable to that extent. However, because the package is obviously related to the hardware environment used for the data base, it is to that degree specific to our system. For example, the data base is accessed by calls to the computer operating system which read specified disk files.

The details of the design have evolved with time and much use. Several groupings of data are used as follows:

*This data base report can be obtained from EPRI as Report NP-933.

- General information, such as fabrication history and manufacturer, related to the materials
- Chemical analyses and specific, heat-related, mechanical properties data
- Mechanical properties (tensile, Charpy V-notch, fracture toughness, and NDTT test data)
- Sigmoidal (tanh) curve fit data for impact and fracture toughness results and associated statistics (residual variance together with the variances and covariances of the parameters)
- Regression curves fitted to the tensile stress data and associated statistics.

Each grouping of data may be contained in several files to facilitate access. For example, a separate file is used for the mechanical properties data for each test type. Within each file, the basic entry is a record which is identified by keywords. Except for the general information group, all records are arranged as a single line of data beginning with the keywords, followed by information such as test temperature, impact energy, lateral expansion and so on in a specified order. Details of this design are given in Reference (9). However, to give the reader an idea of the type and format of the data in the current EPRI data base, several examples of the graphical data are illustrated here. Figure 2-4 shows the type of tensile data available and the graphical format for reporting it. Figure 2-5 shows the data output for V-notch and precracked Charpy tests. All of the available fracture toughness data for a given heat are reported in the format shown in Figure 2-6. Note that the NDTT and RT_{NDT} temperatures are indicated in each figure. Please refer to Reference (9) for a more detailed explanation of these figures.

REFERENCE FRACTURE TOUGHNESS CURVE DEVELOPMENT

The initial work in this area centered on the various philosophies underlying the reference curve concept. This study included: the test data used to normalize the toughness data (Charpy V-notch or precracked Charpy), the use of one stress intensity rate or a combination of loading rates over the full temperature range of interest, and the use of lower bound or mean curves. With regard to more than one loading rate, a limited examination of the EPRI data base revealed four items of interest when considering an overall lower bound:

- In the lower shelf the toughness is independent of loading rate.
- In the transition temperature regime, the dynamic data are lower than the static, and larger section size tends to dictate lower results. This effect is probably due to a Weibull distribution sampling effect.

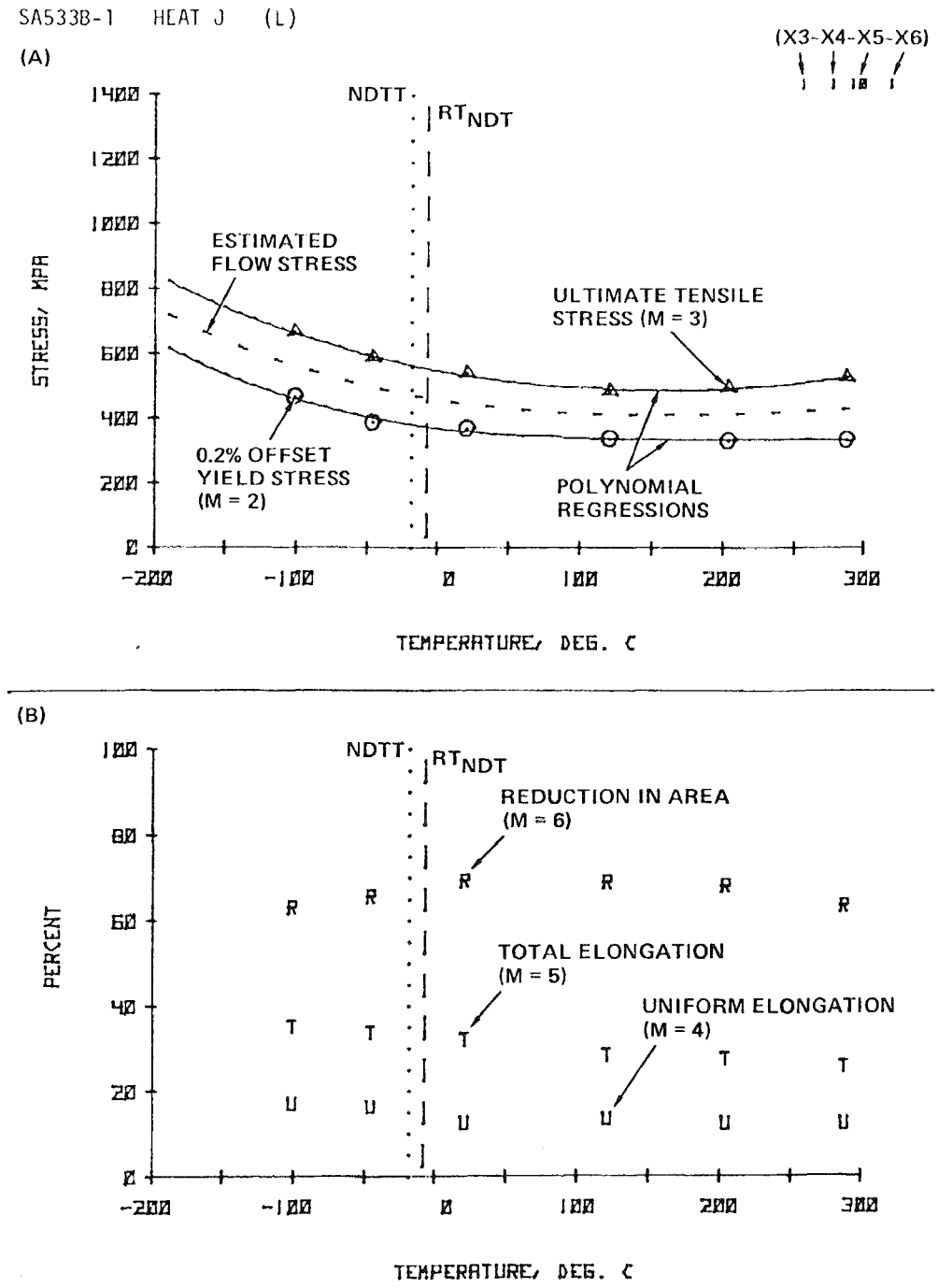

Figure 2-4. Tensile results for heat J, SA533B-1 base metal.

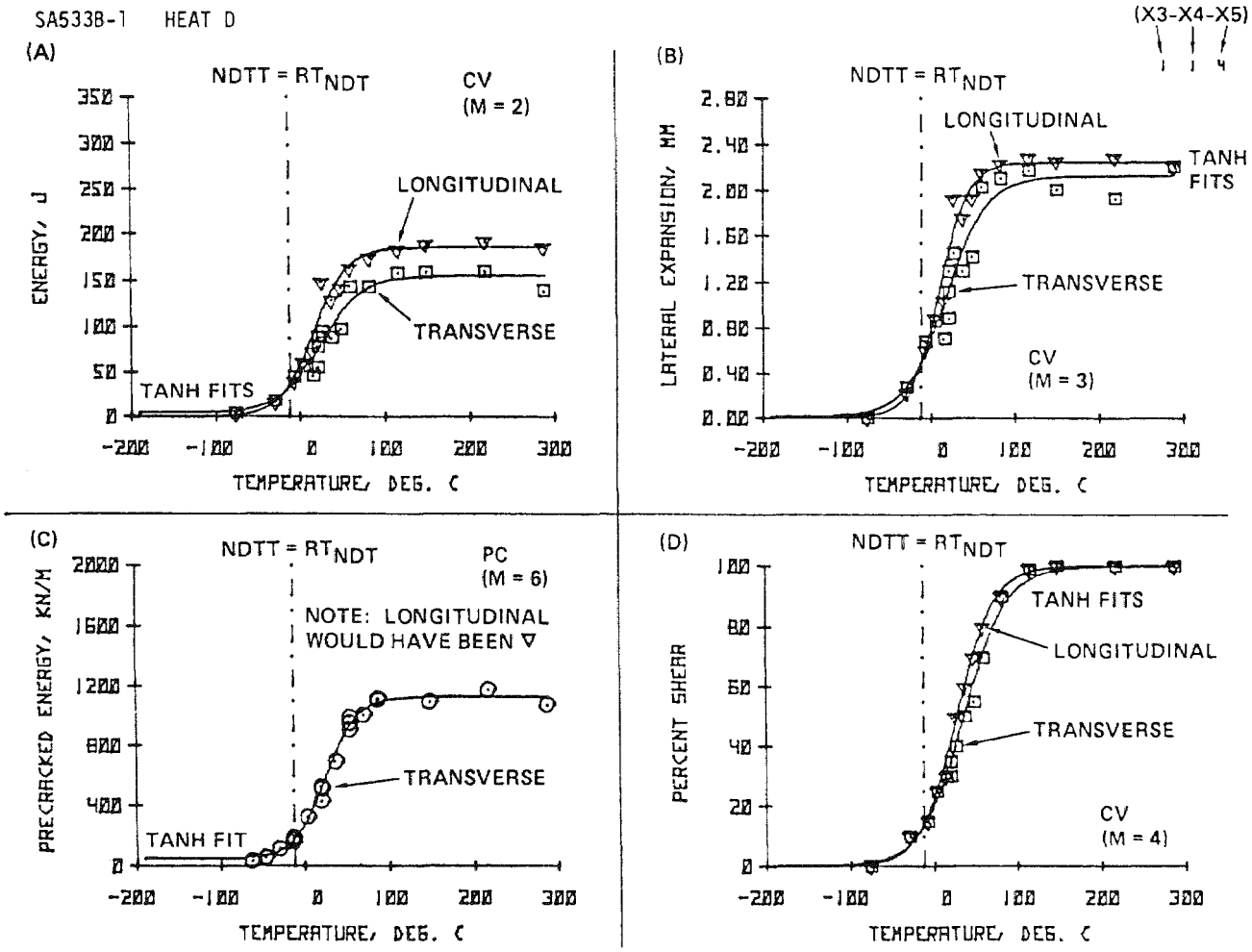

Figure 2-5. Charpy V-Notch and precracked Charpy normalized energy for heat D, SA533B-1 base metal.

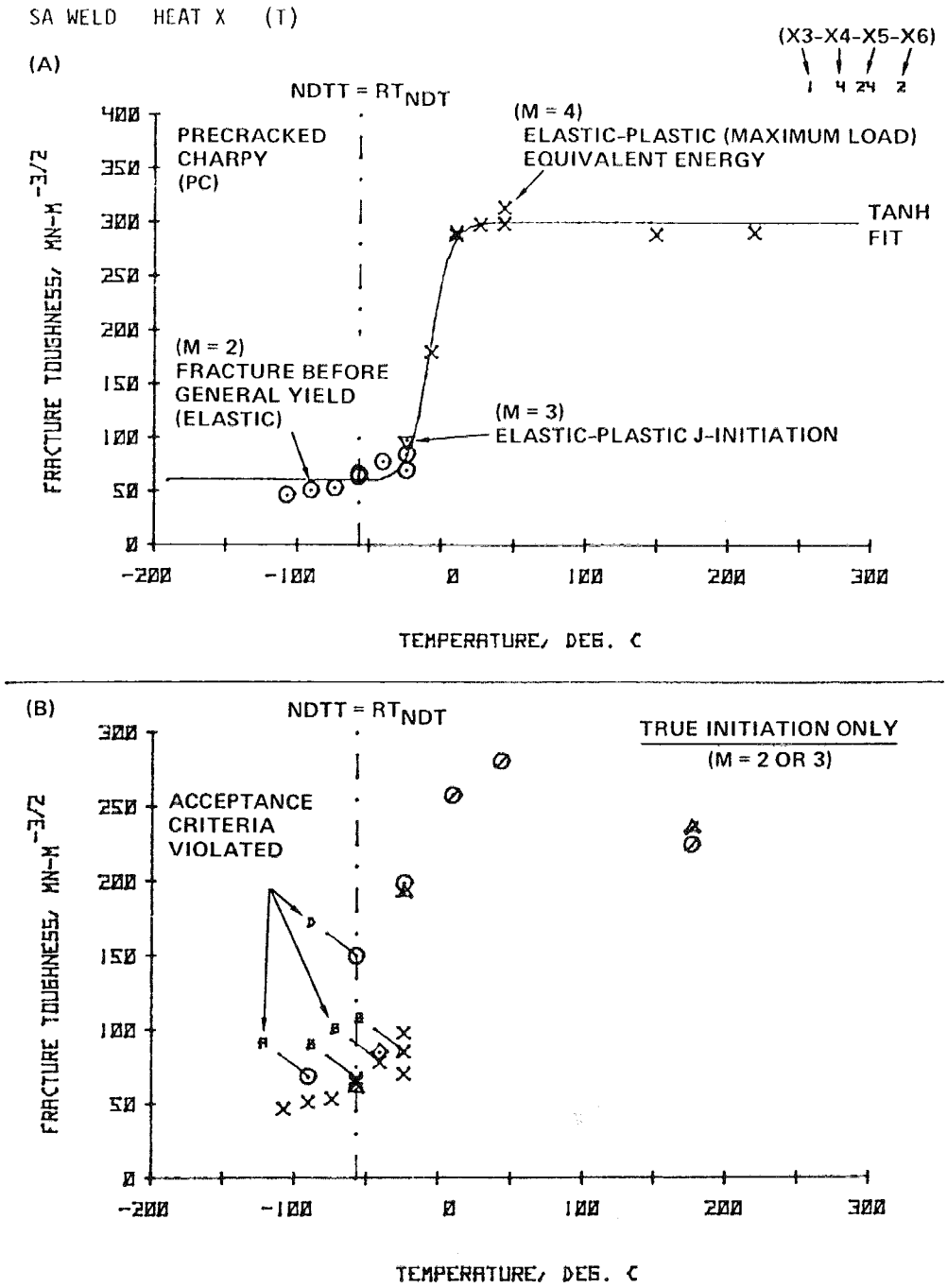

Figure 2-6. Fracture toughness results plotted for precracked Charpy tests and large specimen initiation tests for heat X, submerged arc weld metal (SA533B-1 base).

- At the upper shelf, the dynamic toughness is not the most conservative (22). A change in behavior occurs near the start of the upper shelf which can be attributed to a change in fracture mode.

- The change in mode from cleavage to all fibrous fracture in the Charpy V-notch test occurs at a temperature very near the initiation fracture mode change for the dynamic fracture toughness tests; the static fracture toughness mode change occurs at only a slightly lower temperature. This item reflects the ability to choose the type of test to run relative to the measured Charpy V-notch properties.

These observations indicate the need to consider more than one loading rate when developing an overall physical lower bound for the full temperature range including the upper shelf.

In the RP696-1 program (2), the use of the curve fit parameters from instrumented precracked Charpy toughness data was developed as an alternate referencing procedure (25) to the RT_{NDT} concept. The *tanh* parameter referencing technique was extended in this program to use Charpy V-notch (CVN) energy data which are more readily available for irradiated materials.

Using the revised data base and working in collaboration with a PVRC/MPC Committee, W. Oldfield, under this and other contracts,* has been working to develop the new referencing procedures into practical procedures for possible incorporation into the ASME Codes. Several major developments have occurred out of this work. It was found that the upper shelf had to be referenced in some way when upper shelf initiation data became available through J-integral R-curve work. Otherwise, the predicted toughness bounds would be too low to be useful. Additionally, CVN energy does not have the same dimensions as fracture toughness, so it cannot be used directly to reference toughness (6). The problem was overcome by using a correlation approach, and a reference curve is viewed as simply one form of correlation. It proved to be possible to predict mean toughness, a confidence bound on the mean, or a tolerance bound. Weighted regression procedures were developed to account for changes in variance with position on the curve.

Another development came with the realization that the quality of the referencing procedure needed to be controlled more closely than we had expected. For example, a referencing test cannot reference the lower shelf with adequate precision. This led to the conclusion that, in a practical scheme, there must be alternative approaches which can be used to set bounds when the referencing procedure is not adequate.

*Originally under TPS77-752 and later under RP1021-4 (10).

One of the tools which has proved invaluable in our work is the tanh curve-fit procedure (26). The tanh function is

$$K = A + B \tanh\left[\frac{T - T_0}{C}\right] \qquad (2\text{-}1)$$

where K is toughness, T is temperature, and A, B, T_0, and C are curve fit parameters. Widespread interest has resulted in the development of alternative procedures, partially to correct defects in the form of the tanh method as it was first presented, but which have been removed during this program. To remove confusion, the available published methods have been compared and critically reviewed (27).

To briefly review the new reference curve approach, we shall begin with the precracked Charpy (PCVN) referencing method. It was clear from prior work (25) that an ideal referencing scheme would use four referencing quantities; these quantities would reference the position and the spread of fracture toughness and temperature. Refering to the coefficients in Eq. 2-1, it became clear that A references the position, and B the range of fracture toughness (A is the toughness midway between the shelves, and B is the $\pm$ deviation of the shelves from the midpoint). Similarly, T_0 and C reference the position and range of the transition in the temperature scale. Using the coefficients developed by fitting Eq. 2-1 to PCVN data, referencing can be performed as follows:

$$\text{normalized toughness} = \frac{K - A}{B} \qquad (2\text{-}2)$$

and

$$\text{normalized temperature} = \frac{T - T_0}{C} \quad . \qquad (2\text{-}3)$$

The toughness data from the EPRI programs (9) were then referenced (normalized) by means of the PCVN results for each heat. In this way, reference curves were developed for three types of fracture toughness tests (static and dynamic compact and dynamic bend) using a substantial number of fracture toughness results for each curve. An equation of the form of Eq. 2-1 was fitted to the referenced results, and a piecewise (based on temperature ranges) prediction limit was developed (2). This prediction limit is a bound in which a single future result

might transgress with a stated probability. However, the piecewise prediction limit method was cumbersome and could hardly be termed a practical method. Furthermore, the piecewise statistical bound was technically inappropriate, since it assumed that the position of the mean curve was known exactly.

Working with the ASME Section XI Flaw Evaluation Working Group (and later an MPC/PVRC Committee), we therefore proceeded to give the approach a more practical aspect. The statistical problems were treated first. A weighted non-linear regression scheme was developed which was capable of resolving most of the statistical objections. Next, the statistical bounds to the mean curve were developed, and approximated by Eq. 2-1 (but with different coefficients termed A', B', T_o', and C'). The coefficients can be readily shown to be measures of the bias between the referencing test and the bound. It can be further shown that:

$$\left.\begin{aligned} A &= A + B \cdot A' \\ b &= B \cdot B' \\ t_o &= T_o + C \cdot T_o' \\ c &= C \cdot C' \end{aligned}\right\} \qquad (2\text{-}4)$$

where the desired bound is defined by:

$$K = a + b \cdot \tanh\left[\frac{T - t_o}{c}\right] . \qquad (2\text{-}5)$$

Eq. 2-5 conveniently defines the specific bounding curve to fracture toughness as a function of temperature (28).

Examples of the application of the precracked Charpy referencing technique are shown in the next two figures. Figure 2-7 shows all of the fracture toughness data from static compact fracture tests normalized for toughness (Eq. 2-2) and temperature (Eq. 2-3). The mean to the PCVN referenced data is shown as the upper solid line. The global tolerance bound fitted to the data is shown as a dashed line. This global bound represents a line for which we are 90% confident that 90% of all future measurements will fail above the line; we refer to this confidence level as 90/90. For convenience, the bound was approximated by a tanh function (solid line). The tanh coefficients to the bound are termed A', B_o', T' and C' , as in Eq. 2-4. Figure 2-8 shows the use of the PCVN

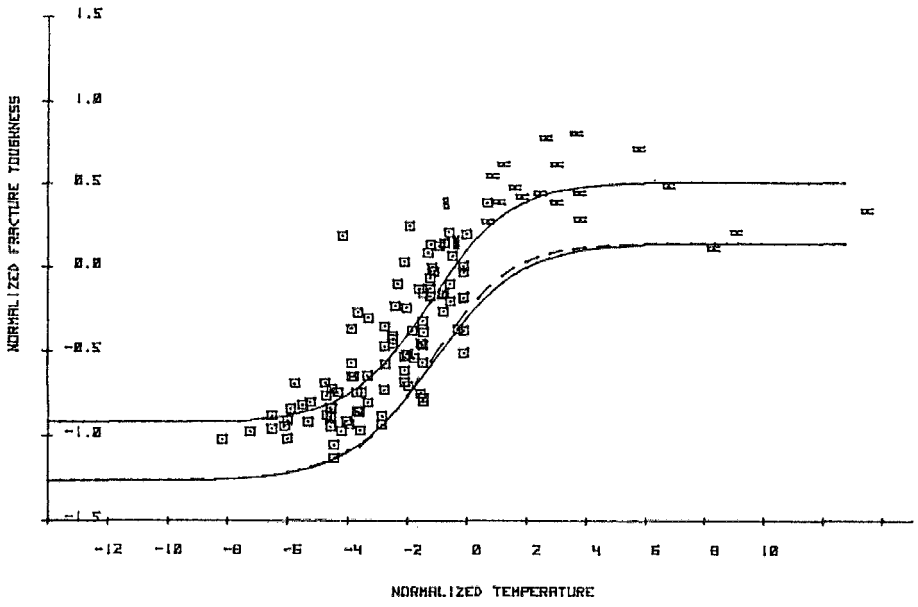

Figure 2-7. Precracked Charpy normalized static compact fracture data.

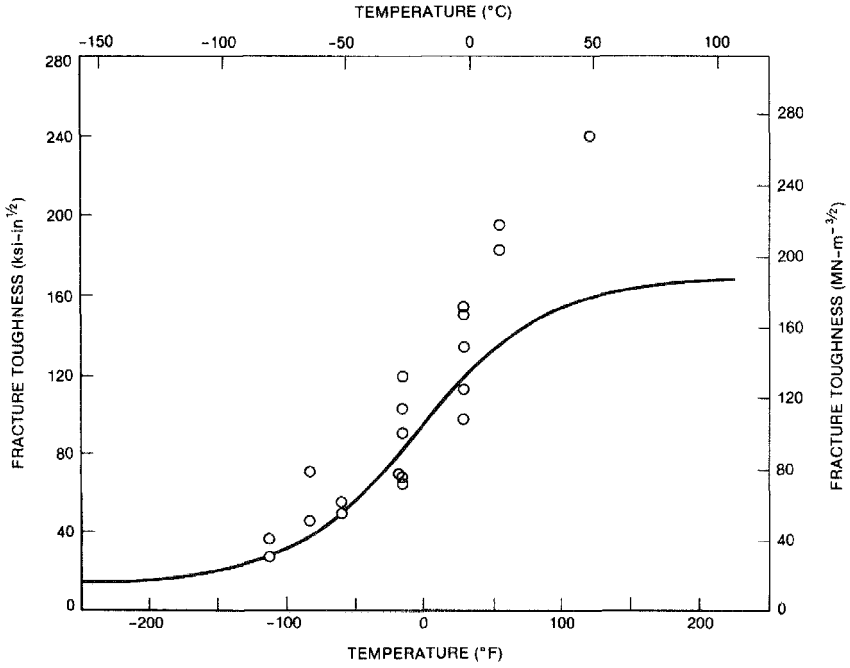

Figure 2-8. Comparison of static compact data for a heat of SA533B-1 steel with predicted 90/90 global tolerance bound using PCVN method.

referencing technique to obtain a lower bound (90/90) static fracture toughness curve for a single heat of SA533B-1 steel arbitrarily selected from the EPRI data base (9). The precracked Charpy dynamic fracture toughness temperature data for this heat were fitted by a tanh function to generate A, B, T_0 and C. These parameters, along with the primed coefficients, were used in Eq. 2-4 to generate the a, b, t_0 and c tanh coefficients which describe the global bound curve in Figure 2-8. Although some data are below the bound shown in Figure 2-8, this would be expected for a 90% tolerance bound. It could be essentially avoided by the use of a stricter bound such as the 99.9%.

The simplification in the referencing technique illustrated by Eqs. 2-4 and 2-5 allowed further steps to be made in the development of a practical and useful referencing scheme. With this approach, the mathematical treatment was available by which any suitable test could be properly referenced to fracture toughness to give a reference curve. The next development illustrates this development. The Charpy V-notch test (CVN) is the most widely used correlative procedure for estimating fracture toughness. So-called correlations are commonly used to reference certain features of the test results to such features as upper shelf toughness or the transition temperature. These correlations are actually referencing procedures which deal with specific portions of the fracture toughness reference curve. Our approach generalizes such correlations and combines them over the total temperature regime. Using the quantity k, defined as:

$$k = (CVN \cdot E)^{1/2} \quad , \tag{2-6}$$

where CVN is the Charpy V-notch energy and E is the modulus of elasticity, the dimensions (in dimensional analysis) become the same as fracture toughness for a specimen of fixed cross section area. By fitting k values for a range of temperatures to the tanh function (Eq. 2-1), four referencing quantities A_k, B_k, $T_{o(k)}$, and C_k can be developed. A set of numerical constants (C_1, C_2, C_3, C_4) relates these to coefficients of similar numerical values for the PCVN reference parameters:

$$\left.\begin{aligned} A &= A_k \cdot C_1 \\ B &= B_k \cdot C_2 \\ T_o &= T_{o(k)} \cdot C_3 \\ C &= C_k \cdot C_4 \end{aligned}\right\} \qquad (2\text{-}7)$$

These quantities were then used to reference the fracture toughness data from the EPRI programs (9). Using a similar analysis to that for the PCVN reference curve, new reference curves were then generated based upon CVN. However, the analysis was carried through to develop sets of bias coefficients which related CVN curves directly to the mean fracture toughness together with the confidence bound and tolerance bound (29). These results are listed in Table 2-2. For example, using the relationship for the lower tolerance bound to fracture toughness measured by dynamic bend tests; Charpy V-notch data for a heat of SA302B material (ASTM surveillance reference heat) were converted to k values using Eq. 2-6, then fitted by a tanh function to generate A_k, B_k, $T_{o(k)}$ and C_k values. These tanh values were then used in the appropriate Table 2-2 expressions to generate (predict) a tolerance bound for dynamic fracture toughness obtained from 1-in (25.4 mm) bend tests. Figure 2-9 compares actual test data with the predicted 90-90 tolerance bound.

At this stage, the analyses have accomplished the majority of the original goals. However, some drawbacks of a practical nature remain. Current work (10) is designed to remove these drawbacks. One major problem relates to the lower shelf. Many sets of Charpy data have too few points at low temperature to properly define the lower shelf position. Also, the distribution of data is skewed high in this region while the statistical analyses generally assume a non-skewed distribution. We propose to remedy both these defects by having a floor on the lower shelf. That is, since the shelf position is fairly uniform for all materials, a non-referenced bound will be determined. This bound will be taken as a minimum which will apply if the referenced curve predicts lower values. Similarly, it is felt that the price in terms of complexity of using k instead of energy data may be too great. If CVN energy is used directly without correction for the changes in modulus with temperature, errors of about 10% may be introduced, which might be acceptable. These possibilities are being explored.

Table 2-2

CVN REFERENCE CURVE COEFFICIENTS

$\dot{K}$ ksi-in$^{1/2}$/s ($MN\text{-}m^{-3/2}/s$)	Mean	90% Confidence Limit	90-90 Tolerance Bound
"Static;" 3×10^0	$a = 0.0440\ B_k + 43.0$	$0.0406\ B_k + 43.0$	$0.0266\ B_k + 43.0$
(3.3×10^0)	$b = 0.0373\ B_k$	$0.0371\ B_k$	$0.0335\ B_k$
	$t_o = T_{o(k)} + 29.3 - 0.676\ C_k$	$T_{o(k)} + 29.3 - 0.602\ C_k$	$T_{o(k)} + 29.3 - 0.672\ C_k$
	$c = 1.10\ C_k$	$1.15\ C_k$	$1.19\ C_k$
"Dynamic;" 3×10^3	$a = 0.0405\ B_k + 43.0$	$0.0380\ B_k + 43.0$	$0.0279\ B_k + 43.0$
(3.3×10^3)	$b = 0.043\ B_k$	$0.0425\ B$	$0.0379\ B_k$
	$t_o = T_{o(k)} + 29.3 - 0.174\ C_k$	$T_{o(k)} + 29.3 - 0.119\ C_k$	$T_{o(k)} + 29.3 - 0.0831\ C_k$
	$c = 1.22\ C_k$	$1.25\ C_k$	$1.31\ C_k$
"Impact;" 2×10^5	$a = 0.0446\ B_k + 43.0$	$0.0431\ B_k + 43.0$	$0.0314\ B_k + 43.0$
(2.2×10^5)	$b = 0.0465\ B_k$	$0.0455\ B_k$	$0.410\ B_k$
	$t_o = T_{o(k)} + 29.3 + 0.578\ C_k$	$T_{o(k)} + 29.3 + 0.637\ C_k$	$T_{o(k)} + 29.3 + 0.665\ C_k$
	$c = 1.207\ C_k$	$1.17\ C_k$	$1.22\ C_k$

Similarly, scanty or excessively variable referencing data might still be acceptable, with some penalty incurred in the position of the bounds.

PRELIMINARY ANALYSIS OF RP886-2 DATA

Unirradiated and irradiated Charpy V-notch and precracked Charpy data from the EPRI program RP886-2 at Naval Research Laboratory (NRL) were digitized from NRL graphs (30). The digitized values were stored on a disc file, later plotted and tanh functions (Eq. 2-1) were fitted (8). Additionally, the Charpy V-notch energy data (CVN) were transformed to estimates of fracture toughness using the procedures discussed in the previous subsection. The transformed quantities of k, when fitted to Eq. 2-1, allowed the prediction of fracture toughness in the irradiated condition. Since the NRL irradiation program did not utilize an efficient statistical design, the reference curve procedures should provide the best possible technique for analysis of the irradiated data. The best prediction of fracture toughness based upon the CVN data are compared to measured fracture toughness results (30) in Figure 2-10. The results from two capsules for the same SA533B-1 steel are combined since they underwent similar irradiation treatment, and as might be expected, the CVN data were quite similar. The results in Figure 2-10 suggest that the data are somewhat more scattered than unirradiated measurements; this fact is not to be unexpected.

The functional behavior indicated in Figure 2-10 forms an interesting contrast to the apparent slope of the data and the NRL interpretation (30) in which they showed the fracture toughness-temperature relationship passing close to the data points with a subsequent steep transition slope. The prediction results here give an interpretation more consistent with the original unirradiated behavior (i.e., the irradiated curve transition slope is decreased due to the neutron embrittlement and in accordance with the irradiated CVN results). The small temperature range and scatter of the actual toughness data possibly prevents the true slope from being ascertained.

Further improvements in the CVN transformation/normalization reference curve procedure as applied to irradiated data are currently being made under EPRI contract RP1021-4 (10). These procedures will hopefully be implemented in future revisions of the ASME Codes.

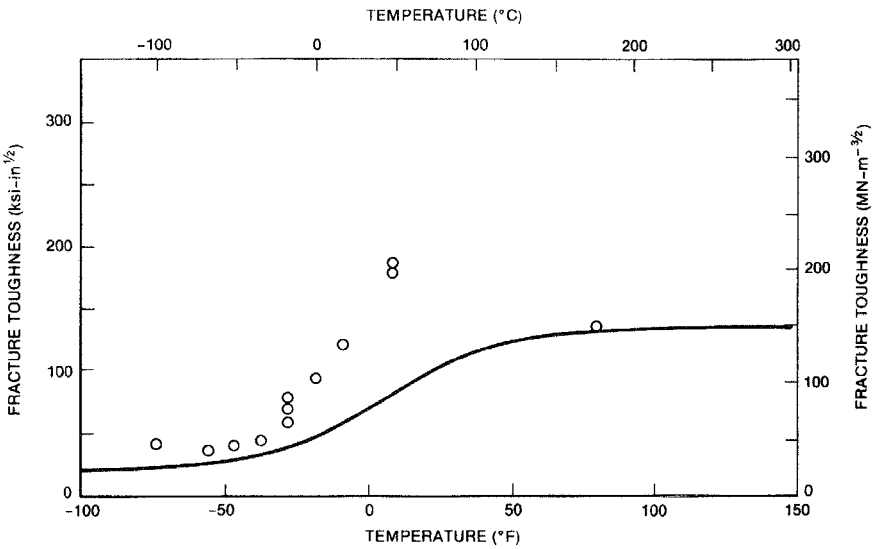

Figure 2-9. Comparison of dynamic bend data for a heat of SA302B steel with predicted 90/90 global tolerance bound using CVN method.

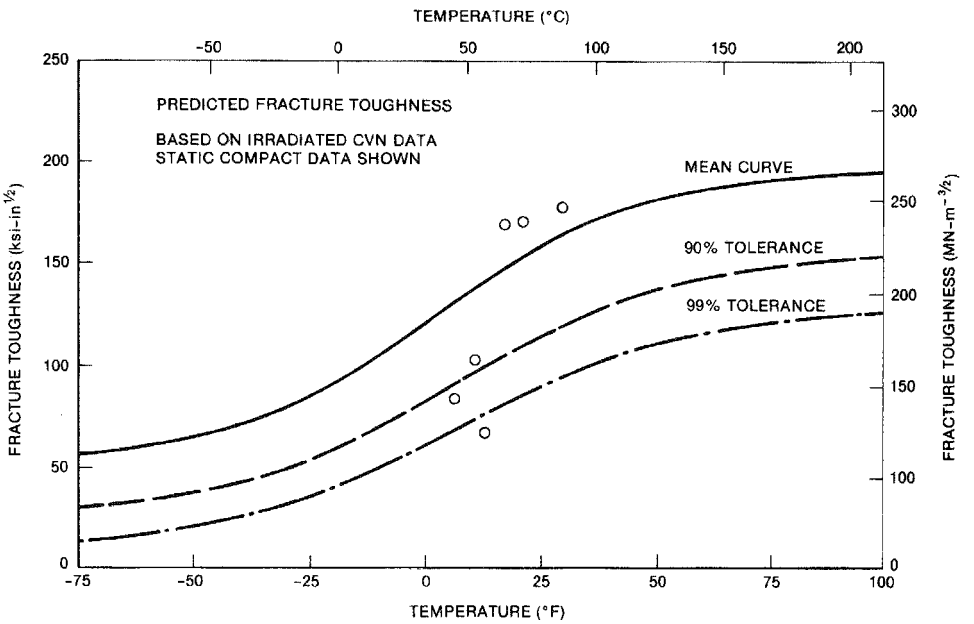

Figure 2-10. Comparison of static fracture toughness data of irradiated SA533B-1 steel from two NRL capsules with CVN predictions.

Section 3

TASK II

FRACTURE TOUGHNESS DATA FROM SURVEILLANCE SPECIMENS*

INTRODUCTION

Nuclear pressure vessel steels commonly used in the reactor beltline area are susceptible to neutron irradiation damage. This damage results in a degradation in toughness properties which can reduce the operability of the reactor vessel. Accordingly, reactor surveillance programs have been devised to periodically monitor irradiation embrittlement, thus allowing critical calculations of the future lifetime of the reactor vessel and its heat-up and cool-down pressurization schedules to be made. Limitations in reactor core space and the expense of irradiating large numbers of surveillance specimens have led to the use of test pieces of Charpy-size dimensions, i.e., 0.394 in (10 mm) square bend bars. Unfortunately, the measurement of fracture toughness at or near operating temperatures requires either exorbitantly large test pieces (thicknesses often in excess of the actual vessel thickness are required to obtain a "valid" ASTM E399 plane strain K_{Ic} toughness value) or costly single and multi-specimen procedures still utilizing larger than 0.394 in (10 mm) dimension specimens [see the proposed ASTM standard for J_{Ic} measurement using a resistance (R) curve approach] (24).

The objective of this task is to develop simple, inexpensive, small-specimen techniques for estimating fracture toughness for possible utilization in future reactor surveillance programs. The importance of ascertaining toughness is especially important where failure occurs beyond general yield by a ductile rupture (microvoid coalescence) mechanism. Two ferritic low strength steels were examined, namely the currently-used nuclear pressure vessel steel, SA533B Class 1 [HSST Plate 02, termed 1bA in the EPRI data base (9)], and the formerly-used material, SA302B (Surveillance Correlation Heat, 4bA in the data base), both in the unirradiated condition. Additionally, some tests were performed using a

*Contributions by W.L. Server, R.A. Wullaert, J.W. Sheckherd, and P.E. McConnell (Fracture Control Corporation), R.O. Ritchie (Massachusetts Institute of Technology), J.S. Perrin, E.O. Fromm, B.D. Trott, and D. Hauser (Battelle Columbus Laboratories), and G.E. Lucas and D. Greenslade (University of California, Santa Barbara).

submerged arc weld metal (1sX in the EPRI data base). Testing was performed under quasi-static and dynamic conditions at temperatures corresponding to the full range of lower shelf, transition, and upper shelf behavior. Extensive data already existed for the three materials studied (9).

The results obtained in this task can be categorized into five areas: (1) single specimen fibrous initiation for static and dynamic loading, (2) critical fracture stress and strain model predictions, (3) other approaches to maximize Charpy-type data, (4) development of surrogate materials, and (5) reconstituted surveillance specimens. Highlights of the major accomplishments in these areas are described next.

SINGLE SPECIMEN FIBROUS INITIATION FOR STATIC AND DYNAMIC LOADING

Due to the fact that initiation does not generally correspond to maximum load for fibrous fracture on the upper shelf, a testing technique was developed in the RP696-1 program (2,22) for determining the dynamic initiation value for ductile fracture. This technique was patterned after the existing ASTM work being performed under static loading (24), and utilized a multi-specimen, controlled displacement procedure for obtaining initiation. Briefly, a vertical drop tower impact machine was used in which hardened steel deflection stops were used to stop the falling impact head at different amounts of specimen deflection. When the impacting tup struck the deflection blocks, a sudden increase in the load signal occurred, marking the stopping event. After loading, each of the 6-8 specimens was heat-tinted at 550°F (288°C) for 15-30 minutes. The specimens were then broken apart at -95°F (-70°C) to reveal the extent of fibrous crack growth. The amount of crack growth (Δa) was measured for each specimen using the maximum growth reading and 3-point and 9-point averaging (Δa_{max}, $\Delta \bar{a}_3$, $\Delta \bar{a}_9$, respectively). J-values were calculated for the three-point bend tests at the point of hitting the deflection stops in the same manner as conventional tests to maximum load were calculated. The J_{Ic} values were determined by the intersection of the J versus Δa straight line fit with the blunting line defined as

$$J = 2\sigma_F \Delta a \quad . \tag{3-1}$$

The values of flow stress, σ_F, for impact tests were estimated from instrumented Charpy V-notch data in a similar manner as impact yield strength values are determined (31), except that a mean between maximum and general yield loads was used in the calculation.

Figure 3-1 shows the dynamic initiation J_{Ic} results for a heat of SA302B steel. It is evident that the three different methods of measuring crack growth (Δa_{max}, $\Delta\bar{a}_3$, and $\Delta\bar{a}_9$) result in markedly different crack growth values due to the sharp curvature of the fibrous crack front. Although this difference has little influence on the J_{Ic} value, the slope of the J-crack growth curves ($dJ/d\Delta a$), and hence the tearing modulus T_J (32),

$$T_J = dJ/d\Delta a \cdot E/\sigma_F^2 \quad , \tag{3-2}$$

where E is Young's Modulus, is substantially changed. It was found that the upper shelf dynamic initiation toughness was almost always higher than static toughness for pressure vessel plates, forgings, and weld metals (22). Logsdon (33) has reported similar results for similar pressure vessel steel plates and forgings.

The problem with the multi-specimen initiation technique is that it requires 6 to 8 specimens and is thus impractical for use with a limited number of irradiated surveillance specimens. Preliminary work was also performed using the single-specimen unloading compliance method for determining J_{Ic} ; this method does work once experimental and interpretation problems are reduced (34), but the technique is only applicable to quasi-static loading and generally to specimens larger than Charpy dimensions (24). Therefore, a simple, inexpensive test technique was needed (7,8,35,36) for determining J-initiation on the upper shelf for both static and dynamic loading using a single, small specimen. Following the work of Green and Knott (37) for mild steel, precracked Charpy specimens were side-grooved, forcing fibrous initiation to occur nearer to maximum load. Figure 3-2 schematically illustrates this effect and shows the procedure for estimating J_{Ic}.

Results for standard size precracked Charpy pieces [original thickness, B , equal to 0.394 in (10 mm)] and over-sized precracked Charpy bars [remaining net thickness, B_o , equal to 0.394 in (10 mm)] are shown in Figures 3-3 and 3-4 for dynamic and static loading. It appears that with a 30% side-groove depth (15% on each side), a conservative, yet accurate, value of J_{Ic} (and thus K_{Jc}) may be determined from a single specimen simply through the measurement of test piece dimensions and maximum load specimen energy. As indicated in Figure 3-4(a) there appears to be a remaining ligament depth (b) size requirement for higher toughness materials tested under quasi-static loading; this requirement appears to be similar to the elastic-plastic requirement for an acceptable J-crack growth test:

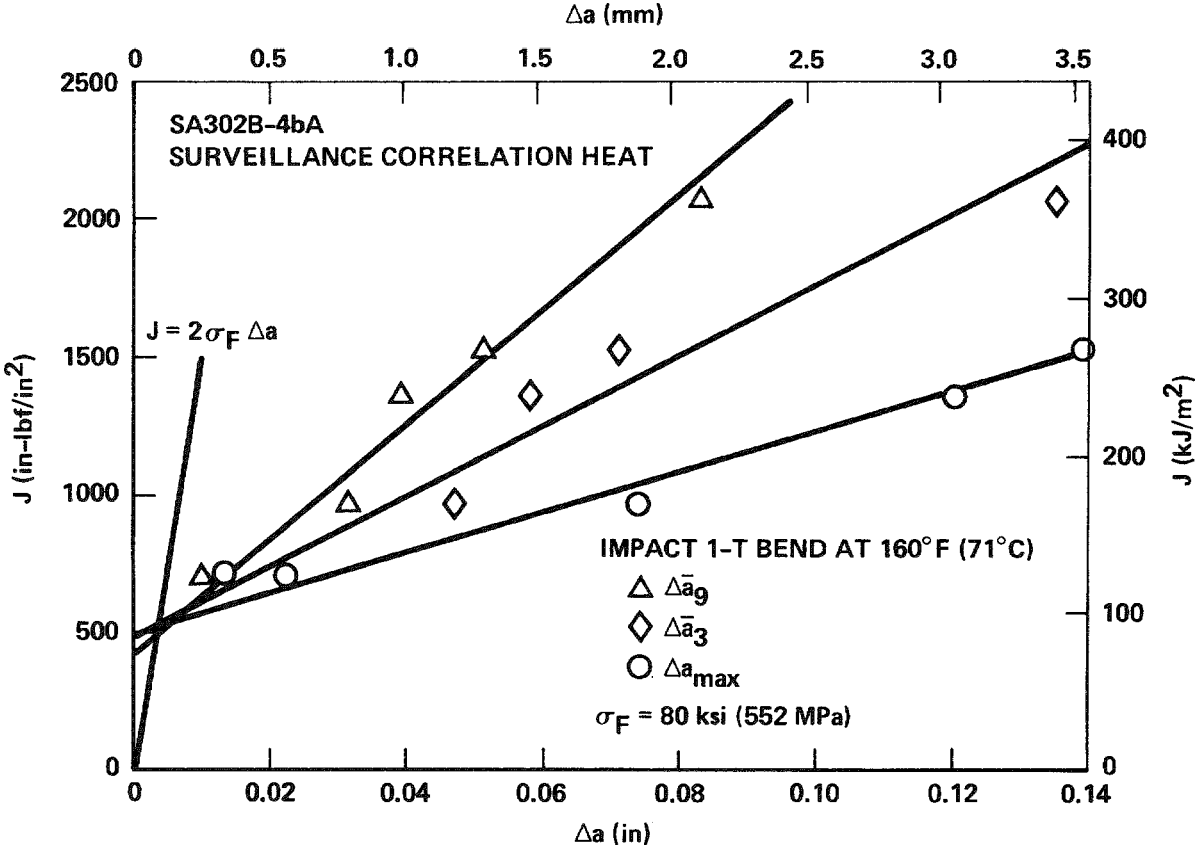

Figure 3-1. Multispecimen J-crack growth results (dynamic bend) for SA302B steel.

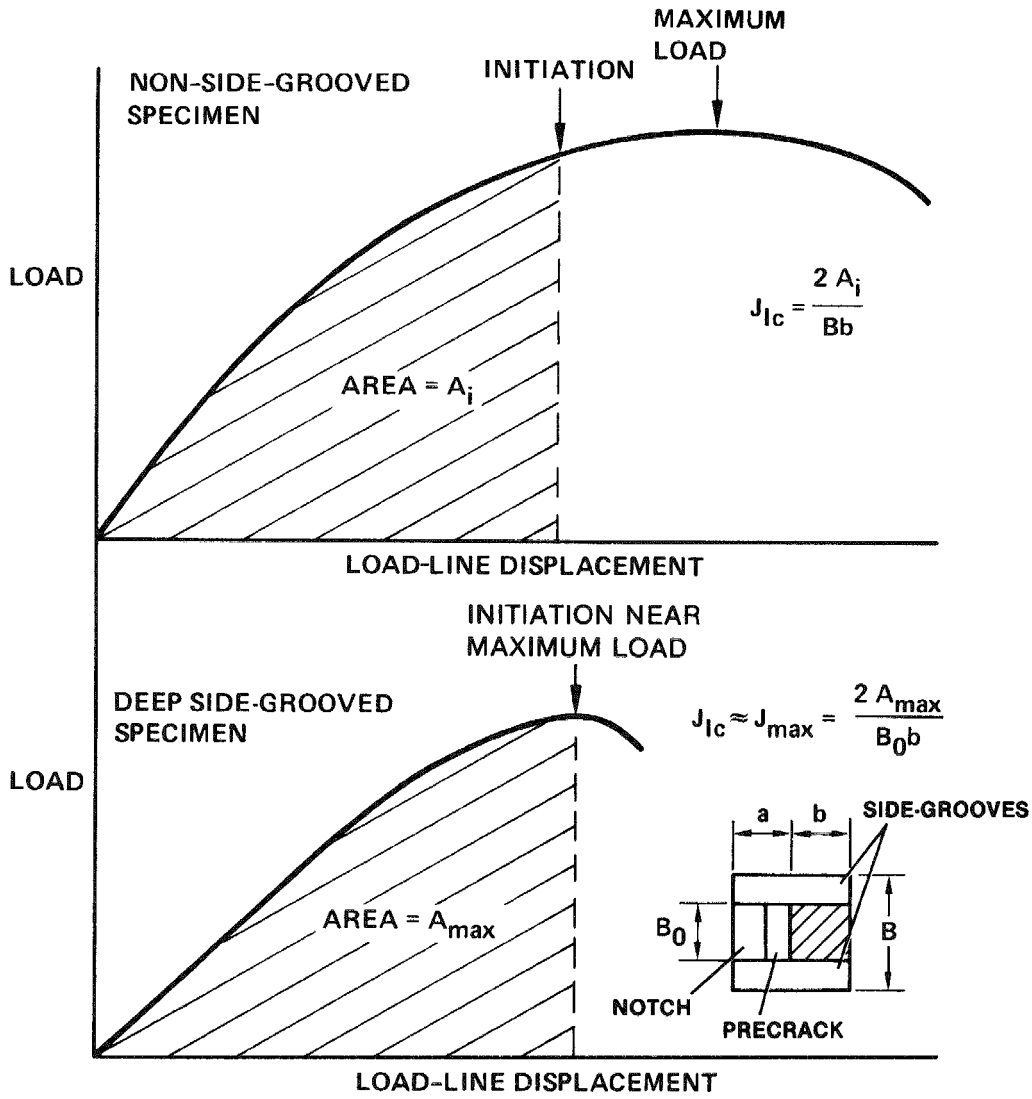

Figure 3-2. Schematic load versus load-line displacement curves for non-side-grooved and side-grooved 3-point bend specimens showing procedure for estimating J_{Ic}.

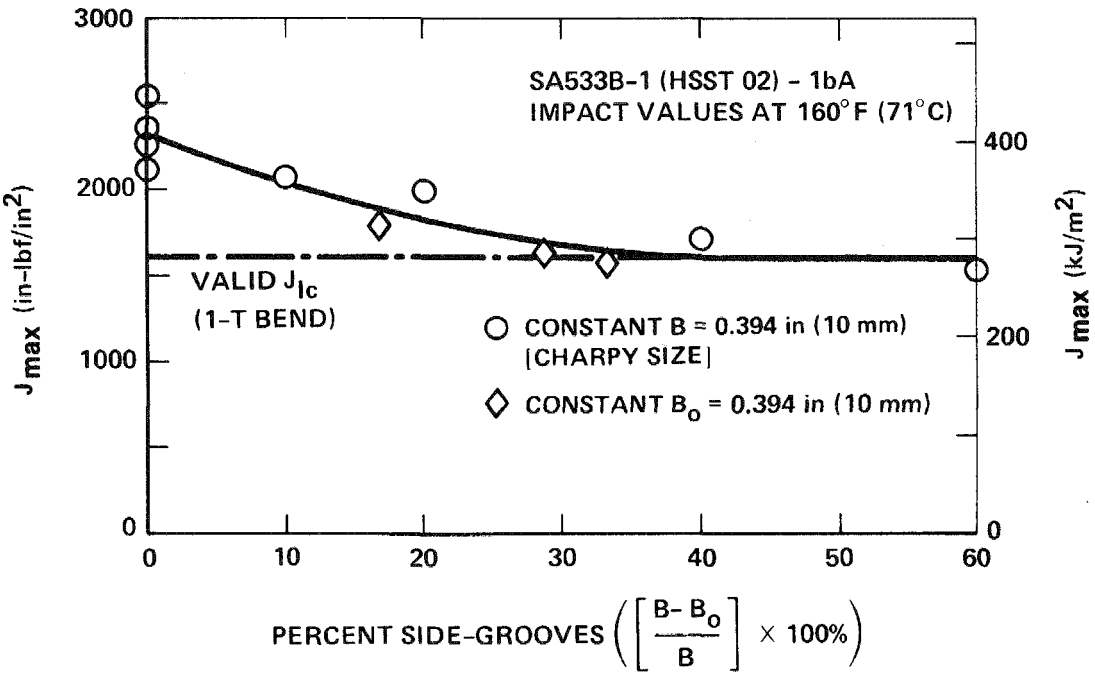

(a)

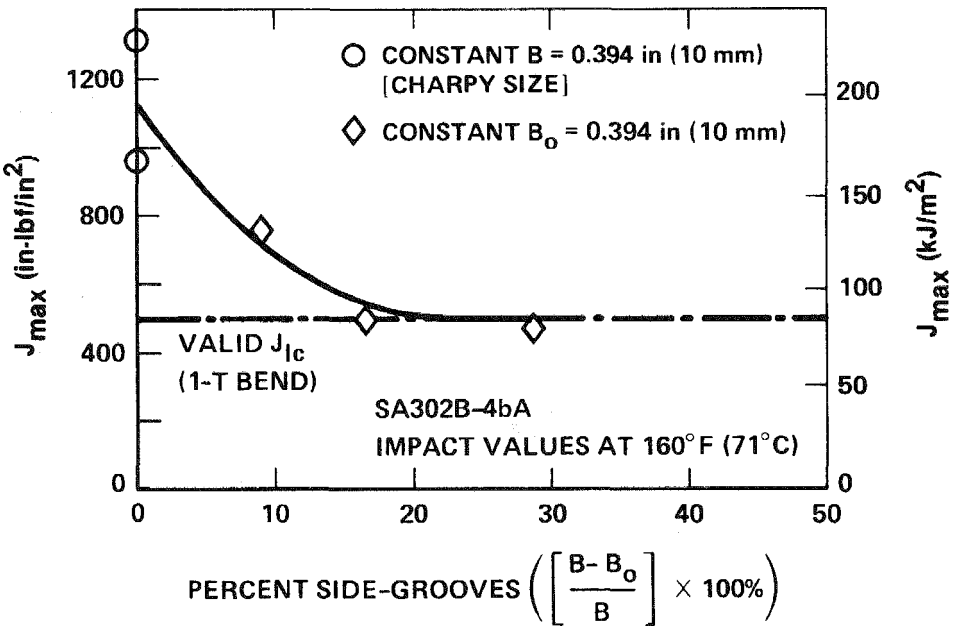

(b)

Figure 3-3. Side-groove results for dynamic bend tests on (a) SA533B-1 steel and (b) SA302B steel.

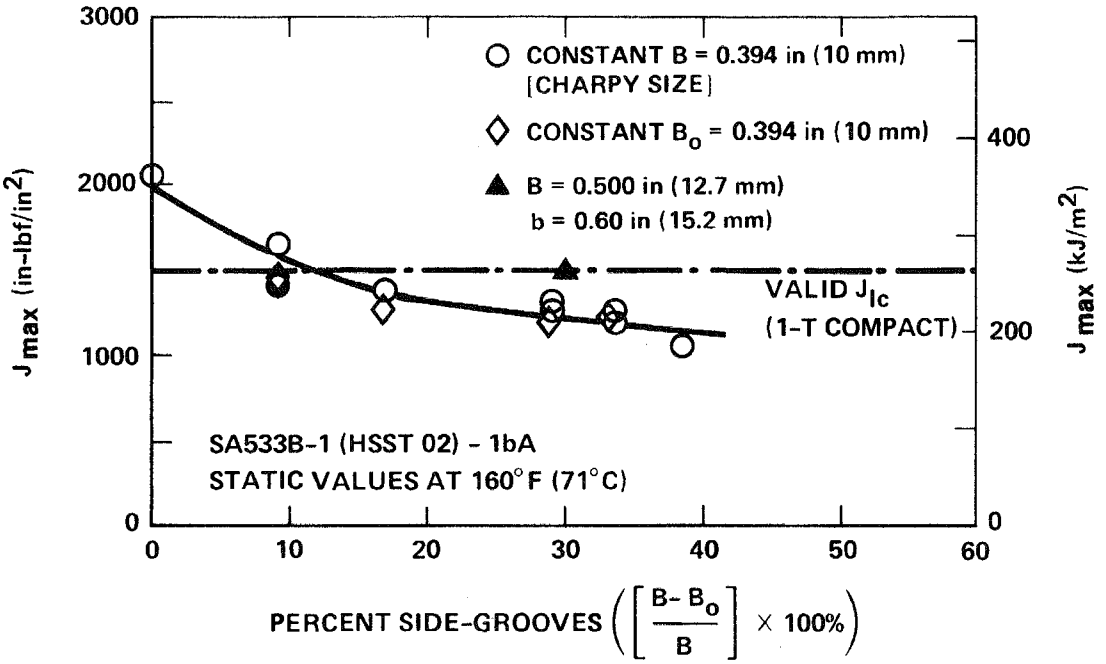

(a)

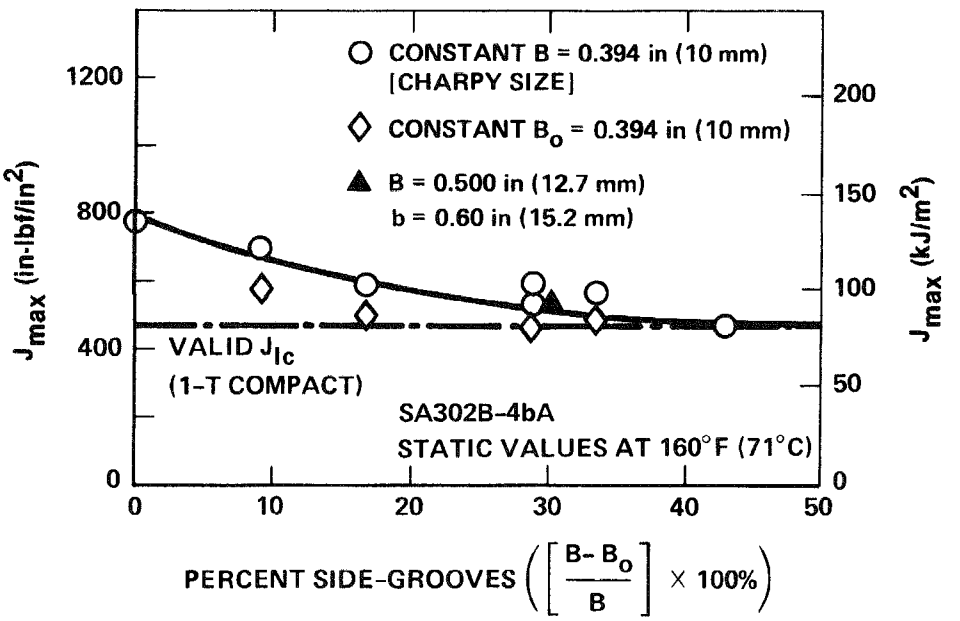

(b)

Figure 3-4. Side-groove results for static bend tests on (a) SA533B-1 steel and (b) SA302B steel.

$$b \geq 25J_{max}/\sigma_F \quad . \tag{3-3}$$

The closed triangular points in Figure 3-4 are for three-point bend test pieces with 30% side-grooves but with a larger remaining ligament depth. The test results for this case agree with the valid J_{Ic} level determined independently from the multi-specimen approach. Violation of the remaining ligament depth criterion (Eq. 3-3) produces low, conservative measures of J_{Ic}. Further support of this size requirement has been shown (36) using a high toughness weld metal tested under quasi-static loading.

It is felt that this test procedure has potential for realistic toughness evaluation in surveillance programs. Existing Charpy V-notch surveillance specimens can be used, merely with the minor modifications of precracking and side-grooving, both for quasi-static and dynamic testing. Thus, there is no need to resort to expensive, multi-specimen procedures or complex and often ambiguous methods for detecting crack initiation. Additionally, the method is expected to work particularly well for irradiated specimens, where irradiation hardening will further reduce the minimum test piece dimension (b) for "valid" measurement, both in terms of increasing σ_F and decreasing J_{Ic} (see Eq. 3-3). However, caution should be exercised before applying this procedure to other materials.

CRITICAL FRACTURE STRESS AND STRAIN MODEL PREDICTIONS

The methodology described here involves the use of simple uniaxial mechanical properties and microstructural information as related to different fracture models depending upon the failure mode. Low temperature, slip-initiated cleavage fracture has been modeled using the critical stress criterion proposed by Ritchie et al. (36). Similarly, failure at the upper shelf has been modeled as fully ductile rupture (microvoid coalescence) using a critical strain model originally proposed by McClintock (39). The application of these models involved determination of critical stress and strain values from bend and notched tensile tests, knowledge of precise analyses for the elastic-plastic stress and strain distributions ahead of sharp cracks, and an evaluation of microstructural size parameters which control the fracture event (40).

Predictions Using the Critical Stress Model

The critical stress criterion for cleavage fracture predicts failure to be dependent upon the degree of work hardening and yield strength in achieving a

high local tensile stress (maximum principle stress) ahead of the stress concentrator (sharp crack tip) which must exceed a critical value (σ_f^*) over a microstructurally significant characteristic distance (ℓ_o^*). With the advent of precise elastic-plastic stress distributions ahead of sharp cracks, it has become possible to relate such a local fracture criterion to macroscopic fracture toughness. Thus, low temperature fracture toughness can be related to a material's yield and fracture stresses. The temperature dependence of static fracture toughness (K_{Ic}) at the lower shelf is illustrated in Figure 3-5 for unirradiated SA533B-1 steel (HSST Plate 02) together with calculated values from the critical stress model. The three predicted lines reflect characteristic distance of 2, 3, and 4 prior austenite grain diameters ($\bar{d}$). Also, yield strength values corresponding to an approximate strain rate ($\dot{\varepsilon}$) of 10^{-2} s^{-1} were used with a work hardening exponent n of 0.1. A critical cleavage fracture stress (σ_f^*) of 1830 MP_a was determined from static four-point bend tests on 45° V-notched, square bars.

The critical stress model predicts values of toughness in agreement with experimental results for temperatures up to the Nil Ductility Transition Temperature (NDTT). Above the NDTT, the critical stress predictions tend to level off due to the smaller temperature variation of yield strength, and the model markedly underestimates the data. This behavior beyond the NDTT is not unexpected since failure at these higher temperatures can no longer be considered unstable cleavage because increasing amounts of ductile tearing between cleavage cracks become evident. Thus, failure above the NDTT is not amenable to an analysis using a purely critical stress model for failure.

Since the complete micro-mechanics of critical failure events in this acicular tempered bainitic steel are not fully understood, it is not possible from first principles to determine the significant characteristic distance. This is the reason for the range of ℓ_o^* values shown in Figure 3-5 as a multiple of $\bar{d}$. Further results (7,40) show that this model works at higher strain rates for this same steel and for a heat of SA302B steel at different loading rates.

The critical stress model can be applied to the prediction of irradiated toughness on the lower shelf as shown in Figure 3-6. Neutron irradiation is assumed to increase the yield strength and reduce the work hardening exponent while leaving the value of σ_f^* unchanged; these assumptions are discussed in more detail in Reference (40). The characteristic distance is also assumed to be unchanged by irradiation since particle spacings and grain sizes remain unaltered. Thus, using ℓ_o^* equal to $3\bar{d}$ and σ_f^* equal to 1830 MP_a,

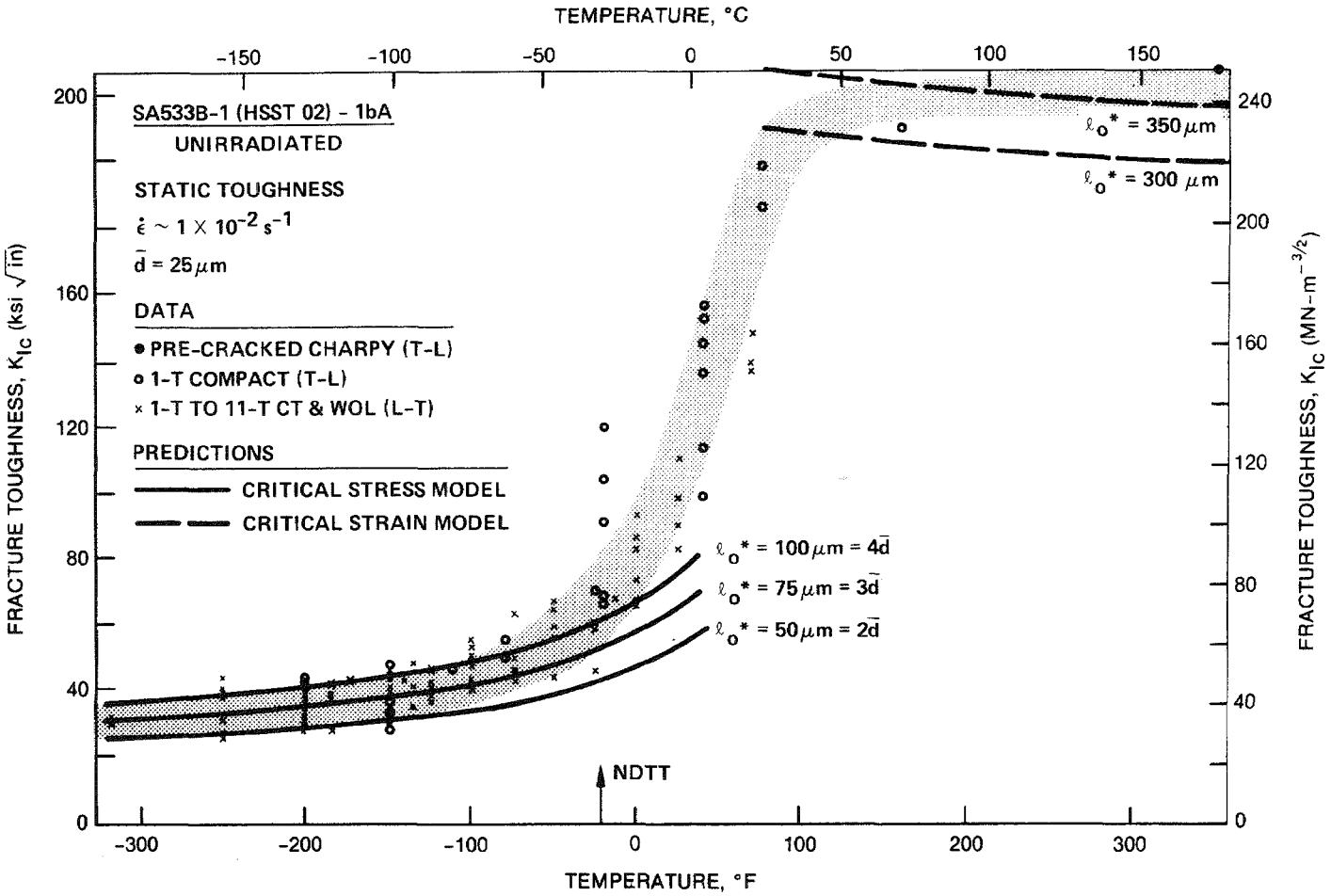

Figure 3-5. Variation of static fracture toughness (K_{Ic}) with temperature for unirradiated SA533B-1, showing comparison and experimental data with critical stress and critical strain model predictions.

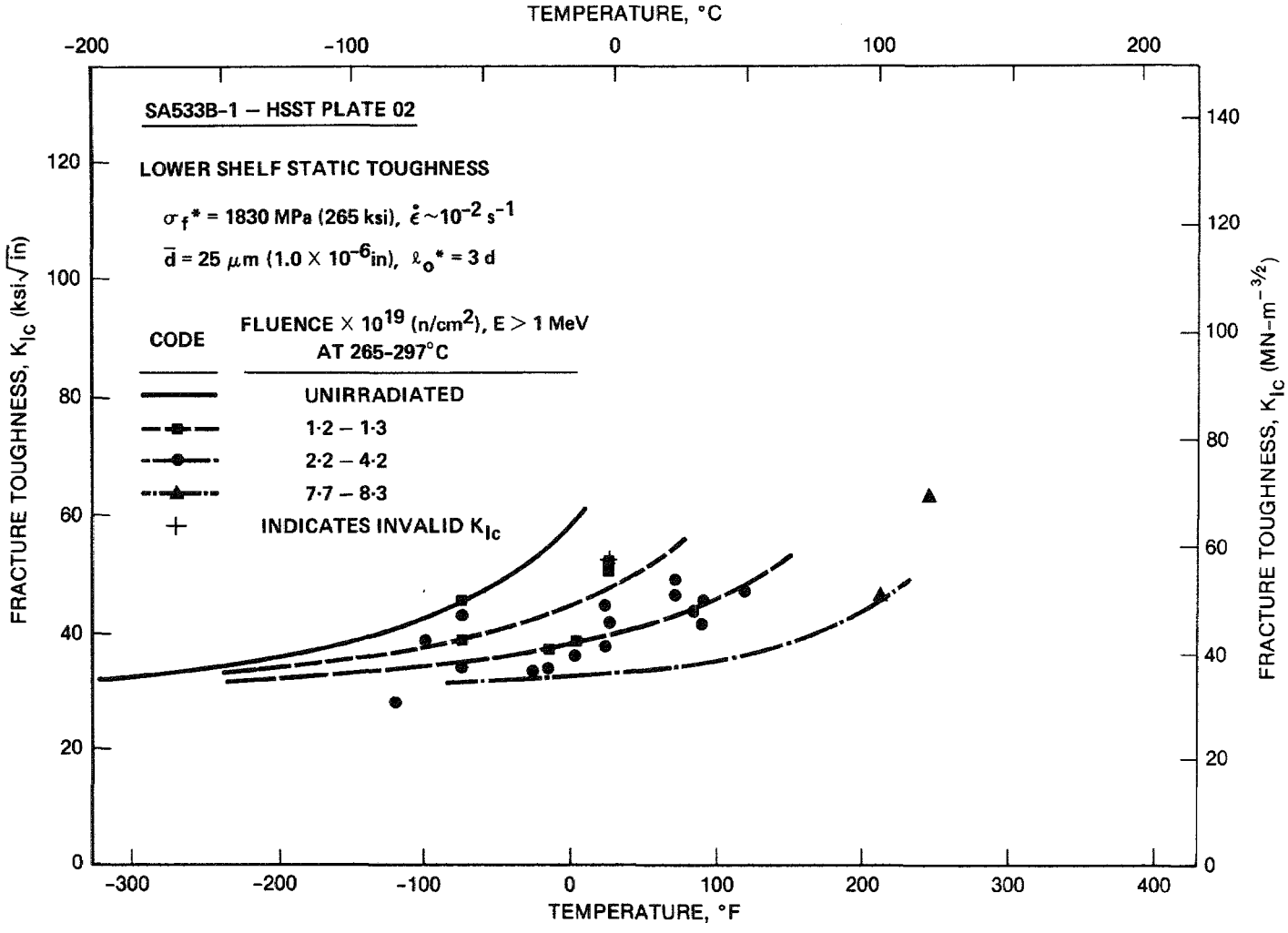

Figure 3-6. Critical stress model predictions of radiation effects on fracture toughness compared with irradiated data on SA533B-1 steel.

the fracture toughness was estimated using irradiated yield stress data corrected for a crack tip strain rate of 10^{-2} s^{-1}, and a work hardening exponent of $n \simeq 0$. The irradiated fracture toughness predictions correctly predict the shift in toughness to higher temperatures with increasing radiation exposure and closely reproduce the available experimental toughness data.

Predictions Using the Critical Strain Model

Macrocrack growth via linking of voids can be modeled as strain-induced fracture (in a simplistic manner) by utilizing the criterion of a critical strain being exceeded ahead of the crack tip. However, void growth during ductile fracture is also a strong function of stress state which varies with distance ahead of the crack tip. Also, in an analogous situation to cleavage fracture, it is not sufficient for the failure criterion to simply use a critical strain to be reached at a single point ahead of the crack tip; instead, this critical strain must be exceeded everywhere over a minimum amount of material which is characteristic of the scale of physical events occurring. Mackenzie et al. (41) have proposed a criterion for ductile fracture in which a critical fracture strain (σ_f^*) is exceeded locally over a microstructurally significant distance (ℓ_0^*) ahead of the crack tip. Their criterion further recognizes the distance variation in stress state away from the crack tip.

The application of this model for the prediction of upper shelf fracture toughness involves experimental determination of the fracture strain or ductility as a function of stress state, together with knowledge of the elastic-plastic strain distribution ahead of the sharp crack. Values of fracture strain were obtained using circumferentially-notched round tension specimens loaded uniaxially to failure; failure originates internally when the most severe hydrostatic stress state occurs and can be varied by using different notch acuity specimens which alter the state of stress. Values of failure strain for different states of stress were thus obtained with different radius-notch specimens. Fracture toughness values were predicted by determining the value of toughness for which the equivalent plastic strain (from blunting solutions for small scale yielding which also consider the state of stress) exceeds, over the characteristic distance (ℓ_0^*), the value of critical fracture strain (ε_f^*) representative of the crack tip stress state at that position. Since the failure event for ductile rupture generally involves coalescence by shear localization between a number of voids nucleated at the largest particles (inclusions), values of ℓ_0^* would be expected to be some small multiple of the inter-particle spacing. The major spacing between voids in SA533B-1 is roughly 50 μm which is

consistent with inclusion distribution studies. The multiple of voids needed to coalesce with the main crack tip for the initiation of a critical crack is unknown and can vary from material to material.

Figure 3-5 shows the upper shelf predictions based upon multiples of 6 or 7 times the inclusion spacing (300 and 350 μm) which best fit the experimental data. Thus, the characteristic distance reflects the critical number of voids needed, in addition to the spacing between particles, for fracture initiation to occur. Results for SA302B steel (7,40) suggest that only one void is needed for this lower toughness steel with an inter-particle spacing of 100-150 μm. Predictions of toughness on the upper shelf for irradiated materials are not possible to make at this time due to the absence of irradiated ductility-stress state data and the sparce upper shelf toughness results for comparison with the model. Additionally, it is quite possible that the reduced strain hardening capacity of irradiated steels will result in earlier coalescence of major voids by plastic shear localization. Thus, a different number of critical voids may be involved at fracture initiation for the irradiated case as compared to the unirradiated condition. At this time we have no way of predicting the change in the number of critical voids needed (after irradiation) for fracture initiation.

OTHER APPROACHES TO MAXIMIZE CHARPY-TYPE DATA

Several investigations were conducted in order to maximize Charpy-size specimen data. These studies also included verification of using a new displacement measuring technique at the load-line for slow bend precracked Charpy testing (42). Four areas of study were: effect of root radius, load-temperature behavior, energy partitioning, and stretch zone measurement and size. A feasibility study of applying improved visioplasticity techniques to slow bend and impact precracked Charpy and Charpy V-notch behavior was also investigated, but the cost and experimental difficulties precluded any actual definitive testing.

The slow bend displacement measuring system described in Reference (42) was built and tested using both Charpy V-notch and precracked Charpy specimens over a wide range of temperatures. The equipment and technique worked well except at low temperatures, where pin sticking was a problem; a comparison of true load-line energies to maximum load with compliance corrected values of load-ram displacement [similar to Reference (43)] gave essentially identical results.

Root Radius Study

The root radius study involved testing various notch root radius specimens to see the effect of notch sharpness (ρ). For the low temperature cleavage

results, the equivalent toughness (K_ρ) was calculated, and plots of K_ρ versus ρ were made (7) as shown in Figure 3-7. The effective root radius (ρ_0) which will produce the same fracture toughness as for a sharp fatigue precrack ($\rho = 0$), was determined for SA533B-1 and SA302B steels at two temperatures and under slow bend and impact loading. For this type of steel and at the temperatures studied, there is a great deal of data scatter which makes the results difficult to interpret. There appears to be little or no difference between the two steels and $\rho_0 \simeq 0.002$ in (0.05 mm). There was, however, a trend for different slopes of the lines passing through the origin and fitting the finite ρ data; these slopes are indicative of the microcleavage fracture stress (σ_f^*), which was determined independently for the critical fracture stress model discussed previously. The magnitude of the difference between σ_f^* values for the two steels can be approximated using the following expression (44):

$$K_\rho = A\sigma_y\left[\exp(\sigma_f^*/\sigma_y - 1) - 1\right]^{1/2}\rho^{1/2} \qquad (3\text{-}4)$$

where A is a constant dependent upon stress state and σ_y is the yield stress (which is essentially equivalent for the two steels). The difference in σ_f^* values between the steels is on the order of 10% which agrees with the independent four-point bend results, and there is a slight trend (again about 10%) towards higher values of σ_f^* with increasing temperature and increasing loading rate--which also agrees with the four-point bend results (40).

The root radius work has also been extended into the fibrous initiation regime (8) on the upper shelf. To obtain fibrous initiation it was necessary to resort to multi-specimen, heat-tinting, R-curve procedures. Charpy-size specimens were machined with varying root radii (ρ) and tested either in slow bend or impact at upper shelf temperatures. Values of absorbed specimen energy (E_m) were calculated from the load-time or load-displacement curves, and the extent of fibrous crack growth was measured optically and computed using a nine point average across the specimen crack ($\Delta\bar{a}_9$). Tests were performed for standard Charpy V-notch specimens for impact loading at several temperatures on the upper shelf, with only a slight tendency towards lower values for the highest temperatures.

Similar results for fatigue precracked Charpy specimens ($\rho = 0$) were also generated. Again, temperatures on the upper shelf were utilized in generating the data, and there does not appear to be a definitive decrease in absorbed energy with increasing temperature. By defining initiation as the intersection of two

fitted lines to the data (as shown in Figure 3-1) the data indicates an increase in absorbed energy for the defined point of initiation with increasing root radius. The SA302B steel has much lower initiation energies and the slopes of the J-Δa curves are much shallower than for the SA533B-1 steel; these small specimen results are consistent with other larger specimen results (2).

Prior work on high strength steels which exhibit ductile (microvoid coalescence) fractures has indicated the existence of an effective root radius (ρ_o) for defining notch toughness (45); this concept is similar to the low temperature cleavage approach discussed earlier. Other work (46) has indicated variance with this concept (for NiCrMoV rotor steel and 6061-T651 aluminum tests) and with a critical strain theory such as suggested by Rice (47). The work in Reference (46) suggests a linear relationship between initiation J and root radius which does not pass through the origin. By estimating our root radius initiation values, as just described, and plotting as a function of root radius, graphs such as Figure 3-8 were obtained. Initiation energies are directly proportional to J (by multiplying by 2) except for the shallow notch depth, finite root radii specimens; the correct formulation for J should include a separation into elastic (U_e) and plastic (U_p) energy components (48). However, the magnitude of the elastic term, as compared to the plastic term, is quite small and can essentially be ignored here.

The relationship as seen in Figure 3-8 is non-linear and does not pass through the origin for both slow bend and impact loading; similar results were obtained for the SA533B-1 steel. The non-linear behavior and data scatter may in part be due to the small size of the Charpy specimens used; however, the SA302B steel has sufficiently low toughness that some of the results meet elastic-plastic size requirements (24). The results of Reference (46) also violated size requirements for many of their test results (in particular, the center-notched panel data). Nonetheless, the applicability of a ρ_o for ductile fracture appears to be dubious.

Load-Temperature Diagrams

Instrumentation of the impact Charpy V-notch and precracked Charpy tests allows the measurement of both critical loads and energies. Since the impact Charpy specimen is the currently used surveillance test specimen, instrumentation is the logical starting point to maximize the data obtained from surveillance testing. Also because of the strain-rate sensitivity of nuclear reactor steels, a need arises to look at both dynamic (impact) and static (slow bend) loading.

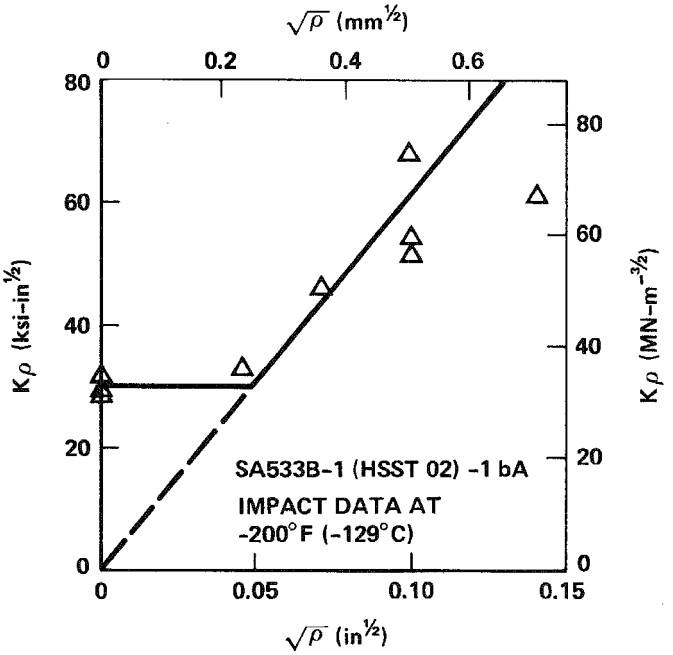

Figure 3-7. Impact root radius results for cleavage initiation for SA533B-1 steel at -200°F (-129°C).

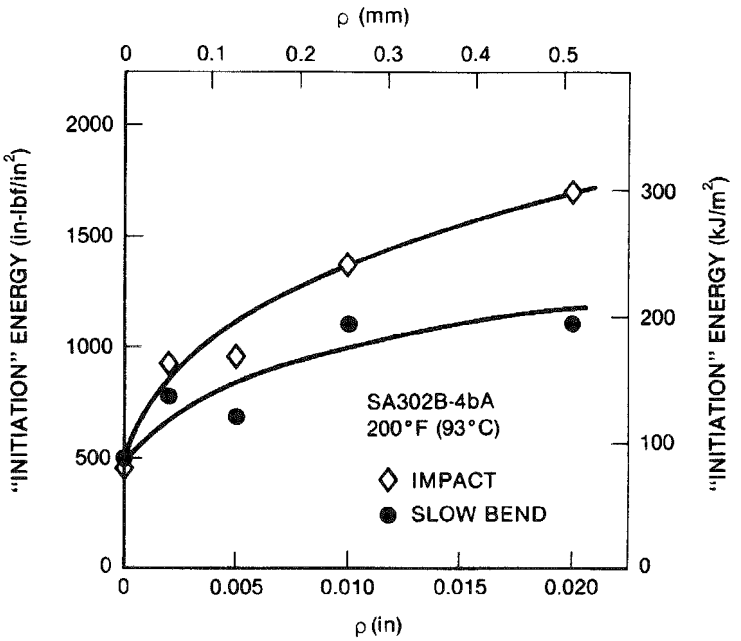

Figure 3-8. Fibrous initiation energy versus root radius (ρ) for SA302B steel at 200°F (93°C).

A load-temperature diagram shows the maximum (P_M) and general yield (P_{GY}) loads as a function of test temperature. Below temperatures where general yielding occurs, the fracture load increases with increasing temperature to the intersection of the P_M and P_{GY} curves, i.e., $P_{GY} = P_M$. This transition temperature is termed T_D and can also be utilized to estimate microcleavage fracture stress values. The fracture instability load (P_M) continues to increase to a temperature T_N at which point strain hardening and plastic constraint are insufficient to achieve a critical fracture stress. In other words, we are near the Nil Ductility Transition Temperature; thus, pure cleavage fracture no longer occurs at temperatures above T_N. Additionally, the general yield loads can be converted to estimates of yield strength as shown in Reference (31).

Load-temperature diagrams for impact Charpy V-notch tests of SA533B-1 and SA302B steel are shown in Figure 3-9. The curves indicate very little difference between orientations for the SA533B-1 steel, but a large difference between the two orientations for the SA302B steel. This difference for the SA302B steel is most likely due to the lack of cross-rolling used during the manufacture of this older quality pressure vessel steel. This difference in behavior also shows up in the absorbed energy values as will be shown later. Additionally, this difference should manifest itself in terms of fracture toughness; unfortunately, we have no longitudinal fracture toughness data for comparison. The shape of the two maximum load curves for the SA302B steel suggests more strain-hardening capacity in the longitudinal orientation; in fact, the longitudinal SA302B load-temperature curve is very similar to the SA533B-1 curves. Note that the general yield (P_{GY}) curves are independent of orientation.

Results for slow bend and precracked Charpy tests have also been analyzed and reported (7,8). To account for varying crack lengths for the precracked specimens, the load scale is normalized as P/b^2. By using this normalization all results can be compared directly. The effect of precracking and impact loading is to shift the curves to higher temperatures (increase T_D). It is interesting that the shift in T_D is greater in the SA533B-1 steel for the effect of root radius (Charpy V-notch to precracked), but the shift in T_D is larger for the SA302B steel when loading rate is considered (slow bend to impact).

Energy Partitioning

The total energy for both impact Charpy V-notch and precracked Charpy tests can be partitioned into components based upon maximum load (i.e., energy to maximum

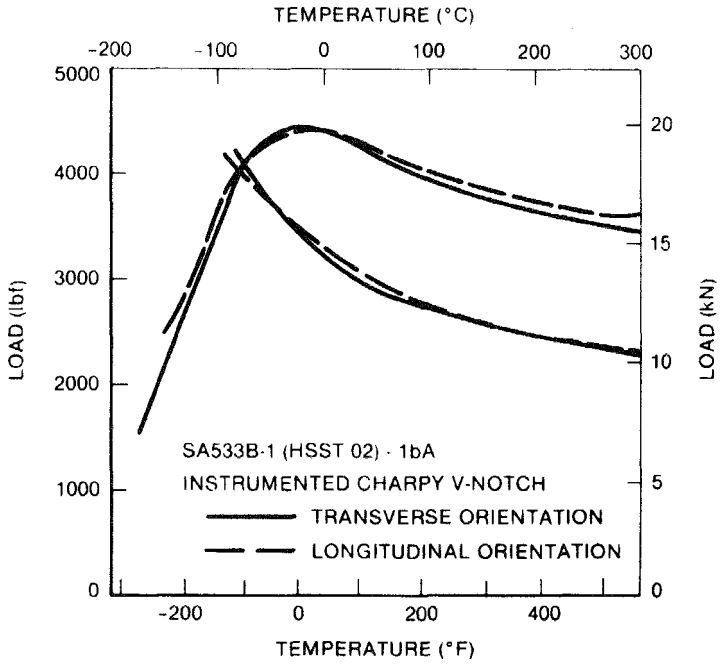

(a)

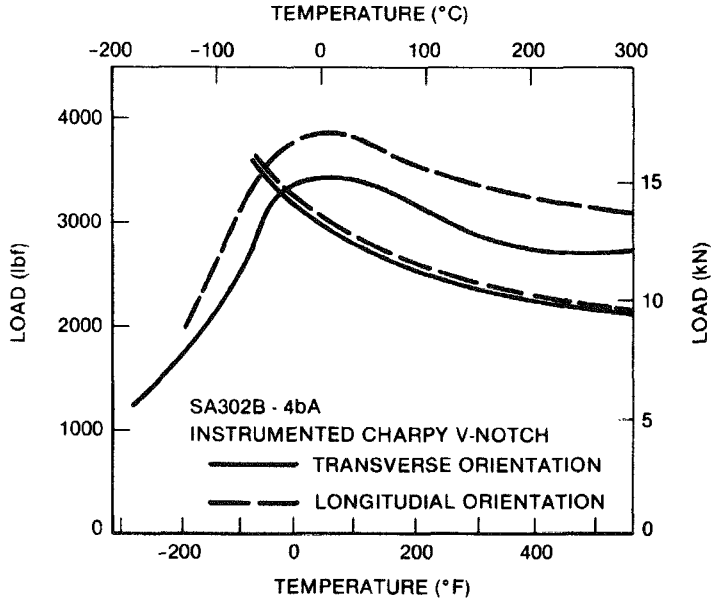

(b)

Figure 3-9. Comparison of load-temperature results between transverse and longitudinal Charpy V-Notch tests for (a) SA533B-1 steel and (b) SA302-B steel.

load and post-maximum load energy). ideally, the true initiation energies should be used rather than the maximum load energy, but these data are not always readily available. Maximum loads generally correspond to initiation when the fracture mode is cleavage; above the fracture mode transition point, the fracture mode is fibrous and R-curve initiation data are required. It is still informative, however, to use the maximum load energy results for partitioning curves. Figure 3-10 shows Charpy V-notch energy-partitioning curves for SA302B steel in both the transverse and longitudinal orientations for the Charpy V-notch test and in the transverse orientation for the precracked Charpy test. Items to be noted are the decrease in upper shelf maximum load energy with increasing temperature, and the increase in post-maximum load energy with temperature to account for the essentially flat total energy on the upper shelf; only the longitudinally oriented SA302B data appear to be flat for all three energies.

For the SA302B steel, the decrease in total absorbed energy in the transverse orientation is due to a decrease in both maximum load energy and post-maximum load energy. Also, the shape of the SA302B transverse orientation curves are markedly lower in transition temperature slope. The maximum load energies for the SA533B-1 steel are essentially identical between the two orientations agreeing with the previous load-temperature results; therefore the difference in total energy is due to an increase in propagation energy (post-maximum load energy). More detailed results for impact and slow bend results were reported in References (7,8).

Stretch Zone Measurement

If we consider a fracture specimen containing an initially sharp fatigue crack, continued propagation of this crack under a monotonically increasing load will require some initial degree of plastic deformation in the vicinity of the crack tip. As idealized in Figure 3-11, significant blunting of the fatigue crack may occur in the material prior to continued crack propagation. This crack blunting results in the formation of a region separating the fatigue crack front from the subsequent crack plane. This intermediate region is termed the stretch zone.

Theoretically, the size of the stretch zone may be correlated with the fracture toughness of the material. For example, consider a low-strength steel tested at a temperature in which ductile fracture occurs and fracture toughness is high. Significant plastic deformation will be required near the fatigue crack tip prior to propagation of the crack, since the formation, growth, and coalescence

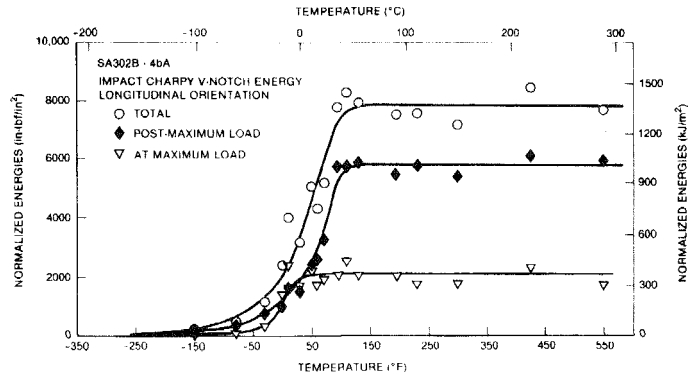

(a)

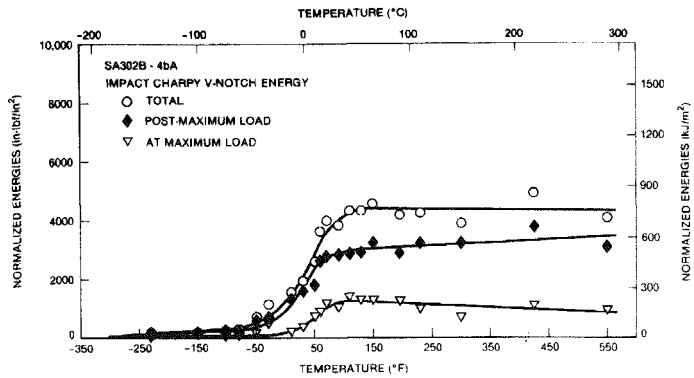

(b)

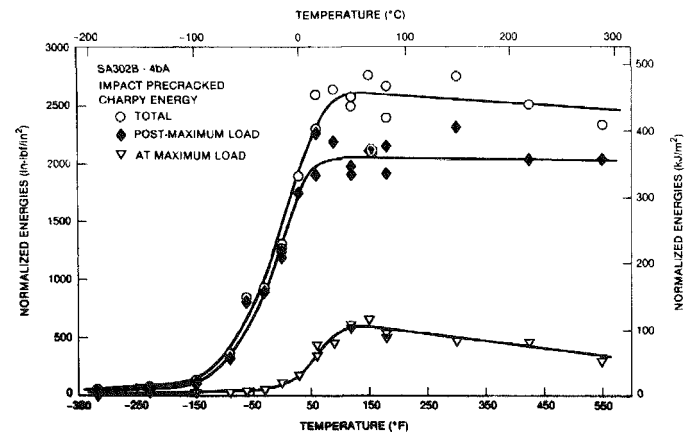

(c)

Figure 3-10. Energy partitioning for SA302B steel for (a) Charpy V-Notch longitudinal orientation, (b) Charpy V-Notch transverse orientation, and (c) precracked Charpy transverse orientation results.

of microvoids in low-strength steel requires large plastic strains. Hence, the stretch zone will be relatively large in the steel when the fracture toughness is high. On the other hand, if the steel is tested at a low temperature where cleavage crack propagation is predominant (and fracture toughness is low), little plastic deformation at the fatigue crack tip will precede crack propagation and the stretch zone will be small.

Quantitatively, the stretch zone height (SZH) may be related to the crack tip opening displacement (CTOD) as shown in Figure 3-12. The CTOD may in turn be correlated to the fracture toughness of the material (49).

The various techniques for evaluating CTOD from stretch zone measurements has been reviewed (50), and the scanning electron microscopy of fracture surfaces appears to be the most reliable technique. However, investigators to date have only analyzed one-half of the fracture surface and assumed that the measured stretch zone height was equal to 1/2 (CTOD). Considerable data scatter has resulted.

Fracture surfaces were sectioned from precracked Charpy specimens of SA302B and SA533B-1 steels which had been tested at a variety of temperatures. Stretch zone height was measured from fractographs (on an ELTEC SEM) taken at an angle $\leq 5°$ from the fatigue crack surface in a direction coincident with the crack propagation direction and at a position within ± 0.04 in (1 mm) from the center of the fracture surface. Early in the investigation it was found that analyzing a single fracture surface was inadequate [i.e., the assumption that stretch zone height equals 1/2 (CTOD) is rarely true]. Consequently, fractographs were taken of matching fracture surfaces for each precracked Charpy test. Corresponding features on matching fractographs were aligned and the CTOD was determined from the sum of the two stretch zone heights measured at corresponding positions on the fractographs. The identification of corresponding features often required a sequence of pictures taken at angles up to 90° from the fracture surface. Despite efforts to carefully match fractographs, however, some scatter and uncertainty in stretch zone height measurements still arose.

The measured CTOD for both SA302B and SA533B-1 steels is plotted as a function of test temperature in Figure 3-13. Although there is some scatter in the data, the following characteristics are definitely apparent:

- The CTOD increases with test temperature, a trend which agrees with the theoretical proportionality between CTOD and K_{Ic}.

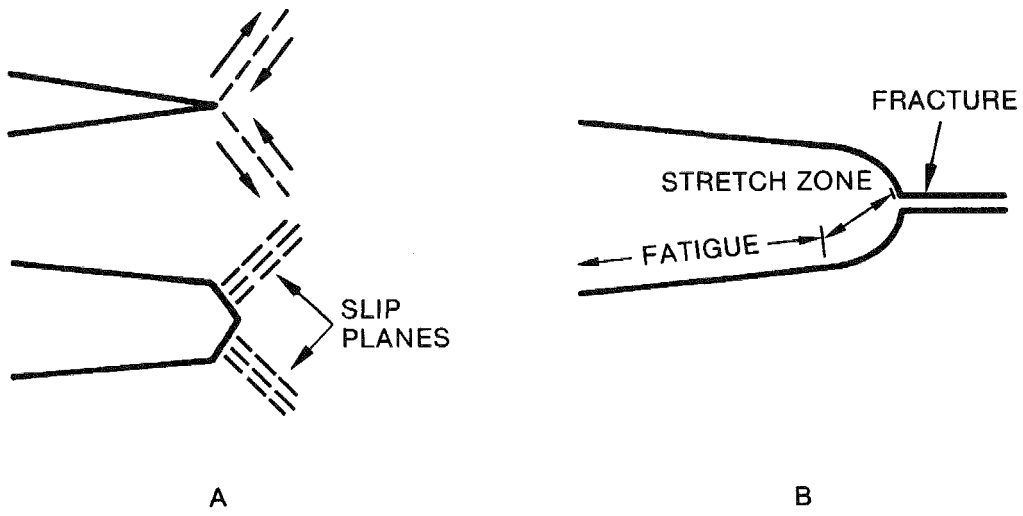

Figure 3-11. Fatigue crack blunting and stretch zone formation in a pre-cracked fracture specimen.

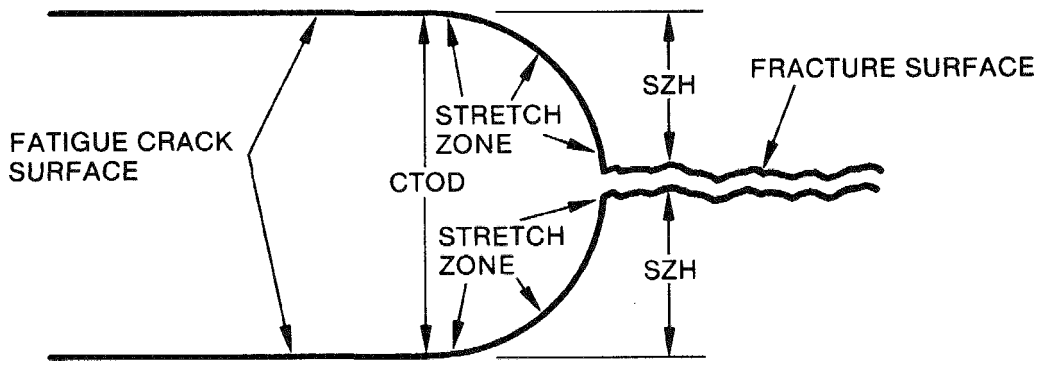

Figure 3-12. Relationship between Stretch Zone Height (SZH) and CTOD.

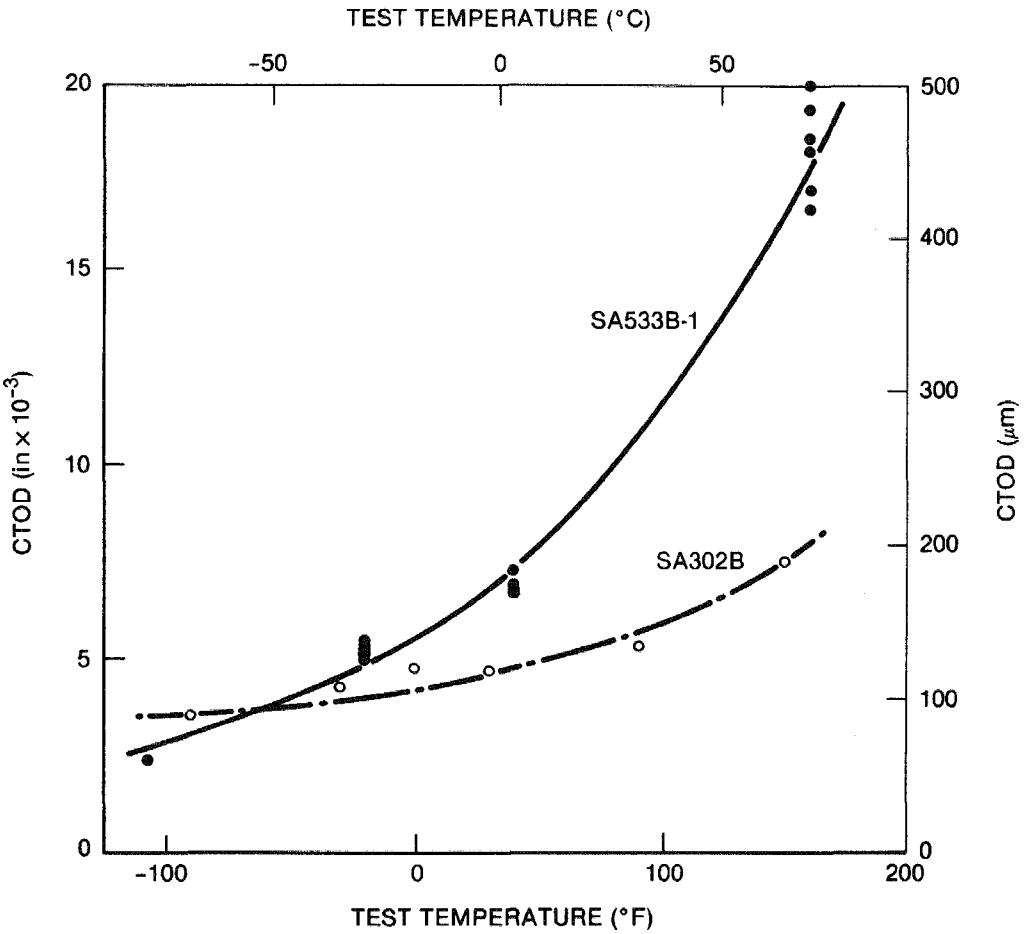

Figure 3-13. Critical crack opening displacement as a function of test temperature.

- The CTOD is much larger for the SA533B-1 steel than the A302B steel. Again this result agrees with the differences in fracture toughness for the two steels.

DEVELOPMENT OF SURROGATE MATERIALS

The purpose of this subtask was to examine the use of shock wave hardening (shock strengthening) to simulate radiation embrittlement. The shock wave embrittlement technique was therefore used to provide surrogate materials that simulated radiation embrittlement. A heat of SA533B-1 steel, heat 1bH (9), was chosen to be shocked and subsequently evaluated.

The primary objective of the experiment was to produce at least a 1 in (25 mm) thick piece of SA533B-1 steel shock hardened to have mechanical properties similar to the same steel irradiated at 550°F to a fluence of approximately 3×10^{19} n/cm^2 (E > 1 MeV). A search of the literature revealed no previous shock-strengthening work on steel of a composition similar to that of SA533B-1. The strengthening desired was to raise the yield strength from approximately 480 MPa (70 ksi) to 760 MPa (110 ksi). A shocking level of near 240 kbar was selected for use in shocking the SA533B-1 material.

An explosive configuration was detonated to produce a planar impact on three steel plates which were at ambient temperature. Post-shock hardness measurements on the top and bottom surfaces of each plate indicated that only the top 1-in plate had been significantly hardened. That is, the Rockwell B hardness (R_b, 1/16 ball, 100 kg load) for the unshocked material and the bottom two plates was similar (around 90). Therefore, only the top plate was sectioned so that hardness profiles could be obtained from the center of impact to the edge of the plate and also through the thickness of the plate (8). The lateral hardness profiles indicated that significant hardness increases occurred out to a position about 4 in (102 mm) from the center of impact. Thus the area that was hardened corresponded to the dimensions of the flyer plate. The through thickness hardness results indicate that uniform hardness of the desired level was obtained only in the top 0.4 in (10 mm) of the plate instead of the entire 1 in (25 mm) thickness. The hardness then drops rapidly over the next 0.4 in (10 mm) and levels out at a hardness level somewhat higher than the unshocked material.

Charpy V-Notch specimens were machined from the top 0.4 in (10 mm) and bottom 0.4 in (10 mm) layers of the top impacted plate. Specimens from these two regions bracket the originally desired hardness and tensile properties to be obtained from the three plates. The comparison of results between the two

layers and the original unirradiated properties is shown in Figure 3-14. The data were also fit to the tanh function (Eq. 2-1), and the subsequent tanh parameters are listed in Table 3-1.

Also listed in Table 3-1 are the estimated equivalent irradiation conditions required to produce the type of shift and shelf drop observed. These estimates were based upon surveying the existing irradiated data base developed in the EPRI 1240-1 program (11). The magnitude and range of the two conditions achieved through shock hardening meet the original objectives of this subtask.

RECONSTITUTED SURVEILLANCE SPECIMENS

The total cost associated with the surveillance of the radiation embrittlement of operating nuclear reactor pressure vessels is substantial. Each utility must bear the cost of fabricating and evaluating up to eight capsules during the expected lifetime of the pressure vessel. Thus the final cost associated with obtaining one Charpy V-notch data point can be in the range of $1,000. If a safety issue concerning radiation embrittlement of the beltline region is raised, having the ability to obtain fracture toughness data for the specified materials could be of great value. Therefore, as part of the overall effort to obtain more information from surveillance specimens, the possibility of reusing broken Charpy specimens to make new (reconstituted) specimens was explored.

The objective of the subtask was to examine low cost techniques for fabricating new Charpy, compact fracture and bend specimens from broken Charpy halves. All of the techniques involved adding material, such as end tabs, to the broken specimen halves. The initial joining techniques evaluated were essentially dependent on a mechanical bond through either threaded connectors, interlocking tabs, shrink fits or press fits. Although successful specimens were developed using these mechanical techniques, it became apparent that most of them were not conducive to automation or hot cell handling. Therefore, the subtask was redirected to consider welding processes which could meet the following requirements: (1) provide sufficient bond strength, (2) not cause annealing of the radiation damage, and (3) be performed economically in a hot cell environment.

The first phase of the study was a comparative analysis of potential welding processes. Those processes given serious consideration were stud welding, friction welding, electron-beam welding, and laser-beam welding. The details of the evaluation are given in Reference (8), and the conclusion reached was that stud welding was the most promising technique.

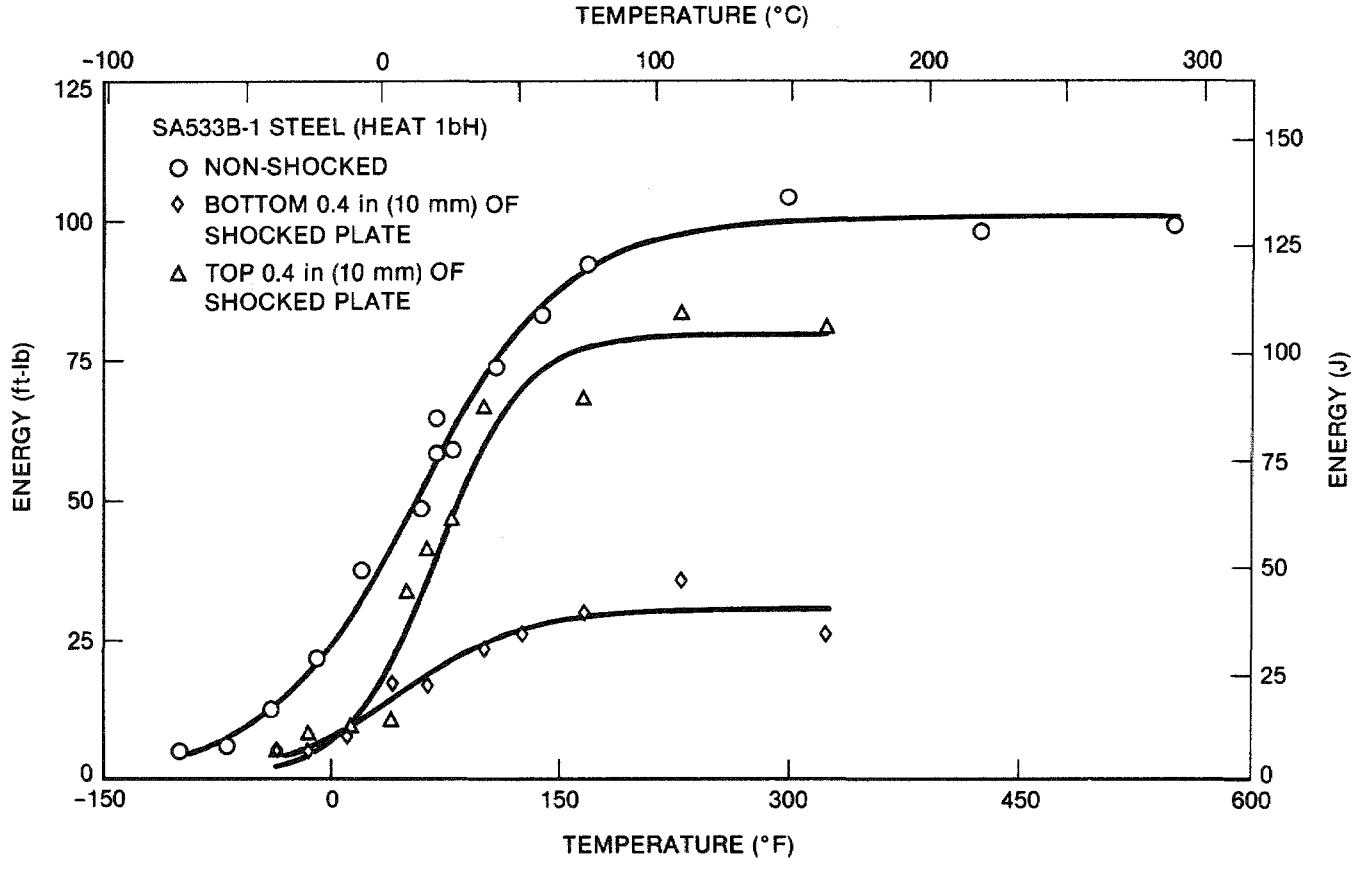

Figure 3-14. Non-shocked and shock-simulated-irradiated Charpy V-Notch energy curves for SA533B-1 steel.

Table 3-1

SHOCK-HARDENED SA533B-1 STEEL PROPERTIES

Condition	Hardness	Estimated Ambient Flow Properties, ksi (MPa)		Tanh Fit Parameters				ΔT 30	Δ Shelf	Corresponding** Irradiation Conditions	
				ft-lbf (J)		°F (°C)				φ	φt
		Yield	Tensile	A	B	T_o	C	°F (°C)	ft-lbf (J)	$n/cm^2/s$	n/cm^2
Non-Shocked	90	65 (450)	87 (600)	50.1 (67.9)	50.1 (67.9)	56.2 (13.4)	97.8 (54.3)	--	--	$U_{N_{I_{R_{R_{A_{D_{I_{A_{T_{E_D}}}}}}}}}}$	
Bottom Layer	93	77 (530)	97 (670)	39.7 (53.8)	39.7 (53.8)	69.1 (20.6)	57.8 (32.1)	40 (22)	21 (28)	0.2-0.5 × 10^{11}	1.3 × 10^{18}
Top Layer	103	115 (795)	130 (895)	15.2 (20.6)	15.2 (20.6)	44.8 (7.1)	80.0 (44.4)	--*	70 (95)	--	>13 × 10^{18}

*The upper shelf is only barely above the 30 ft-lbf (40.7 J) level.

**These estimates based upon SA533B-1 irradiation data obtained from EPRI RP1240-1 irradiated pressure vessel steel data base (11).

The second phase of the study involved experiments to establish the feasibility of stud welding square tabs to broken Charpy specimen halves. A successful experimental stud welding apparatus was developed, and welding parameters were determined for producing sound welds in unirradiated SA533B-1 steel without excessive heating of the central portion of the original broken Charpy sections. Reconstituted Charpy V-notch specimens were tested to determine an energy transition curve, and the data were compared to the data obtained from the original Charpy specimens in Figure 3-15. Additional reconstituted Charpy V-notch specimens were precracked and used to determine dynamic fracture toughness. A comparison of dynamic fracture toughness from reconstituted and original specimens is shown in Figure 3-16. It is clear from Figures 3-15 and 3-16 that stud welding can produce reconstituted specimens with no change in properties from the original specimens.

The next phase of the program was to demonstrate that the stud welding technique could produce acceptable reconstituted irradiated Charpy specimens in a hot cell environment. Broken Charpy halves from irradiated SA533B-1 plate and submerged arc weld metal (SA508-2 base metal) were used to make reconstituted Charpy V-notch specimens. A comparison of the data from the reconstituted specimens and the original irradiated specimens is shown in Figures 3-17 and 3-18. Again, the comparison is quite good except for a few points in Figure 3-18. The high values for the two data points tested around room temperature for the reconstituted weld metal are not believed to be related to welding induced annealing of the radiation damage. Extensive experiments were performed to establish that the time-temperature conditions near the root of the reconstituted Charpy specimens could not lead to annealing. A more likely explanation for the high values is fluence variations in the original specimens since the broken specimens selected for the study had the lowest radiation (activity) readings. Thus, the reconstituted specimens may correspond to a fluence which is less than the average fluence for the original set of specimens.

The results of this subtask demonstrate that it is feasible to produce new reconstituted test specimens. In particular, it has been shown that the stud welding process provides a relatively simple and inexpensive means for generating reconstituted surveillance specimens in a hot cell environment. Thus, a procedure now exists for significantly increasing the amount of toughness data that can be obtained from the very limited number of specimens in a pressure vessel surveillance capsule.

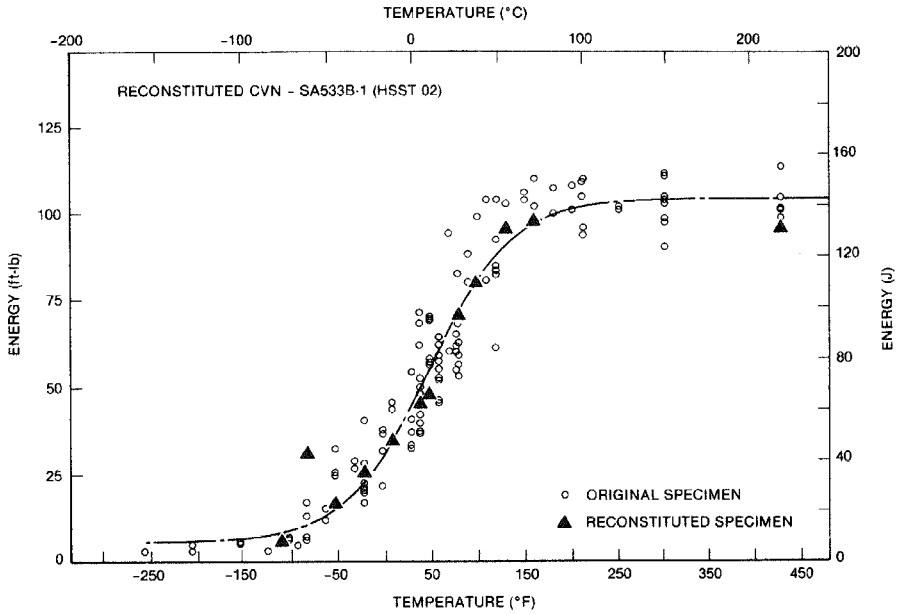

Figure 3-15. Comparison of Charpy V-Notch data from reconstituted and original specimens of unirradiated SA533B-1 steel.

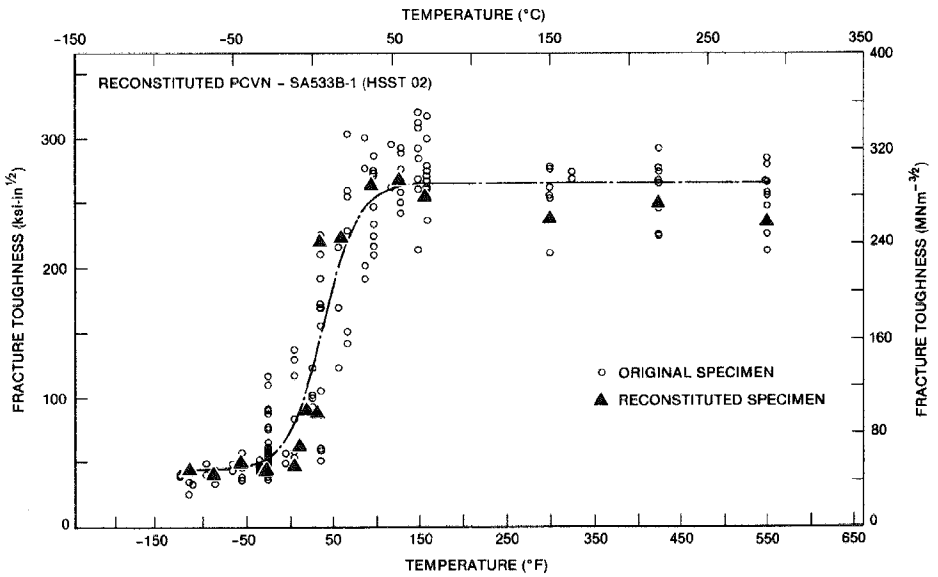

Figure 3-16. Comparison of dynamic fracture toughness data from reconstituted and original specimens of unirradiated SA533B-1 steel.

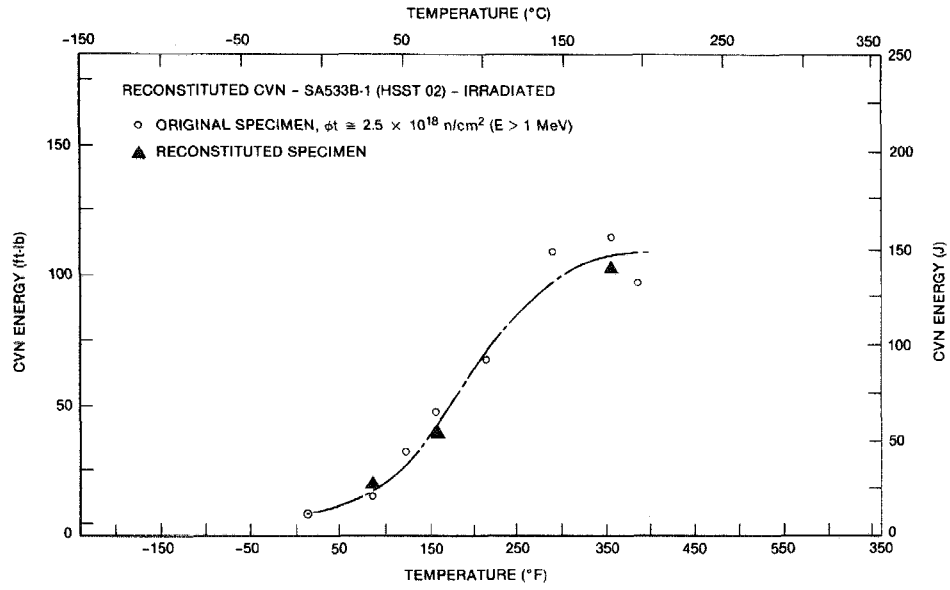

Figure 3-17. Comparison of Charpy V-Notch data from reconstituted and original specimens of irradiated SA533B-1 steel.

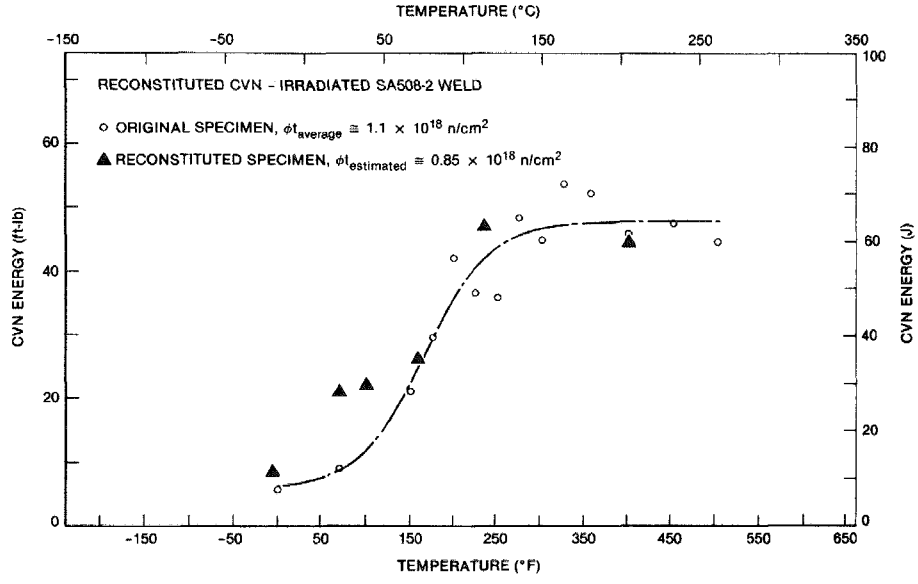

Figure 3-18. Comparison of Charpy V-Notch data from reconstituted and original specimens of irradiated submerged arc weld metal.

Section 4

RADIATION DAMAGE ANALYSIS AND MODELING*

INTRODUCTION

Predicting the time-dependent embrittlement parameters of light water reactor pressure vessel alloys requires the development and synthesis of several types of information. This information includes: (1) changes in embrittlement parameters, such as transition temperature, upper shelf energy, and toughness, as a function of both metallurgical and irradiation environment variables; (2) specification of these metallurgical (initial composition, microstructure, microchemistry, etc.) and environmental (temperature, spectrum-flux-fluence, and their time-history) variables; (3) correlation of data from both test reactor and surveillance programs and extrapolation of the data to predict time-dependent in-service material behavior.

Damage analysis is concerned with items (2) and (3) above; that is, characterizing the irradiation environment and correlation/extrapolating data. Historically, inadequate damage analysis procedures have been a significant source of uncertainty in embrittlement predictions. The embrittlement data base is characterized by very large scatter. This scatter is due, in part, to poor characterization of initial microstructure and chemistry and inaccurate dosimetry and temperature control (as well as failure to properly correlate these variables). The data base is also relatively sparse with respect to potentially important variable (and variable combination) regimes, making purely empirical approaches to data correlation difficult. Finally, these factors coupled with the overall complexity of the problem and the historical emphasis on developing engineering "trend curves" has resulted in a significant lack of basic understanding of embrittlement mechanisms.

---

*Contributions by G.R. Odette and G.E. Lucas (University of California, Santa Barbara), D.M. Schwartz, C.R. Glazer, and J.H. Shively (California State University Foundation), R.A. Wullaert and J.W. Sheckherd (Fracture Control Corporation), and R. Heinrich (Argonne National Laboratory).

The objectives of this task were to: assess the status of various problem areas, provide a strategy for dealing with the highest priority problems in a cost-effective manner using state-of-the-art techniques, and lay the groundwork for follow-on efforts aimed at significantly improved damage analysis procedures. Three major efforts were undertaken in response to these objectives: (1) assessment of the historical accuracy of the dosimetry component of embrittlement analysis and conduct of an advanced dosimetry experiment in the National Research Laboratory irradiation location in the Bulk Shield Reactor (BSR) located at the Oak Ridge National Laboratory (ORNL); (2) development and application of advanced physical correlation models; and (3) initiation of some selected critical irradiation experiments aimed at providing more fundamental information on embrittlement mechanisms. This section of the report deals with these efforts.

Before reviewing accomplishments in each of these areas, the overall strategy behind the various efforts should be emphasized. First, we assumed that the historical data base, taken as a whole, is not of sufficient accuracy; and, hence, the data base should be improved both by adding new high quality data and by eliminating, or at least giving low weight to, inaccurate data. This action requires some systematic quantitative criteria for establishing the quality of the data ultimately used in the embrittlement analysis. Second, it is recognized that new, and presumably high quality, data are and will continue to be generated by several sources outside the EPRI irradiation programs (i.e., those sponsored by the Nuclear Regulatory Commission, utilities, reactor vendors, and several foreign countries). Hence, emphasis was placed on providing a basis for EPRI to contribute to a self-consistent data base of high relative precision. Third, high priority was placed on developing physically-based models of embrittlement to mitigate the various limitations of the empirical data base. Fourth, and finally, an effort was made to take advantage of relatively low-cost opportunities to develop additional data, and to avoid the future difficulty and expense of attempting to reconstruct important experimental information easily taken or recorded during the course of this program.

NEUTRON DOSIMETRY

The first step in addressing the dosimetry issue was a semi-quantitative assessment of the sources and magnitudes of uncertainties in establishing neutron exposures (5). The most significant source of uncertainty was found to be flux-fluence measurements based on combinations of reactor physics calculations and

nuclear reaction rate measurements for both test and surveillance irradiations. There are numerous factors (at least five categories with several individual sources in each category) which contribute to dosimetry uncertainties; and, historically, a one standard deviation net relative uncertainty in fluence was estimated to be about ±30-40%. Hence, a maximum error in the fluence parameter in the embrittlement data base by a factor of 2 to 4 can be easily anticipated. Other exposure-related uncertainties involve extrapolation of fluence data into the vessel, which must be based on calculation only and the appropriate physical basis of measures of damage exposure (i.e., fluences > 1 MeV, termed $\phi t > 1$). Review of the literature suggested that extrapolation of fluences into the vessel could add considerable additional uncertainty (i.e., factors of 2). Use of artificial exposure parameters such as fluences > 1 MeV and relative uncertainties in spectrum were found to add large errors only in special circumstances; in particular, this error is important in assessing embrittlement to out-of-vessel components.

This analysis was used to establish a set of recommended procedures for dosimetry in EPRI irradiation programs. Further, it was, in part, utilized by the Nuclear Regulatory Commission (NRC) and its prime contractor, the Hanford Engineering Development Laboratory (HEDL), in planning a comprehensive dosimetry improvement program (55). This program, known as the LWR Pressure Vessel Surveillance Dosimetry Improvement Program, has two prime objectives: establishing a self-consistent set of practical procedures for both test and surveillance dosimetry and extrapolating fluences in the vessel; and providing a very high quality set of engineering embrittlement data for a variety of engineering alloys at a reference condition [$T = 550°F$ (288°C); $\phi t_{>1} \approx 2 \times 10^{19}$ n/cm^2]. Other secondary objectives include verifying the use of displacements per atom (dpa) as a reliable irradiation exposure unit for purposes of data correlation and developing some additional information on flux/time-at-temperature effects by conducting the irradiation over an extended period of two years. Finally, the NRC study provided an opportunity to irradiate specimens aimed at providing mechanistic data.

The NRC program includes a number of U.S. and foreign participants and involves extensive dosimetry/calculational verification in standard reference fields and the irradiation experiment discussed above. The irradiation experiment began in May 1980 at a simulated pressure vessel facility at the Oak Ridge Research Reactor (ORR). Further details of this effort are given elsewhere (55).

Since it is data of this type which provide the basis for an improved embrittlement data base, it is important that data generated in the EPRI programs be compatible and of roughly the same quality. To achieve this goal (in the specific context of the NRL RP886-2 program to generate embrittlement reference toughness curves), a dosimetry mapping experiment was jointly planned by FCC and the dosimetry group at the Argonne National Laboratory (ANL) under the direction of Dr. R. Heinrich.

Because of limitations in resources, only a limited dosimetry study was conducted to provide neutron spectral information for the NRL-EPRI irradiation experiments. Ten dosimeter sets (both gadolinium covered and uncovered) have been irradiated in the BSR in Position No. 76 at various axial positions using the NRL all-steel dummy irradiation block. Reactor rates for approximately 170 dosimeters and gradient wires have been measured for this irradiation. Comparison of relative flux gradients from this study to earlier NRL data shows excellent agreement. No neutron spectral data have been derived from these reaction rates due to a current lack of an appropriate reactor physics calculaion for this BSR core configuration. A report describing the dosimetry experiment and tabulating the reactor rates is on file with FCC (56). As soon as the calculation becomes available, it is possible that neutron spectra will be derived and appropriate damage parameters will be calculated. However, consistent with the strategy outlined above, a good set of basic reference dosimetry data is now available for any future analysis. Hence, there will be a reliable basis for adding the EPRI data to any improved data base. The general recommendations developed in this effort have also been implemented in other EPRI irradiation programs conducted at the University of Virginia Reactor.

DEVELOPMENT OF PHYSICAL CORRELATION MODELS

Many material and irradiation variables influence embrittlement. Further, there are clearly interactive effects between variables (e.g., composition-flux-temperature) which are difficult to establish in a completely empirical manner. In addition, actual in-service conditions are generally not conveniently accessible. Hence, there is a real need for a marriage of theory and experiment in the form of physically-based correlation models. Because of the paucity of reliable and fundamental data and the complexity of the phenomena, these models must be, in general, partly phenomenological; additionally, even the mechanistic components often will be based on rather simplified sub-models. However, when coupled with proper statistical methods of analysis, the models can be used effectively to analyze the data base. In particular, these models can be used to:

- Estimate the effect of uncertainties in the irradiation parameters and separate this effect from intrinsic data scatter, variables not considered, and implicit uncertainties in the model.
- Interpolate and to some extent extrapolate from sparse experimental matrices and provide approximate estimates of interpolation-extrapolation uncertainties.
- Assess the data base and exclude or weight data which is likely to be spurious.
- Synthesize various types of experimental information such as post-irradiation annealing and surveillance and test irradiation data.

Perhaps most importantly, the models provide physical insight into important embrittlement mechanisms and guidance in designing and analyzing new experiments.

Schematically, the correlation model consists of a function (or more complex model) which operates on material and irradiation variables to predict embrittlement. The completeness versus detail of the model must be tailored to the data under analysis; that is, detailed models for mechanistic data and composite, more phenomenological models for the engineering data base.

The effort on model development began with a review of the component processes of embrittlement -- primary defect production, microstructural evolution and microstructurally-induced property changes (7). An assessment of the state-of-knowledge in each of these areas, and pertinent programs aimed at improving our understanding, were outlined.

Following this general discussion, a model for the transition temperature shift ΔTT was applied to a set of SA302B standard reference material data taken from both test reactor and surveillance irradiations. The model was structured to account for a variety of processes including temperature-dependent initial defect production, thermal-aging, and self annealing processes. The model included a large number of parameters; approximate values of these parameters were developed from the literature or other "independent" sources of information.

It was found that the qualitative predictions of this fairly detailed physical model were consistent with experimental observations and that excellent quantitative fit could be achieved with only minor "eyeball" adjustments of the model parameters. These results suggested that at long time-at-temperature conditions

associated with low-flux surveillance irradiations both aging (perhaps enhanced by irradiation) and self-annealing effects could be important at low fluxes; these both tend to flatten the ΔTT versus fluence curve and lead to a steady-state regime of constant shift at high fluences. These results (initially arrived at independently) tended to support the experimental observations of Westinghouse that a saturation in ΔTT occurs under some conditions.

Parametric sensitivity studies with the model suggested that these general results would hold over a fairly wide range of self-annealing times for low-flux vessel conditions. Other calculations indicated that basic information about the kinetics of the embrittlement process could be developed experimentally by conducting tests for a range of temperatures and flux levels. Finally, the model was applied to a temperature, flux, fluence sensitivity study; results of these calculations indicated that much of the scatter in the engineering data base could be attributed to uncertainties in these parameters.

Subsequent to this initial study, a simplified version of the model was applied to the Materials Property Council (MPC) embrittlement data base (57);* the model was also modified to account for copper content (largely based on an empirical basis), and the data analysis was restricted to an irradiation temperature = 550 + 11°C (338 $\pm$ 6°C) and fluences $\phi t_{>1} < 10^{20}$ n/cm^2 . The simplified model can be expressed as

$$\Delta TT = A\left[1 - \exp\left(-\frac{\phi t}{\phi \tau_a}\right)\right] Cu^2 + R\left\{\phi\tau_r\left[1 - \exp\left(\frac{\phi t}{\phi \tau_r}\right)\right]\right\}^{1/2} Cu \qquad (4\text{-}1)$$

where ϕ is the flux and Cu is the copper content in weight percent. The parameters A, R, τ_a , and τ_r were found from a nonlinear multiple parameter regression analysis. Physically, the first term of Eq. 4-1 derives from the treatment of thermal aging; $A\,Cu^2$ is the maximum magnitude of the aging contribution and τ_a is the relaxation time of the transformation leading to aging. The second term of the equation accounts for the irradiation-induced shift with a proportionality constant R with provisions for in-situ recovery, as characterized by the self-annealing time parameter τ_r . Average values of flux of 2.5×10^{12} and 2.5×10^{11}, n/cm^2/s were assumed for test and surveillance conditions, respectively; these estimates are probably good only to a factor of 2-4.

*Permission to use the MPC embrittlement data base is greatly appreciated.

The correlation provided by the model for 219 MPC data points was quite good, with a standard error of ~32°F (18°C) and a correlation coefficient of 0.96. Further, the standard error in the value of τ_r was about 40%, suggesting that the defect recovery time falls within a range where flux effects should be observed for vessel operating conditions.

Table 4-1 shows the least square fit (LSF) parameters and "approximately equivalent" parameters derived in the analysis of the SA302B correlation monitor material discussed previously (57); the "approximate equivalence" derives from the fact that there were some differences between the models, and the parameters for the previous analysis were only for the chemistry of the correlation monitor heat (i.e., Cu = 0.2 wt%).

It is notable that the present results agree well with the previous analysis which involved a more detailed physical model but a much smaller set of data. Figure 4-1 shows the predictions of the latest model and the correlation monitor material data; clearly, the agreement is reasonably good, although the later model predictions are slightly low.

Table 4-2 shows some additional tests of the model in the form of "blind" comparisons with some recent low flux data which was not considered in either the previous analysis of the reference correlation monitor material or the statistical analysis of the MPC data base. Predictions for test reactor conditions (i.e., ignoring a flux effect by applying the calibrated model to test reactor

---

Table 4-1

LEAST SQUARE FIT PARAMETERS FOR EMBRITTLEMENT MODEL FOR THE MPC DATA BASE

Parameter	LSF Value	"Equivalent" Value From Reference (57)
$A(°C/Cu^2)^*$	630	700
$R(°C - cm/n^{1/2} - Cu \times 10^8)$	6.19	6.63
$\tau_a(s \times 10^{-7})$	0.12	20.5
$\tau_r(s \times 10^{-7})$	5.64	7.8

*Cu in weight %.

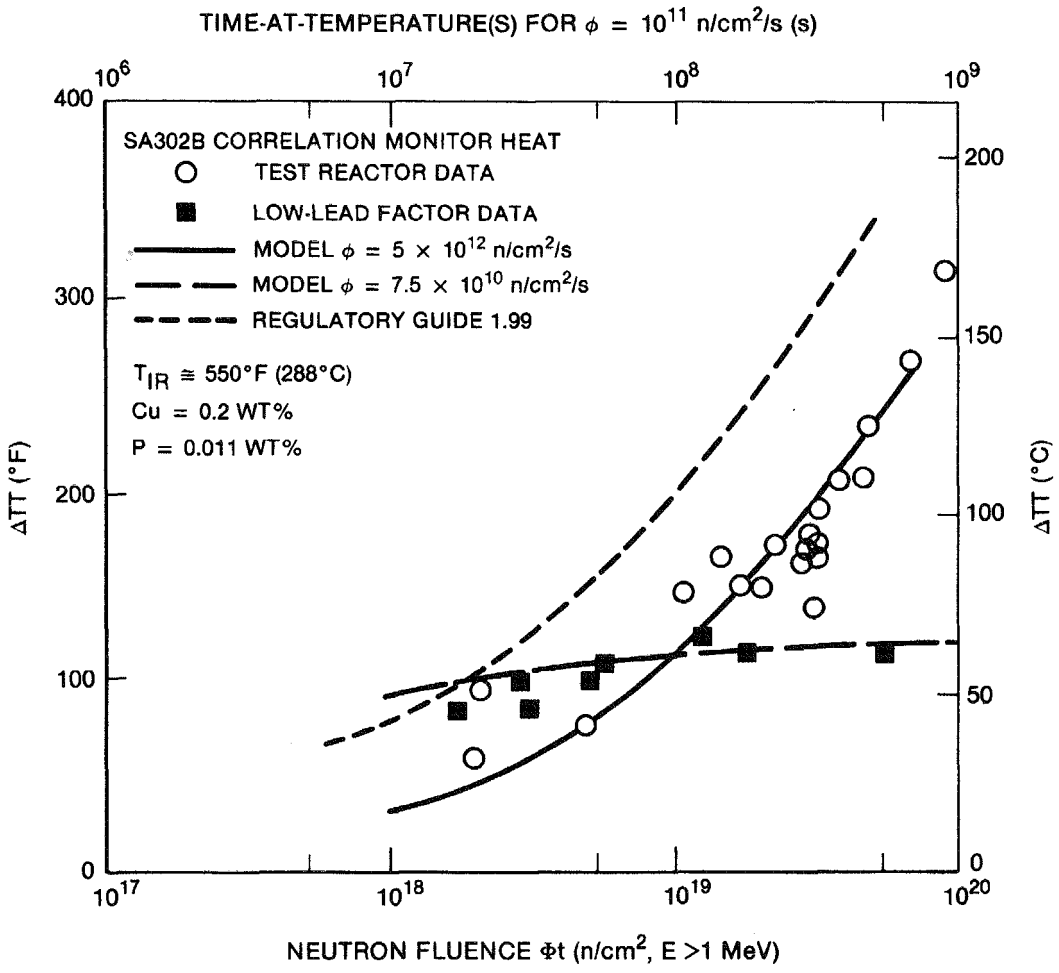

Figure 4-1. A comparison of model predictions for parameters from the MPC data base to SA302B correlation monitor heat data.

Table 4-2

SOME BLIND COMPARISONS OF MODEL PREDICTIONS WITH NEWLY REPORTED DATA

Source	Cu Chemistry (wt %)	Estimated Flux n/cm^2	Estimated Fluence $n/cm^2/s$ ($E > 1$ MeV)	ΔTT, °F(°C)*** Predicted	Measured	Extrapolated Test Data	Extrapolated Regulatory Guide 1.99
SA302B German Data	?**	6×10^{11}	1.2×10^{20}	126(70)	99(55) and 198(110)	288(160)	603(335)
Point Beach Weld	0.24	9.4×10^{10}	2.2×10^{19}	135(75)	153(85)	189(105)	297(165)
Point Beach Plate*	0.19	9.4×10^{10}	2.2×10^{19}	99(55)	99(55)	144(80)	234(130)
Point Beach Plate*	0.11	9.4×10^{10}	2.2×10^{19}	36(20)	45(25)	72(40)	144(80)
Conneticut Yankee Plate*	0.10	5.7×10^{10}	1.8×10^{19}	27(15)	27(15)	54(30)	108(60)
Conneticut Yankee Plate*	0.12	5.7×10^{10}	1.8×10^{19}	36(20)	45(25) and 72(40)	72(40)	117(65) and 135(75)
Ginna Weld	0.23	4×10^{10}	7.6×10^{19}	90(50)	135(75)	126(70)	180(100)

*SA302B steel plate.

**Assumed 0.2 Cu/0.011P.

***Values rounded to nearest 9°F (5°C).

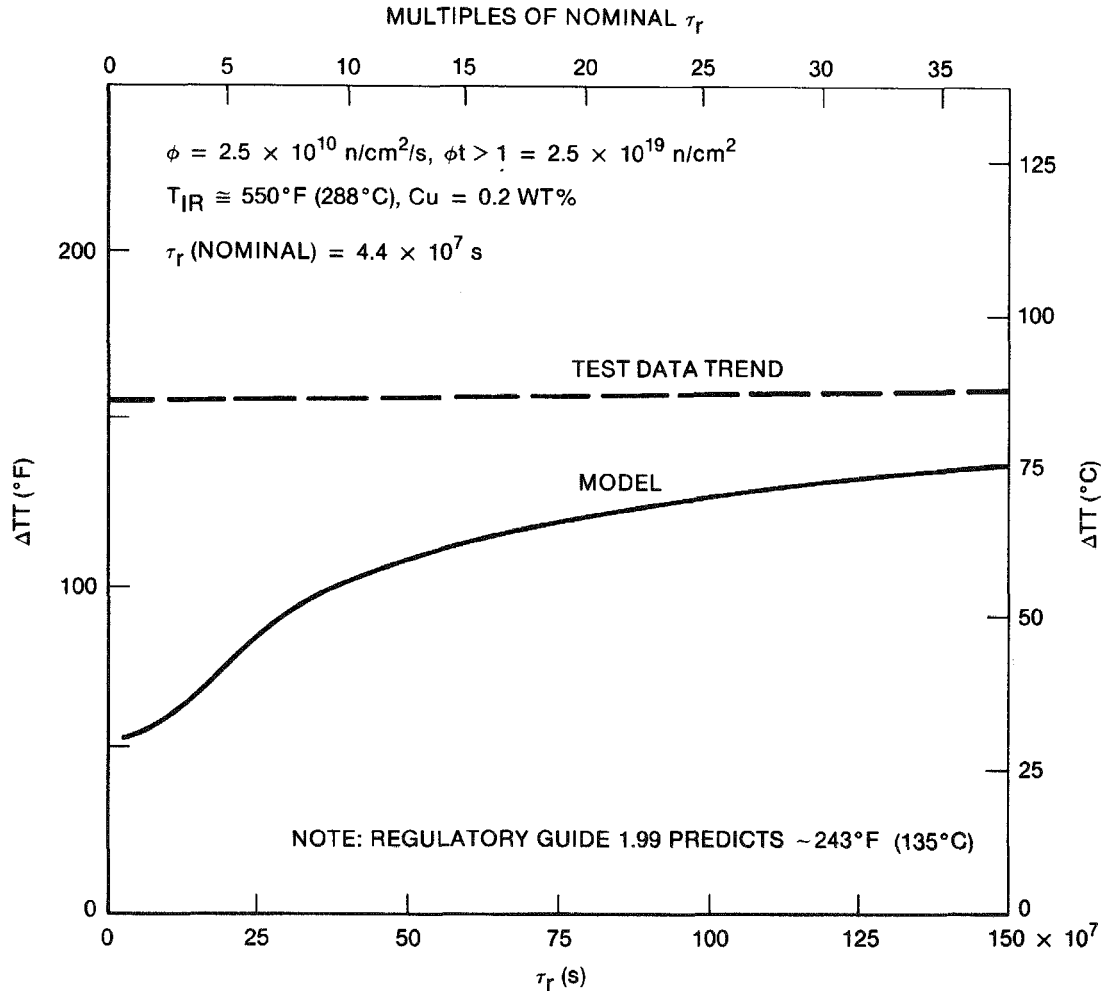

Figure 4-2. Results of a sensitivity study of predicted ΔTT at typical end-of-life conditions as a function of the defect recovery (self-annealing) time parameter τ_r

fluxes) are given in Table 4-2. Again, it is evident that agreement between the model predictions and experiment are quite good.

Figure 4-2 illustrates the effect of uncertainties in τ_r for $\phi t_{>1}$ = 2.5×10^{19} n/cm^2 ; here nominal $\tau_r = 5.64 \times 10^7$ s is increased by integral factors and the LSF analysis repeated with τ_r fixed at those values. These results show that, even if the τ_r value derived is highly inaccurate, a significant flux effect lowering ΔTT might be expected for in-service conditions if another mechanism (such as enhanced long-term aging) does not intervene.

Hence, it is concluded that there is qualitative support for the model in the MPC data base indicating a flux effect. This effect derives not so much from a large quantitative and "obvious" difference in the test and surveillance data sets, but in the trends (fluence-dependence) displayed by the collective data base.

Probably the greatest single source of uncertainty in this analysis is due to potential errors in the irradiation temperatures; indeed, sensitivity studies indicate that systematic differences between the actual irradiation temperatures between test and surveillance data [for a nominal 550°F (288°C)] as low as 27-36°F (15-20°C) could also result in the observed trends in the data. The other significant approximation is in the assumed values for flux. Hence, it is important to emphasize again the limits of this analysis; while suggestive of a potentially significant flux effect, the results at present cannot be regarded as conclusive. The predictions are not unique and depend on the correlation model parameter sets and the data base used. Ultimately, predictive sensitivity of the full range of plausible mechanisms and parameters must be explored by comparing comprehensive physical models to a reliable data base. Neither the present data base nor correlation models fully meet these requirements.

One important application of such models is sensitivity studies of the effect of uncertainties in the damage variables and the interactive effects between variables. A modified version of the model discussed previously was used to make such a study (58). Table 4-3 gives estimated ΔTT errors, based on model calculations, associated with uncertainties in ϕ, ϕt, T and wt.% Cu (the latter is used as an overall surrogate metallurgical variable). Dosimetry uncertainties contribute on the order of 20-40% error in ΔTT for historical accuracies of $\delta\phi$, $\delta\phi t$ = +100/-50% ; for improved dosimetry of $\delta\phi$, $\delta\phi t$ = to ±15% , the ΔTT errors are only 5-7%. The effect of temperature uncertainties may be even more

Table 4-3

ESTIMATED TEMPERATURE SHIFT ERRORS

Estimated ΔTT Errors Due to Dosimetry Uncertainties

Irradiation Conditions			Nominal ΔTT	+/-% ΔTT Error for δφt, δφ ; Uncertainties of	
$\phi t_{>1}$ ($\times 10^{19}$ n/cm^2)	$\phi_{>1}$ ($\times 10^{12}$ n/cm^2/s)	T(°F;°C)	(°F;°C)	+100%/-50%	±15%
2.5	5	550;288	151;84	28/20	5
2.5	0.05	550;288	90;50	21/15	4
0.5	5 or 0.05	212;100	169;94	35/28	6/7

Estimated ΔTT Errors Due to Irradiation Temperature Uncertainties

Irradiation Conditions			Nominal ΔTT	+/-% ΔTT Error for δT; Uncertainties of	
$\phi t_{>1}$ ($\times 10^{19}$ n/cm^2)	$\phi_{>1}$ ($\times 10^{12}$ n/cm^2/s)	T(°F;°C)	(°F;°C)	±31°F(17°C)	±9°F(5°C)
2.5	5	550;288	151;84	22/27	11/7
2.5	0.05	550;288	90;50	131/36	21/15

Estimated ΔTT Errors Due to Alloy Cu Chemistry Uncertainties

Irradiation Conditions			Nominal ΔTT	+/-% ΔTT Error for CU Uncertainty	
$\phi t_{>1}$ ($\times 10^{19}$ n/cm^2)	$\phi_{>1}$ ($\times 10^{12}$ n/cm^2/s)	T(°F;°C)	(°F;°C)	±50%	±10%
2.5	5	550;288	151;84	70/56	13/13
2.5	0.05	550;288	90;50	88/63	16/15
0.5	5 or 0.05	212;100	169;94	46/50	9/10

---

significant. With δT = ±31°F (17°C) the ΔTT errors ranged from 20-40% except in the case of a negative temperature deviation at low flux; in this case ΔTT was in error by ~130%. Again for improved temperature control of ±9°F (5°C) the ΔTT errors were significantly reduced ranging from 5-20%. Uncertainty in the metallurgical variable δCu = ±50% project to ΔTT errors of

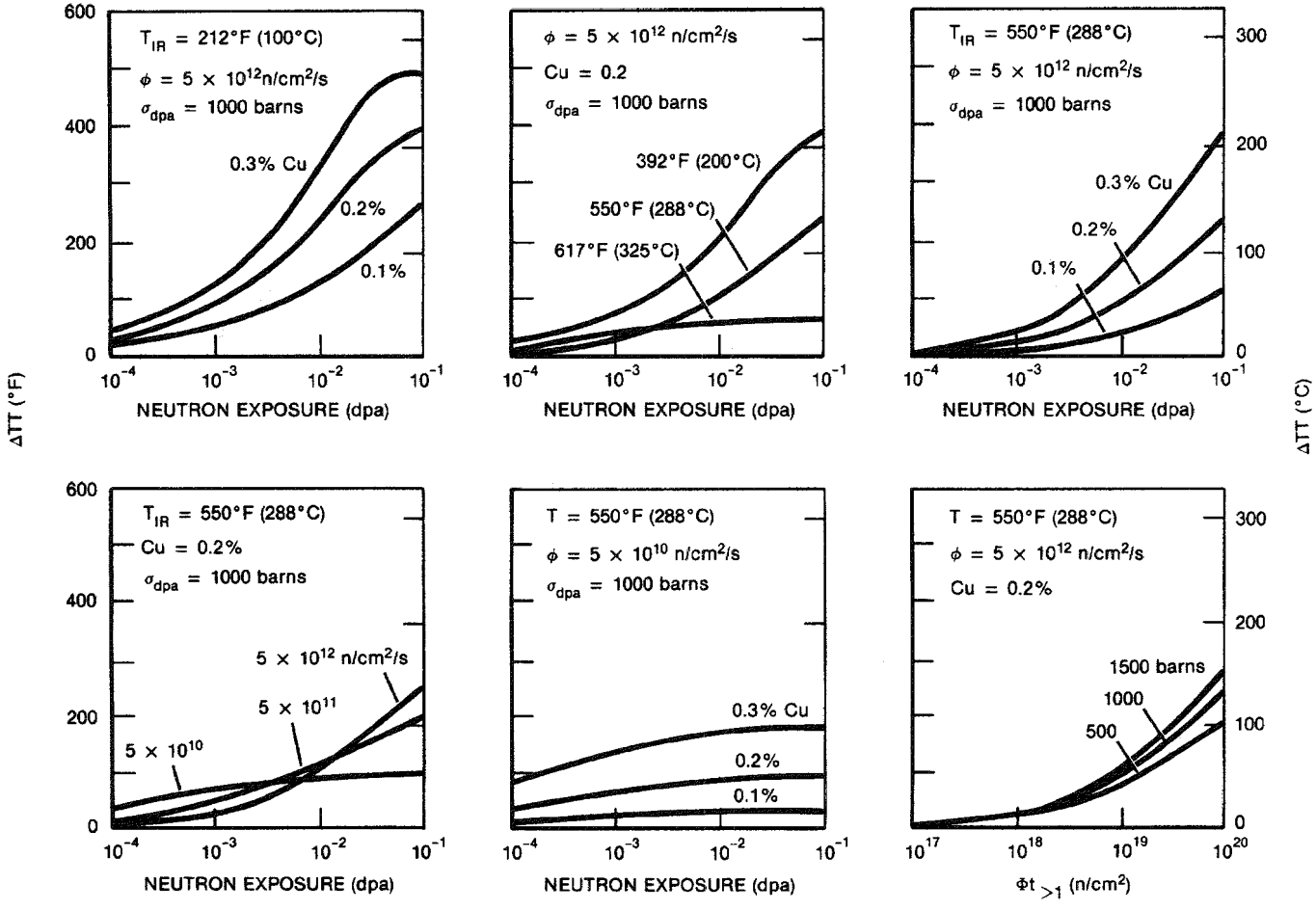

Figure 4-3. Exposure/fluence dependence of ΔTT as a function of irradiation on metallurgical variables.

50-90% percent, while improved characterization of $\delta Cu = \pm 20\%$ leads to ΔTT errors of about 10-15%. A root mean error total of these contributions gives net ΔTT errors of $\pm 75\%$ for test and +160/-100% for surveillance conditions, which is consistent with observed scatter in the data base. For improved variable characterization, the ΔTT uncertainties are only about ±15-25%. Further uncertainties can be added by ΔTT measurement errors (relatively small) and possibly by "imperfect" correlation procedures (which may be large).

Another study using the model was conducted to examine the exposure dependence of ΔTT for various conditions (59). Some results are shown in Figure 4-3. Clearly, the "shape" of a ΔTT versus exposure curve depends on the particular combination of variables; hence, the typical practice of using simple mathematical forms (e.g., $\Delta TT = A + B\ \phi t^p$) to correlate data can be very misleading.

It should be emphasized that since the models are only approximate and have not been fully verified, these sensitivity studies give only estimates of errors and functional behavior. The most important conclusion that can be derived from these calculations is that, once having recognized the physical complexity of the problem and the sensitivity of the results to the precision in characterizing the irradiation variables, it should be possible to develop a new and more accurate data base and less conservative approaches to correlating embrittlement based on better physical understanding of the underyling mechanisms.

The model development discussed previously has focused on a relatively broad phenomenological approach which is consistent with existing engineering data. As more detailed mechanistic data (e.g., model alloy and microstructural results) become available, however, a more detailed and refined analysis capability will be needed. We have, therefore, initiated the development of a generalized computer framework for such an analysis; the most unique feature of the computational approach is its flexibility and the capability for analysis of the coupled evolution of defect-microchemical structures. The framework is a computer code called SODAK. This is an acronym for Simulation of Defect Production and Annealing Kinetics (8). The code was developed by Professors Shively and Schwartz of California State University at Northridge in collaboration with FCC. This code has the capability of handling a wide range of models and mechanisms as described by sets of coupled differential-difference (kinetics) equations. As currently structured, the code can calculate the detailed kinetics of cluster (point defect, point defect-solute and solute) formation and decay; hence, it

provides a basis for developing better understanding of microstructural and compositional effects on embrittlement. Some typical results of calculations of SODAK are shown in Figure 4-4. Figure 4-4(a) shows maximum cluster densities as a function of binding energy; Figure 4-4(b) shows the time dependent concentration of copper precipitate nuclei formed by point defect transport mechanisms.

A final effort initiated, in part, under this task was an analysis of the neutron energy spectral dependence of lower temperature (<451°F; 233°C) embrittlement data (58). The usual expedient of correlating exposure data on the basis of fluence greater than 1 MeV ($\phi t_{>1}$) was found to be inaccurate and not physically justified. Consistent with several other studies, displacements per atom exposure units were found to provide a good correlation [i.e., a standard deviation of ~31°F (17°C) compared to 56°F (31°C) for $\phi t_{>1}$]. However, the use of $\phi t_{>1}$ added relatively small errors in correlating data between "typical" test and surveillance environments. Improved exposure correlation units are most important when extrapolating into, and particularly through, the vessel to assess embrittlement to out-of-vessel components.

CRITICAL IRRADIATION EXPERIMENTS

In an effort to achieve some of the needed fundamental information on radiation embrittlement mechanisms and to resolve some of the critical points used in the last subsection, FCC and its consultants collaborated with cognizant personnel involved in other programs and machined specimens for two critical experiments. These experiments will be completed after this program is terminated. The two experimental programs will be briefly discussed next.

PSF Space Compatible Test Program

The Pool Side Facility (PSF) experiment is a pressure vessel steel irradiation experiment funded by the Nuclear Regulatory Commission and managed by the Hanford Engineering Development Laboratory. As an international collaborative effort, the goal of the experiment is to characterize the effect of neutron flux spectrum on the embrittlement of pressure vessel steels. To accomplish this characterization, several packages of compact and Charpy V-notch (CVN) specimens are being irradiated in the Oak Ridge Reactor Pool Side Facility (ORR-PSF) under precisely controlled and well characterized irradiation conditions.

As part of the involvement of EPRI (FCC/UCSB) in the PSF experiment, plans were formulated for use of four CVN-size spaces in each of the PSF packages as irradiation volume for piggy-back experiments pertaining to the pressure vessel

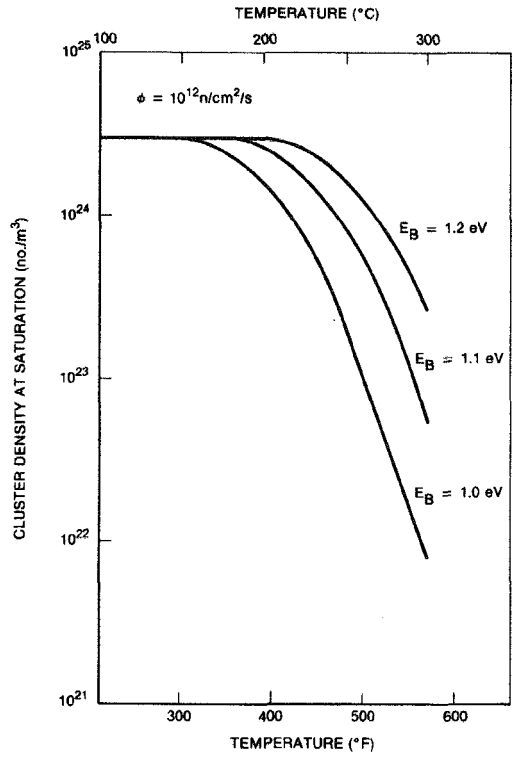

Figure 4-4(a). Prediction of cluster density at saturation as a function of temperature and vacancy-cluster binding energy.

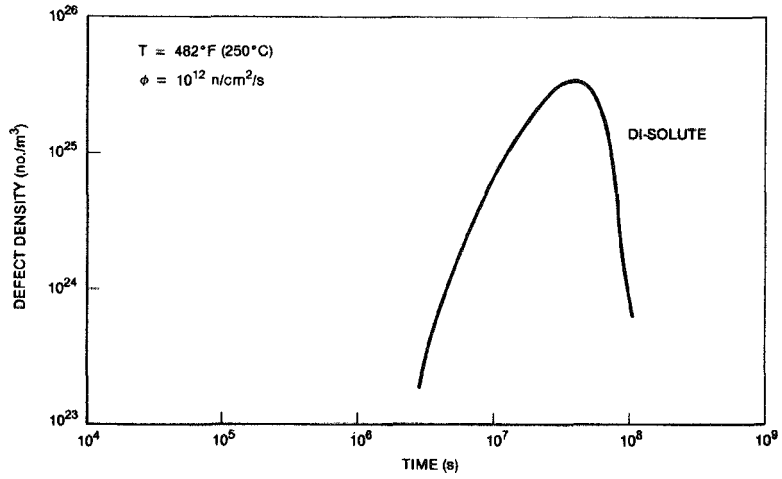

Figure 4-4(b). Predicted time dependent concentration of copper solute cluster nuclei taken as di-solute atom clusters.

steel embrittlement problem. A detailed irradiation test matrix was formulated which provides optimum use of this limited PSF space as irradiation volume for a set of engineering and model alloy specimens. Tests on these specimens will be performed to answer important questions regarding pressure vessel steel embrittlement that are not addressed by the basic PSF experiment.

The materials selected for these irradiations consist of seven engineering materials and eight model materials. Details of these materials are described in a previous report (8). It was decided that with these materials several basic questions could be addressed with relatively few tests.

The specific goals of the PSF space-compatible specimen (PSF-SCS) test program are: (1) to ascertain the variation of the damage function G(E) for pressure vessel steel embrittlement with material conditions; (2) to determine the nature of the damage microstructure produced in selected, irradiated pressure vessel steels; (3) to determine in part the nature and extent of alloy and impurity atom segregation in these steels during irradiation; and (4) to determine the thermal stability of both the as-fabricated and the irradiation-induced microstructure in the selected steels. To provide the required information to achieve these goals, several specimen/test technique combinations were selected; these techniques were:

- Compression tests on cylindrical specimens
- Transmission Electron Microscopy/Scanning Transmission Electron Microscopy (TEM/STEM) analyses on TEM discs
- Field Ion Microscopy (FIM) analyses on wire specimens
- Hardness tests on discs

Again, specific details on specimen geometries and quantities are given elsewhere (8).

Nine PSF-SCS packages have been prepared, each consisting of compression cylinders and hardness and TEM discs machined from the engineering and model materials. Some packages also contain FIM wires. Six of these packages are being irradiated along with the master PSF packages at surveillance, front face, quarter thickness, half-thickness and void box positions. Specimen holder designs for the PSF-SCS in these irradiations have been developed and described previously (8). In addition to these irradiations, one package has been prepared for baseline tests, one for thermal aging tests, and one for archival purposes.

Void Box Experiment

The main PSF irradiation (just described) is being performed in a reactor irradiation configuration designed to simulate a pressure vessel wall. As part of the attempt to obtain accurate dosimetry characterization of a pressure vessel wall irradiation environment, a void box has been located outside the simulated pressure vessel wall to reproduce the void space between the pressure vessel and normal support structures (neutron shield tank). Because of current utility interest in the potential effect of low energy neutrons ($E < 1$ MeV) on neutron shield tanks, EPRI (FCC/UCSB) and Virginia Electric Power Company (VEPCO) have assisted NRC in the planning and implementation of a void box irradiation experiment.

The experiment consists of one ambient temperature metallurgical capsule which will fit up against the back of the void box. The capsule contains only Charpy-size test specimens in a configuration of 4 across by 39 high by 1 specimen deep for a total of 152 specimens. Dosimetry in the void box capsule is provided in approximately the same locations as in the main capsules used in the simulated pressure vessel experiment. The irradiation is expected to last for approximately two years.

The main responsibility of FCC in this experiment has been to suggest, locate and machine appropriate materials for encapsulation by ORNL. The materials selected are considered typical of those that would be exposed to neutron irradiation at temperatures less than approximately 150°F (66°C) outside the main pressure vessel. These materials are described elsewhere (8).

Section 5

CONCLUSIONS

This section of the report summarizes the major technical accomplishments achieved under each of the three tasks of the program.

STATISTICAL ANALYSIS AND DEVELOPMENT OF REFERENCE FRACTURE TOUGHNESS CURVES

- The requirements and options available in developing an efficient, statistical, experimental design for radiation embrittlement programs were reveiwed with emphasis on developing probability diagrams and the importance of proper confounding of experimental qualities.

- A round robin program involving three laboratories was statistically designed to check the calibration of the equipment used in small specimen instrumented impact testing; the results indicate a need to improve the calibration of the test.

- The existing EPRI testing and analysis procedures were simplified and revised to include current state-of-the-art techniques, especially for elastic-plastic fracture toughness testing. New data report forms were developed for tensile, drop weight NDTT, Charpy V-notch, three-point bend, and compact specimen tests to assure that all pertinent data are adequately reported.

- Several sets of EPRI program results were consolidated into a new computer data base in which the data were qualified with respect to the revised analysis procedures, statistically analyzed in terms of curve fit parameters, and printed in both graphical and tabular form for user convenience. The computer data base includes chemical analysis, processing history, curve-fit parameters and statistics, and mechanical properties data.

- The precracked Charpy reference curve approach developed in the RP696-1 program was improved by developing a weighted non-linear regression scheme and global tolerance bounds resulting in a simple, statistically-based technique.

- The referencing technique developed for precracked Charpy referencing was extended to the use of standard Charpy V-notch data. The new Charpy V-notch approach has exceptional potential for irradiation data since the Charpy is the current surveillance test specimen. Equations have been developed whereby a Charpy V-notch curve can be referenced to the master fracture toughness curve, and mean, confidence, and global tolerance bounds can be predicted (computed) directly.

- Initial RP886-2 data generated by the Naval Research Laboratory (NRL) were analyzed, and mean and tolerance bounds were generated to predict the lower bound fracture toughness. Comparison was made with measured fracture toughness values also generated by NRL.

FRACTURE TOUGHNESS DATA FROM SURVEILLANCE SPECIMENS

- Additional static and dynamic multi-specimen J_R-curves were produced using 1-in (25.4 mm) thickness test pieces for comparison with upper shelf, small specimen tests.

- A simple, inexpensive, single-specimen test technique was evaluated in which precracked Charpy specimens are side-grooved by 30%, and the resulting maximum load J-integral value was found to agree favorably with the larger specimen J_{IC} (for both static and impact loading). Although high toughness material was found to require a longer ligament depth to force side-grooved initiation closer to maximum load, this technique has excellent potential for assessing the true loss in initiation upper shelf toughness due to irradiation exposure.

- A critical stress model for low temperature, slip-initiated fracture was used to accurately predict fracture toughness up to the Nil Ductility Transition Temperature for unirradiated steels under both impact and slow loading. The method was applied to irradiated data on SA533B-1 steel in which limited linear elastic fracture toughness data exists, and the model predicts the toughness changes due to irradiation with good accuracy.

- A critical strain model was used to predict the unirradiated upper shelf toughness where fracture involves a fully ductile rupture (microvoid coalescence) mechanism. Predictions for irradiated material were impossible due to the absence of needed irradiated ductility-stress state data and the paucity of upper shelf initiation toughness results for comparison with the model.

- A root radius study was used to determine the existence of a limiting root radius (ρ_0) in which the same toughness is obtained as in the fatigue precracked case; a ρ_0 exists for low temperature cleavage fracture, but there does not appear to be such a value for ductile rupture fracture.

- Static and dynamic instrumented precracked Charpy and standard Charpy V-notch results for two steels were analyzed with respect to load-temperature diagrams and energy-partitioning curves. The results provide insight into the nature of differences between the steels and the effects of testing in different plate orientations.

- A fractography study was conducted to measure the stretch zone height at the end of a fatigue precracked Charpy specimen; this measurement was then related to the crack tip opening displacement which is a measure of toughness for the steels studied.

- A surrogate material designed to simulate radiation damage was developed by explosively shock-hardening a SA533B-1 steel. Testing of this surrogate material produced Charpy V-notch energy

results consistent with the temperature shift and upper shelf energy drop seen in irradiated materials.

- Reconstituted surveillance specimens were produced by stud welding end tabs on broken Charpy V-notch specimens. The results of testing unirradiated and irradiated reconstituted specimens (both Charpy V-notch and precracked Charpy) were consistent with the original test data. This technique may provide an opportunity to maximize the data that can be obtained from expensive irradiation programs.

RADIATION DAMAGE AND MODELING

- The assessment of the historical accuracy of the dosimetry component of embrittlement analysis has revealed the most significant source of uncertainty is the flux-fluence measurements based upon combinations of reactor physics calculations and nuclear reaction rate measurements for both test and surveillance irradiations. Values of the fluence parameter may vary by as much as a factor of 4.

- An advanced dosimetry experiment was conducted to provide neutron spectral information (mapping) for the Naval Research Laboratory program RP886-2; thus, basic reference dosimetry data are now available for future analysis.

- The status of light water reactor damage analysis programs was reviewed and recommendations were made concerning future experiments and coordination of the overall programs. Consistent with these recommendations was involvement in the Pool Side Facility Space Compatible Test Program (PSF-SCS) and the Void Box Experiment.

- A physically-based, semi-empirical correlation model for predicting embrittlement was developed to incorporate primary defect production, development of damage microstructure, and the relationship between microstructure and mechanical properties. The model was able to quantitatively predict, with reasonable accuracy, the results of recent observations of a damage rate effect in low lead-factor surveillance experiments.

- Another computer model (SODAK) was developed to track the development of defect microstructures during irradiation, post-irradiation annealing, and reirradiation. The model explicitly considers the effects of both irradiation induced defects and impurity or alloying elements (i.e., copper). The results from SODAK support the phenomenological modeling approach previously developed.

- The various models, even though not perfect, were useful in providing a systematic identification of future experimental efforts. Significant progress in current modeling and data correlation efforts cannot be made until additional mechanistic data are available and the irradiation environment is more precisely defined.

- Contributions were made to the Nuclear Regulatory Commission program for the PSF and Voix Box experiments by helping design the experiment, procure materials, and machine specimens.

Section 6

REFERENCES

1. Wullaert, R.A., W. Oldfield, and W.L. Server, "Fracture Toughness Data for Ferritic Nuclear Pressure Vessel Materials," Electric Power Research Institute Report NP-121, Final Report on Research Project 232-1, April 1976.

2. Server, W.L., W. Oldfield, and R.A. Wullaert, "Experimental and Statistical Requirements for Developing a Well-Defined K_{IR} Curve," Fracture Control Corporation Final Report on Research Project RP696-1 to the Electric Power Research Institute, EPRI NP-372, May 1977.

3. Stahlkopf, K.E., W.L. Server, R.E. Smith, and R.A. Wullaert, "A Methodology for Evaluating Variability in Fracture Properties of Ferritic Nuclear Pressure Vessel Steels," Journal of Pressure Vessel Technology, Vol. 99, Series J, No. 3, August 1977.

4. Oldfield, W., R.A. Wullaert, W.L. Server, and K.E. Stahlkopf, "Statistically Defined Reference Toughness Curves," Proceedings of the Third International Congress of Pressure Vessel Technology, Tokyo, Japan, April 1977.

5. Oldfield, W., W.L. Server, G.R. Odette, and R.A. Wullaert, "Analysis of Radiation Embrittlement Reference Toughness Curves," Semi-Annual Progress Report No. 1 to Electric Power Research Institute on RP 886-1, Fracture Control Corporation Report FCC 77-1, March 1977.

6. Oldfield, W., W.L. Server, and R.A. Wullaert, "Analysis of Radiation Embrittlement Reference Toughness Curves," Semi-Annual Progress Report No. 2 to Electric Power Research Institute on RP 886-1, Fracture Control Corporation Report FCC 77-6, October 1977.

7. Odette, G.R., W.L. Server, W. Oldfield, R.O. Ritchie, and R.A. Wullaert, "Analysis of Radiation Embrittlement Reference Toughness Curves," Semi-Annual Progress Report No. 4 to Electric Power Research Institute on RP 886-1, Fracture Control Corporation Report FCC 78-11, November 1978.

8. Wullaert, R.A., Editor, "Analysis of Radiation Embrittlement Reference Toughness Curves," Semi-Annual Progress Reports Nos. 5 and 6 to Electric Power Research Institute on RP 886-1, Fracture Control Corporation Report FCC 79-5, October 1979.

9. Server, W.L., and W. Oldfield, "Nuclear Pressure Vessel Steel Data Base," Fracture Control Topical Report to Electric Power Research Institute on RP 886-1, EPRI Report NP-933, December 1978.

10. Oldfield, W., "Fracture Toughness Correlations and Reference Curves," Annual Report No. 1 to Electric Power Research Institute on RP 1021-4, April 1980.

11. McConnell, P., G.R. Odette, W. Oldfield, J.W. Sheckherd, and R.A. Wullaert, "Collection and Evaluation of Data for Irradiated Pressure Vessel Steels," Final Report to Electric Power Research Institute on RP 1240-1, March 1980, to be published by EPRI.

12. Server, W.L., "Impact Three-Point Bend Testing for Notched and Precracked Specimens," Journal of Testing and Evaluation, Vol. 6, No. 1, January 1978, pp. 29-34.

13. Davies, D.L. and P.L. Goldsmith, Statistical Methods in Research and Production, Hafner Publishing, New York, 1972.

14. Ireland, D.R., W.L. Server, and R.A. Wullaert, "Procedures for Testing and Data Analysis," Effects Technology, Inc., Report 75-43, October 1975.

15. Oldfield, W., R.A. Wullaert, W.L. Server, and T.R. Wilshaw, "Fracture Toughness Data for Ferritic Nuclear Pressure Vessel Materials; Task A--Program Office, Control Material Round Robin Program," Effects Technology, Inc., Report TR 75-34R, July 1975.

16. Wullaert, R.A., J.W. Sheckherd, W.L. Server, and W. Oldfield, "HTGR Fracture Toughness Program," Final Report on RP 337-1 to the Electric Power Research Institute, NP-120, April 1976.

17. Server, W.L., R.A. Wullaert, and J.W. Sheckherd, "Verification of the EPRI Dynamic Fracture Toughness Testing Procedures," Effects Technology Report TR 75-42, October 1975.

18. Server, W.L., R.A. Wullaert, and J.W. Sheckherd, "Evaluation of Current Procedures for Dynamic Fracture Toughness Testing," Flaw Growth and Fracture, ASTM STP 631, American Society for Testing and Materials, 1977, pp. 446-461.

19. Marston, T.U., M.P. Borden, J.H. Fox, and L.D. Reardon, "Fracture Toughness of Ferritic Materials in Light Water Nuclear Reactor Vessels," Electric Power Research Institute Report EPRI 232-2, Final Report on Research Project 232-2, December 1975.

20. Van Der Sluys, W.A., R.R. Seeley, and J.E. Schwabe, "Determining Fracture Properties of Reactor Vessel and Forging Materials, Weldments, and Bolting Materials," Electric Power Research Institute Report NP-122, Final Report on Research Project 232-3, July 1976.

21. Server, W.L., J.W. Sheckherd, and R.A. Wullaert, "Fracture Toughness Data for Ferritic Nuclear Pressure Vessel Materials; Task B--Laboratory Testing," Electric Power Research Institute Report EPRI NP-119, Final Report on Research Project 232-1, April 1976.

22. Server, W.L., "Static and Dynamic Fibrous Initiation Toughness Results for Nine Pressure Vessel Materials," Elastic-Plastic Fracture, ASTM STP 668, American Society for Testing and Materials, Philadelphia, 1979, pp. 493-514.

23. Borden, M.P. and L.D. Reardon, "Sub-Critical Crack Growth in Ferritic Materials for Light Water Nuclear Reactor Vessels," Electric Power Research Institute Report EPRI NP-304, Final Report on Research Project 232-4, August 1976.

24. "Recommended Procedure for J_{Ic} Determination," Preliminary Draft From ASTM E24.01.09, March 1977.

25. Oldfield, W., W.L. Server, R.A. Wullaert, and K.E. Stahlkopf, "Development of a Statistical Lower Bound Fracture Toughness Curve," International Journal of Pressure Vessels and Piping, Vol. 6, 1978, pp. 203-222.

26. Oldfield, W., "Curve Fitting Impact Test Data: A Statistical Procedure," ASTM Standardization News, Vol. 3, No. 11, November 1975, pp. 24-29.

27. Oldfield, W., "Fitting Curves to Toughness Data," Journal of Testing and Evaluation, Vol. 7, No. 6, 1979, pp. 326-333.

28. Oldfield, W., "Development of Fracture Toughness Reference Curves," Journal of Engineering Materials and Technology, Vol. 102, January 1980, pp. 107-117.

29. Oldfield, W. and T.U. Marston, "Revised Fracture Toughness Reference Curves," Transactions of the 5th International Conference on Structural Mechanics in Reactor Technology, Vol. G, Paper G2/7, 1979.

30. Hawthorne, J.R. and F.J. Loss, "Evaluation and Prediction of Neutron Embrittlement in Reactor Pressure Vessel Materials," Annual Progress Report to Electric Power Research Institute on Research Project RP 886-2, May 1979.

31. Server, W.L., "General Yielding of Charpy V-Notch and Precracked Charpy Specimens," Journal of Engineering Materials and Technology, Vol. 100, No. 2, April 1978, pp. 183-188.

32. Paris, P.C., H. Tada, A. Zahoor, and H. Ernst, "The Theory of Instability of the Tearing Mode of Elastic-Plastic Crack Growth," Elastic-Plastic Fracture, ASTM STP 668, J.A. Begley and J.D. Landes, Eds., American Society for Testing and Materials, 1979, pp. 5-36.

33. Logsdon, W.A., "Static and Dynamic Fracture Toughness of ASTM A508 C12 and ASTM A533 GrB C11 Pressure Vessel Steels at Upper Shelf Temperatures," Ductility and Toughness Considerations in Elevated Temperature Service, MPC-8, G.V. Smith, Ed., The American Society of Mechanical Engineers, 1978, pp. 149-165.

34. Andrews, W.R. and C.F. Shih, "Thickness and Side-Groove Effects on J- and δ-Resistance Curves for A533-B Steel at 93°C," Elastic-Plastic Fracture, ASTM STP 668, American Society for Testing and Materials, 1979, pp. 426-450.

35. Ritchie, R.O., W.L. Server, and R.A. Wullaert, "A Simple Test Method for Measuring 'Valid' J_{Ic} Fracture Toughness in Charpy-Size Surveillance Specimens of Nuclear Pressure Vessel Steel," International Journal of Fracture, Vol. 14, December 1978, pp. R329-334.

36. Server, W.L., R.A. Wullaert, and R.O. Ritchie, "The Use of Side-Grooves in Estimating J_{Ic} Fracture Toughness With Charpy-Size Specimens of Nuclear Pressure Vessel Steel," Journal of Engineering Materials and Technology, Vol. 102, No. 1, April 1980, pp. 192-199.

37. Green, G. and J.F. Knott, "Effects of Side Grooves on Initiation and Propagation of Ductile Fracture," Metals Technology, Vol. 2, September 1975, pp. 422-427.

38. Ritchie, R.O., J.F. Knott, and J.R. Rice, "On the Relationship Between Critical Tensile Stress and Fracture Toughness in Mild Steel," Journal of Mechanics and Physics of Solids, Vol. 21, 1973, pp. 395-410.

39. McClintock, F.A., "Plasticity Aspects of Fracture," Fracture, An Advanced Treatise, H. Liebowitz, Ed., Vol. 3, Academic Press, New York, 1971, pp. 47-225.

40. Ritchie, R.O., W.L. Server, and R.A. Wullaert, "Critical Fracture Stress and Fracture Strain Models for the Prediction of Lower and Upper Shelf Toughness in Nuclear Pressure Vessel Steels," Metallurgical Transactions A, Vol. 10A, October 1979, pp. 1557-1569.

41. MacKenzie, A.C., J.W. Hancock, and D.K. Brown, "On the Influence of State of Stress on Ductile Failure Initiation in High Strength Steels," Engineering Fracture Mechanics, Vol. 9, 1977, pp. 167-188.

42. Succop, G., R.T. Bubsey, M.H. Jones, and W.F. Brown, Jr., "Investigation of Some Problems in Developing Standards for Precracked Charpy Slow Bend Tests," Developments in Fracture Mechanics Test Methods Standardization, ASTM STP 632, American Society for Testing and Materials, 1977.

43. Server, W.L., "Compliance Correction for Determining Load-Line Energies for Compact Fracture Toughness Specimens," Journal of Testing and Evaluation, Vol. 17, No. 1, January 1979, pp. 29-32.

44. Malkin, J. and A.S. Tetelman, "Relationship Between K_{IC} and Microscopic Strength for Low Alloy Steels," Engineering Fracture Mechanics, Vol. 3, No. 2, 1971, pp. 151-169.

45. Ritchie, R.O. and R.M. Horn, "Further Considerations on the Inconsistency in Toughness Evaluation of Ultra-High Strength Steel Austenitised at Increasing Temperatures," Metallurgical Transactions A, Vol. 9A, 1978, pp. 1039-1053.

46. Begley, J.A., W.A. Logsdon, and J.D. Landes, "Ductile Rupture Blunt-Notch Fracture Criterion," Flaw Growth and Fracture, ASTM STP 631, American Society for Testing and Materials, 1977, pp. 112-120.

47. Rice, J.R., "A Path Independent Integral and the Approximate Analysis of Strain Concentration by Notches and Cracks," Journal of Applied Mechanics, Vol. 35, 1968, pp. 379-386.

48. Sumpter, J.D.G. and C.E. Turner, "Method for Laboratory Determination of J_c," Cracks and Fracture, ASTM STP 601, American Society for Testing and Materials, 1976, pp. 3-18.

49. Wells, A.A., "Unstable Crack Propagation in Metals: Cleavage and Fast Fracture," Proceedings of the Crack Propagation Symposium, Vol. 1, pp. 210-230.

50. Robinson, J.N. and A.S. Tetelman, "The Critical Crack-Tip Opening Displacement and Microscopic and Macroscopic Fracture Criteria for Metals," University of California, Los Angeles, Report UCLA-ENG-7360, August 1973.

51. Erkman, J.O. and A.B. Christensen, "Attenuation of Shock Waves in Aluminum," Journal of Applied Physics, Vol. 38, No. 13, 1967, pp. 5395-5403.

52. Trott, B.D., et al., "ARPA Order 854 Impact Sensitivity of Explosives," Battelle Research Report to The Naval Research Laboratory, AD 886-3236, July 1971.

53. Wilcox, B.A., et al., "Research on Metallurgical Synthesis," Air Force Materials Laboratory Technical Report AFML-TR-72-238, Part II, January 1974.

54. Champion, A.R. and R.W. Rhode, "Hugoniot Equation of State and the Effect of Stress Amplitude and Duration on the Hardness of Hadfield Steel," Journal of Applied Physics, Vol. 41, No. 5, 1970, pp. 2213-2223.

55. McElroy, et al., "LWR Pressure Vessel Surveillance Dosimetry Improvement Program," 1979 Annual Report NUREG/CR-1291/HEDL-SA 1949, 1980.

56. Heinrick, R.R. and R.J. Popek, "Dosimetry Study for the NRL-EPRI Dual-Material BSR Irradiation Experiments," Final Report to Fracture Control Corporation from Argonne National Laboratory, March 1980.

57. Stahlkopf, K.E., G.R. Odette, and T.U. Marston, "Radiation Damage Saturation in Pressure Vessel Steels: Data and a Preliminary Model," to be published in Journal of Pressure Vessel Technology.

58. Odette, G.R., "A Quantitative Analysis of the Implications of Accuracy of Dosimetry to Embrittlement Predictions: Past, Present, and Future," Proceedings of the 3rd ASTM-Euratom Symposium on Reactor Dosimetry, Ispra, Italy, October 1979.

59. Odette, G.R., "Neutron Exposure Dependence of the Embrittlement of Reactor Pressure Vessel Steels: Correlation Models and Parameters," Proceedings of the IAEA Technical Committee Meeting on the Accuracies in Correlation Between Property Changes and Exposure Data From Reactor Pressure Vessel Steel Irradiations, Julich, W. Germany, September 1979.

Appendix A

ALUMINUM ROUND ROBIN PROGRAM

The experimental design was based upon preliminary experimentation at Fracture Control Corporation (FCC) which allowed the initial characteristics of the experiment to be predicted in terms of n, α, β, and δ. The experiment highlights any differences which might exist between laboratories in terms of maximum load measurement, dial energy reading, or integrated energy computation. At the same time, the experiment will reveal any inhomogeneities in the plate, as shown by differences between edge (material A) and center (material B) samples, and will show whether different testing procedures give results which differ from those generated by the EPRI standard procedures. The basic design and preliminary experimental characteristics are shown in Table A-1; this design basically employs a 2×2 factorial design with 8 replicates per test condition. For the first row of tests, the usual test procedures at each laboratory are replaced by a standardized set of procedures common to both laboratories. The second row is developed by the laboratory using its usual procedures. Approximately seven laboratories had agreed to participate in this experiment and were sent machined specimens, but unfortunately only three organizations submitted their results.

An analysis of variance was used to analyze the results for each quantity measured; maximum load, dial energy, and integrated total energy. With this method, the variance of all data was first determined by assuming each to be an equally valid estimate of a single quantity. This total variance estimate does, of course, contain the effects of all experimental variables being studied. The total variance was then analyzed to determine the variance resulting from the experimental variables and their interactions. Any effects that the experimental variables do have can be found with great sensitivity and precision. The computer procedure used here first normalized all data about the mean to enhance the computational accuracy. Then the analysis of variance was performed using three main effect variables: (1) laboratories, (2) type of handling (testing procedure), and (3) portion of the original 0.50-in (12.7 mm) plate (edge or center). The analysis of variance results for maximum load data are shown in Table A-2.

Table A-1

ALUMINUM ROUND ROBIN EXPERIMENTAL DESIGN CHARACTERISTICS

Impact Energy	Maximum Load
σ^2 = 0.0521 ft^2-lbf^2 (0.0958 J^2)	σ^2 = 547.16 lbf^2 (10.826 N^2)
n = 8	n = 8
α = 0.05	α = 0.05
(S.E. diff) = 0.1141 ft-lbf (0.1547 J)	(S.E. diff) = 11.696 lbf (52.03 N)
Δ = 0.2579 ft-lbf (0.3497 J)	Δ = 26.436 lbf (117.59 N)

β	δ ft-lb (J)	β	δ lb (N)
0.1	0.4668 (0.6329)	0.1	47.84 (212.8)
0.05	0.5159 (0.6995)	0.05	52.86 (235.1)
0.025	0.5638 (0.7644)	0.025	57.78 (257.0)
0.01	0.6288 (0.8525)	0.01	64.44 (286.5)
0.005	0.6791 (0.9207)	0.005	69.59 (309.6)
0.001	0.8035 (1.0894)	0.001	82.34 (366.3)

	Number of Samples			
	Laboratory A		Laboratory B	
	Material A	Material B	Material A	Material B
Standard Conditions	4	4	4	4
Laboratory Procedures	4	4	4	4

The results from this experiment indicate the following important areas of concern:

- Instrumented impact load calibration does not yet appear to be properly controlled. The biases between laboratories amount to 8% of the peak load levels. There seems to be no reason that the variance for all laboratories should not be as low as the preliminary experiment at FCC.

Table A-2

ANALYSIS OF VARIANCE OF MAXIMUM LOAD DATA FROM ALUMINUM ROUND ROBIN STUDY

ANALYSIS OF VARIANCE TABLE

SOURCE	S.S.	D.F.	M.S.
MAIN EFFECT 1	0.2804739E 7	2.	0.1402370E 7
MAIN EFFECT 2	0.2310187E 4	1.	0.2310187E 4
MAIN EFFECT 3	0.6526875E 3	1.	0.6526875E 3
INTERACTION 1 x 2	0.5782812E 4	2.	0.2891406E 4
INTERACTION 1 x 3	0.5514312E 4	2.	0.2757156E 4
INTERACTION 2 x 3	0.3466875E 3	1.	0.3466875E 3
3-TERM INTERACTION	0.1960212E 5	2.	0.9801062E 4
TOTAL AMONG GROUPS	0.2827304E 7	11.	0.2570276E 6
RESIDUAL VARIATION	0.2889160E 6	36.	0.8025445E 4
TOTAL VARIATION	0.3116220E 7	47.	0.6630256E 5

S.S. -- Sum of Squares
D.F. -- Degrees of Freedom
M.S. -- Mean Square Variation

- Both the dial energy and integrated energy values revealed bias. These differences were real but on the order of 0.4 ft-lb (0.5 J), which is probably unimportant from a practical standpoint.

- Special handling had an effect on energy measurements with different effects at different laboratories.

- The material was uniform as far as the precision of the experiment could show. The variance estimates are therefore giving the variance of the method and not the material. The variance in these quantities can thus be used to predict the variance in fracture toughness predictions made from them using a reference curve procedure.

In conclusion, this experiment indicates a clear need for improvement in the calibration of the instrumented Charpy test. Additionally, the variance of test data does not arise totally from material variability; thus variance can impose a severe penalty on reactor operation since all of the variance is generally assumed to be in the material when operation standards are written.

Appendix B

COMPACT SPECIMEN TEST PROCEDURES

STANDARDS AND REFERENCES

The following ASTM standards (1,2) and references should be used to insure compliance with existing standard test methods: E4, Standard Methods of Verification of Testing Machines; E74, Standard Methods of Calibration of Force-Measuring Instruments for Verifying the Load-Indication of Testing Machines; E399, Standard Test Method for Plane-Strain Fracture Toughness of Metallic Materials; and E220, Calibration of Thermocouples by Comparison Techniques. Reference should also be made to the EPRI RP 232-1 Procedures (3), and the RP696-1 Final Report (4).

An area not covered by these procedures is the machining, orientation, and selection of specimens. It is assumed that all contractors draft detailed cutting diagrams and mark orientation on all specimens and archive pieces such that any anomaly in test results can be traced back to the original slab of material. The selection of samples should be made in a randomized fashion.

INSPECTION AND CALIBRATION

A complete inspection and calibration report for the entire test system should be written prior to any testing. The report should contain at least the following information:

A. Type, manufacture, and calibration results of the testing machine and recording devices to be used. Also, details of periodic calibration checks should be included.

B. Description of the speeds of testing to be used and the methods employed in measuring and controlling the speed.

C. Type, manufacture, and calibration results for the thermocouple readout device along with a description of the thermocouples used (including placement and attachment procedures).

D. Type and manufacture of the furnace/cooling device and temperature controller. Also include details of temperature gradients that the specimen may see (including overshoots).

E. Method, apparatus, and accuracy of measuring particular specimen dimensions.

F. The time of holding at temperature should be specified along with any data showing when thermal equilibrium is reached.

G. Type, manufacture, and calibration results of the clip gage and recording device used. Details of linearity and absolute accuracy over the entire working range should be reported as well as daily calibration check procedures.

H. Description of the test specimen(s) to be used.

I. Frequency response information pertaining to both the load cell, clip gage, and related electronics (i.e., both electronic and mechanical response).

TEST DATA REPORT

Figure 2-3 in this report illustrates the data form used in evaluating compact fracture specimen tests. All necessary information and calculations are indicated on the form.

Definitions of Terms and Symbols

The following list of definitions are important to the understanding of the test and required calculations:

Electronic Response Time (T_R)--0.915 dB rise time for the electronics based upon a sine wave signal.

Test temperature (T)--equilibrium temperature at the time of testing.

Thickness (B)--specimen breadth.

Width (W)--specimen depth from the load-line.

Ligament Depth (b)--remaining depth of the specimen below the fatigue crack.

Crack Length ($\bar{a}$)--the three-point interior average of the total crack depth (machined notch plus fatigue crack) measured after the sample has been fractured.

Fracture Area (A)--the ligament area over which fracture occurs.

Secant Offset Load (P_Q) and Time (t_Q)--5% secant offset load and time from the initial linear portion as determined from the load-clip gage displacement record.

Maximum Load (P_M) and Time (t_M)--the maximum load and associated time attained in the test.

Conditional Fracture Toughness (K_Q)--the linear elastic toughness value calculated using the load P_Q ; this value may not be acceptable due to size limitations and/or excessive plasticity.

Young's Modulus (Y_σ)--the elastic modulus for steel.

J-Integral Value (J_M)--the calculated J value at maximum load.

Strength Ratio (R_{sc})--the ratio of the net section stress to the yield stress.

Yield Stress at $\sim \dot{\varepsilon}$ (σ_y)--the estimated value of yield stress at the appropriate temperature and strain rate (4).

Flow Stress at $\sim \dot{\varepsilon}$ (σ_{fl})--the estimated value of flow stress (one-half yield plus ultimate) at the appropriate temperature and strain rate (4).

Stress Intensity Factor (K_{Ic} or K_{Jc})--the measure of mode I deformation of the stress-field intensity near the tip of a perfect crack in a perfect crack in a linear elastic field. K_{Ic} is a direct small-scale yielding measure of this intensity factor, while K_{Jc} is a post-general yield energy measure converted to an equivalent K_{Ic}.

Stress Intensification Rate ($\dot{K}$)--the measure of loading rate obtained by dividing the K_{Ic} or K_{Jc} value by the time to maximum load.

Fibrous Crack Extension ($\Delta\bar{a}$)--the nine-point average of the stretching plus fibrous growth occurring below the fatigue precrack.

Fracture Initiation Mode--either cleavage or fibrous as determined from observation of the broken specimen fracture surface.

Fatigue Stress Intensity Factor (K_f)--the linear elastic stress intensity factor during fatigue loading.

Calculations

1. $Y_\sigma = 207.2 - (0.0571T)$ (GPa)

   T is in degrees Centigrade

2. $$J_M = \frac{2\int_0^{\delta_M} P d\delta}{bB}$$

3. $$R_{sc} = \frac{2P_M(2W + \bar{a})}{Bb^2\sigma_y}$$

4. $K_{Ic}(K_Q)$, K_{Jc}:

a. When $P_M/P_Q \leq 1.10$

$$K_Q = \frac{P_Q}{BW^{1/2}}\left[29.6\left(\frac{\bar{a}}{W}\right)^{1/2} - 185.5\left(\frac{\bar{a}}{W}\right)^{3/2} + 655.7\left(\frac{\bar{a}}{W}\right)^{5/2} - 1017.0\left(\frac{\bar{a}}{W}\right)^{7/2} + 638.9\left(\frac{\bar{a}}{W}\right)^{9/2}\right]$$

$$\text{If } B,b,a \geq 2.5\left(\frac{K_Q}{\sigma_y}\right)^2 \quad ; \quad K_{Ic} = K_Q$$

(This criterion is generally too restrictive for ferritic pressure vessel steels); if the thickness criteria are not met then proceed to the K_{Jc} calculation.

b. When $P_M/P_Q > 1.10$

$$K_{Jc} = (Y_\sigma J_M)^{1/2}$$

5. $$\dot{K} = \frac{(K_{Ic}, K_{Jc})}{t_M}$$

6. Acceptance Criteria:

Criteria	Elastic $P_M/P_Q \leq 1.10$	Elastic-Plastic $P_M/P_Q > 1.10$
Size	$a,b,B \geq 2.5\left(\frac{K_{Ic}}{\sigma_y}\right)^2$	$a,b,B \geq \frac{50J_M}{\sigma_{fl}}$ (cleavage initiation) $a,b,B \geq \frac{25J_M}{\sigma_{fl}}$ (fibrous initiation)
Crack Depth	$0.45 \leq \frac{\bar{a}}{W} \leq 0.55$ $(\bar{a} - a_o) \geq 1.3$ mm	$0.50 \leq \frac{\bar{a}}{W} \leq 0.70$ $(\bar{a} - a_o) \geq 1.3$ mm
Fatigue Crack Shape	$a(1/4B)$, $a(1/2B)$, $2(3/4B) \leq 0.95\ \bar{a}$ a(surface 1), a(surface 2) $\leq 0.90\ \bar{a}$ Symmetry of the plane of notch and fatigue crack surface do not deviate by more than 10 degrees	(Same as for Elastic)
Fatigue Precrack	K_f over last 2.5% of $\bar{a} \leq 0.6K_S$; K_S is the minimum 1. $\frac{\sigma_{yp}}{\sigma_{yt}} K_Q$ $\sigma_{yp} \equiv$ yield stress at precracking $\sigma_{yt} \equiv$ yield stress at testing conditions 2. $0.0033Y_\sigma$	(Same as for Elastic)
Response Time*	$t_Q \geq 1.1T_R$	(Same as for Elastic)

*Only valid for RC-type filter circuits.

7. Mode of Initiation:

If fast fracture occurs at maximum load, a check on whether the amount of stretching (blunting) exceeds a certain amount dictates if the fracture is cleavage initiated in ferritic steels:

$$\Delta\bar{a} \leq \frac{0.55J_M}{\sigma_{fl}} \quad \text{(cleavage)}$$

If $\Delta\bar{a}$ is larger than the quantity above, the mode of initiation is fibrous.

NOTE: The form shown in Figure 2-3 is used for an R-curve type J-initiation test where J_M and $\Delta\bar{a}$ values are required.

REFERENCES

1. 1976 Annual Book of ASTM Standards, Part 10, ASTM, Philadelphia, PA, 1976.

2. 1976 Annual Book of ASTM Standards, Part 44, ASTM, Philadelphia, PA, 1976.

3. Ireland, D.R., W.L. Server, and R.A. Wullaert, "Procedures for Testing and Data Analysis," Effects Technology, Report TR75-43, October 1975.

4. Server, W.L., W. Oldfield, and R.A. Wullaert, "Experimental and Statistical Requirements for Developing a Well-Defined K_{IR} Curve," Fracture Control Corporation Final Report of Research Project RP696-1 to the Electric Power Research Institute, EPRI NP-372, May 1977.